GETTING THE MOST OUT OF A TRAINING SESSION: A MOTOR LEARNING APPROACH TO GAIT REHABILITATION IN STROKE

by
Kevin Andrew Day

A dissertation submitted to Johns Hopkins University in conformity with the requirements for the degree of Doctor of Philosophy

Baltimore, Maryland
August, 2019

Abstract

Gait following stroke often presents with multiple impairments. These can include step length asymmetry, decreased paretic knee flexion, pelvic tilt, and abnormal ankle plantar/dorsiflexion, among others. Given the tight time and financial restrictions that many patients face, it is important that we look to make therapy as efficient as possible. Here, we first studied how altering the training schedule influenced the storage of a motor memory across multiple days. We used a split-belt treadmill to train participants to walk with one belt moving twice as fast as the other. When exposed to this perturbation, participants are forced to adapt their walking pattern to restore symmetrical step lengths. When re-exposed to the same perturbation, participants are able to adapt faster—a phenomenon termed savings. By manipulating the delivery of this perturbation over five days, we were able to achieve an equivalent level of savings as a daily training regime in just one-fourth of the training time. We then focused on methods in which we could target kinematic impairments other than step length asymmetry. We explored how healthy participants could learn multiple kinematic features of a modified walking pattern using real-time visual feedback. We delivered the visual feedback of four kinematic features in one of two forms: 1) a single stream of visual information representing a composite of all four kinematic dimensions in a one-dimensional summary of performance or 2) four concurrent streams of visual information, each of which contained information for a single feature of walking. We found that healthy participants were able to use the one-dimensional summary visual feedback to improve their performance faster and more completely. Last, we used this summary visual feedback in a stroke population

to allow them to correct multiple patient-specific deficits. This feedback algorithmically weighed the input kinematic dimensions based on the patient's baseline walking deficits. Patients were able to use this individualized visual feedback to bias multiple features of their walking toward a prescribed goal walking pattern. These results indicate that this feedback has promise for altering multiple features of a complex movement and individualized rehabilitation of gait following stroke.

Thesis Committee

Amy J. Bastian

Kathleen E. Cullen

Ryan T. Roemmich

Adrian M. Haith

Acknowledgements

There are many people I would like to thank who have made this dissertation possible. First, I would like to thank the research subjects who participated in these walking studies. Without their participation, we would know slightly less about gait rehabilitation in stroke as a product of this dissertation.

I would like to thank Amy Bastian for being an incredible advisor. You have helped me become a better scientist and have shown me how to ask interesting questions as well as how to design the right experiment to answer these questions. You were always approachable and I really enjoyed the opportunity to learn from you over the past five years. I consider myself lucky to have been your graduate student.

I would like to thank the members of the Center for Movement Studies, both past and present. You made coming to work enjoyable and always provided insightful feedback for my projects. In particular, I would like to thank Ryan Roemmich for introducing me to key motor learning principles as well as the lab equipment to answer our questions when I first joined the lab. Your continuous feedback throughout all of these projects was invaluable.

To the friends I have gained in Baltimore, I would like to thank you for helping me legitimately enjoy my time in graduate school. We all came to Baltimore not knowing anyone and it was amazing to gain such a great group of friends. Spending time with you was always a welcome distraction from the grind of doctoral research.

To my family, I would like to thank you for your continuous support throughout my educational journey. Thank you for your encouragement and understanding why I

wanted to go to school forever. To my parents, thank you for instilling in me a love for engineering and science and always supporting my career aspirations. I would like to thank my identical twin, James, who joined a Biomedical Engineering PhD program the same time as me and offered someone to compare graduate school notes with. Even though we always say we are not competitive, I think it's worth mentioning that I beat you to the dissertation defense by three months. Maybe next time!

Finally, I would like to thank my fiancé, Kaci. We first met during my first week in Baltimore so I can truly say you have been there the entire time during this journey. Thank you for your constant support, encouragement, and friendship. I am so grateful, that thanks to you, I am leaving Baltimore with more than a PhD. I've gained a best friend and I cannot wait to see what the future holds for us.

Dedication

To my parents, Marlene and Dennis, and my fiancé, Kaci.

Table of Contents

List of Tables

List of Figures

Chapter 1 Introduction

Our ability to modify our movement is remarkably flexible. This flexibility allows us to navigate a wide range of environments smoothly and effortlessly. Beyond allowing us to pick up a new hobby such as playing the piano or playing basketball, this flexibility affords us an opportunity for rehabilitation when movement becomes impaired due to orthopaedic, neurological, or any other type of injury. Recent rehabilitation approaches have focused on the brain's ability to modify its output to compensate for changing environmental demands[1-2]. This phenomenon is termed motor learning and is thought to rely on a suite of learning mechanisms that act in combination to grant us an ability to modify or expand our movement repertoire[3-5].

A classic example of motor learning is our ability to adapt our movement in response to wearing prism goggles that shift the visual field either rightward or leftward[6-7]. Consider a task where we are instructed to throw a dart to a target directly in front of us. When first donning the goggles, we will tend to miss the target in the same direction of the visual shift. Over a number of throws, however, we will be able to adapt our movement so that our throws become closer to the target[6-7]. Interestingly, when we take the goggles off and attempt to hit the target, our throw will miss in the opposite direction of the visual shift—a product of a motor learning process. This miss—termed an aftereffect—is the hallmark of a type of motor learning called sensorimotor adaptation and is indicative of a recalibration between sensory input (e.g. visual field) and motor output (e.g. our throw)[6-10]. Because this type of learning is automatic and unconscious, hitting the target is not just a matter of re-aiming when we take the goggles off. Our brain

has now stored a new 'normal' that we must actively unlearn, now with the context of a normal visual field[6-7].

When considering the use of motor learning principles for rehabilitation, their application to walking presents a promising approach. Walking is the predominant form of mobility for most people and is known to predict independence[11], risk for disability[12], and survival[13] in older adults. Walking, like upper-limb movement in the prism example, is flexible to motor learning and adaptation processes[1,4,14-15]. Thus, when walking is impaired, it is important that we use all of the tools available to us to lead to the most effective and efficient therapy.

The focus of this dissertation is to determine how we can most efficiently and effectively modify a walking pattern, in both healthy individuals and individuals post-stroke. The work here has implications to basic neuroscience principles as it provides insight into how the nervous system learns and stores a new walking pattern as well as implications to rehabilitation as we look to inform methods in which we can optimize therapy for those with gait impairment.

1.1 Gait impairment post-stroke

Gait deficits are often a product of several types of neurologic injury, of which stroke is the most common. With improved acute care following stroke, stroke mortality is steadily decreasing and stroke has become the leading cause of long-term disability in the United States[16]. Furthermore, over 75 percent of stroke survivors display gait deficits[17]. This presents a clear need for effective neurorehabilitation to restore healthy function for the increasing number of stroke survivors with pathological gait.

Stroke, either ischemic or hemorrhagic, often results in unilateral damage to the motor cortex. Such damage most commonly manifests itself as a diminished ability to generate voluntary muscle contractions on one side of the body[18-19]. This loss of control could be due to a combination of a decreased ability to activate motor units, a reduced number of functional motor units, or a decreased drive (i.e. firing rate) of motor units to a particular muscle[19-21]. In addition to the loss of strength, persons post-stroke often experience abnormal spasticity due to decreased inhibitory drive from the central nervous system[22]. Because of this unilateral decrease in strength and increase in spasticity, a paretic gait is generally asymmetric. Thus, restoring symmetry is a common rehabilitation goal for therapists when treating persons post-stroke.

Gait deficits post-stroke are multiple and heterogeneous in nature. Some of the most common include reduced gait speed[17], prolonged stance phase[18], greater proportion of stride in double support[18], asymmetrical step length[23], hip hiking[24], hip circumduction[24], decreased knee flexion[25-26], and decreased ankle dorsiflexion[27]. Often times, these deficits are related and consequences of each other. For example, people who exhibit 'stiff-knee gait' have reduced knee flexion during swing and thus compensate with their hip (e.g. via hip hiking or circumduction) to progress their foot forward without tripping[24-25]. Thus, it is common to distinguish deficits as an impairment (i.e. directly due to the injury) or a compensation (i.e. due to trying to mitigate the primary impairment)[18].

Spatiotemporal deficits and kinematic deficits represent two prominent domains of walking deficits after stroke. Spatio-temporal deficits rely on the coordination between the two legs (step length asymmetry, double support time, etc) while kinematic deficits

are largely within-limb and arise within each step (decreased knee flexion, decreased ankle dorsiflexion, etc)[18]. Often, different therapies are more effective at targeting a certain class of deficits. Thus, it is important to consider for a given person with stroke that a specific therapy or intervention may not be ideal to target their individual deficits.

1.2 Introduction to locomotor adaptation

Similar to upper-limb movement described in the prism goggle example, lower-limb movement (i.e. walking) is able to adapt to changing environmental demands. That is, our brain is able to recalibrate how we walk in response to changing sensory inputs—a process termed locomotor adaptation[1,4,14-15]. In everyday life, this process helps us navigate varying environments such as a sandy beach or an icy driveway. In the lab, locomotor adaption is studied by introducing participants to a novel walking environment. Specifically, we can drive adaptation using a split-belt treadmill, a treadmill with individually-driven belts under each foot. In this environment, we have people walk with one belt moving faster than the other. Initially, people begin to limp in response to this perturbation but over the course of steps, they begin to normalize their walking, such that the limp decreases. By a few minutes of walking in this split-belt environment, it would be difficult for a naïve observer to know that one belt was moving faster than the other just by looking at the participant's walking pattern.

During the deadaptation phase of the experiment, the belts return to the same speed to test for learning. Indeed, healthy participants will exhibit a limp in the opposite direction (i.e. an aftereffect). Even though the tied belts are 'normal', the brain perceives this transition as an error and must unlearn the calibration it built when the belt speeds were split during the adaptation phase of the experiment[14-15]. These aftereffects are

transient, however, and walking returns to baseline behavior after a few minutes on tied belts[14-15, 28].

Previous studies have revealed exactly which features of gait are changing when adapting to a split-belt environment. Reisman et al. studied both spatial and temporal features of walking during split-belt adaptation[14]. They observed that interlimb gait parameters (e.g. step length, percent double support, etc.) showed the most robust adaptation and aftereffects while intralimb gait parameters (e.g. stride length, percent stance time, etc.) changed rapidly to accommodate the changing environments but were not learned (i.e. no aftereffects). A primary measure used to describe adaptation processes in walking is step length asymmetry. Step length is defined as the distance between the feet at heel strike of each foot. Step length asymmetry is the difference between step lengths on each side, normalized by the total magnitude of the step lengths. Thus, a larger limp will correspond to a large step length asymmetry. Step length asymmetry has been shown to exhibit a large error at the beginning of adaptation, followed by an incremental reduction over training as well as a robust aftereffect when returned to tied-belts during deadaptation[14]. Because it is a normalized parameter, we can fairly compare across individuals of different height and stride length.

Further research has demonstrated that these interlimb adaptation parameters can be parsed into temporal and spatial components[29]. That is, we change *where* we place our feet relative to one another (i.e. spatial) and *when* we move our legs relative to one another (i.e. temporal) as we adapt to a split-belt environment. Temporal and spatial adaptation have been observed to operate on differing time-scales and be responsive to differing interventions[30-31]. For example, temporal adaptation is more resistant to

cognitive manipulations than spatial adaptation[30]. Thus, they are thought to be independent of one another and possibly arise from differing neural substrates[30,32-33].

When re-exposed to the same split-belt perturbation, people show the ability to achieve faster learning even after unlearning[34-36]—a phenomenon termed savings. Savings is thought to be due to the faster retrieval of a motor pattern in response to a previously experienced perturbation[37], and demonstrates that the nervous system stores features of previously experienced adaptive environments. Savings of a split-belt environment is driven by previous exposure to similar abrupt changes in the environment as well as the amount of exposure to the new environment[35]. The ability to save a new motor pattern presents a promising tool for rehabilitation as therapists can build on what was learned in previous training sessions.

1.3 Adaptive gait training in stroke

Previous work suggests that the ability to adapt to a split-belt environment is largely driven by cerebellar processes[15]. In this work, the authors demonstrated that participants with cerebellar disorders were not able to restore symmetry when walking on a split-belt treadmill and did not display the characteristic aftereffects that would be expected if learning had occurred[15]. Indeed, inducing cerebellar lesions in cats abolishes their ability to adapt to a novel walking environment[38] (Yanagihara and Kondo, 1996). Furthermore, previous work studying the ability of decerebrate cats to adapt to novel walking environments suggests that the ability to modify inter- and intralimb coordination of gait remains intact even without cerebral inputs[38-39]. Thus, locomotor adaptation provides a promising avenue for modifying gait in those who have

experienced cerebral damage but may still have other motor pathways (e.g. cerebellar) intact.

Often, those who have experienced cerebral damage due to stroke exhibit asymmetrical walking[40-42]. Work by Reisman et al. has shown that patients with cerebral stroke who normally walk with a limp are able to adopt a new, more symmetric walking pattern after exposure to a split-belt environment that exaggerates their limp[43]. That is, a split-belt environment that results in an initial asymmetry that is greater than their baseline asymmetry induces a negative aftereffect that places them in a more symmetrical walking pattern compared to baseline[43]. Thus, an adaptation learning mechanism can uncover the latent ability of stroke survivors to walk with a symmetric pattern.

Although participants were able to display an aftereffect that resulted in a more symmetrical walking pattern, this walking pattern washes out due to adaptation to the now tied-belt environment[43]. This is the paradox of using adaptive mechanisms for rehabilitation of gait: the mechanism that allowed participants to achieve an improved walking pattern is the very mechanism that is responsible for washing it away as they restore baseline behavior. Still, adaptive training offers some benefit to people post-stroke. Previous work demonstrated that the adaptive effects achieved on a split-belt treadmill transfer to over ground walking for people post-stroke[44]. Additionally, repeated split-belt training over the course of months has proven to improve step length asymmetry relative to baseline by increasing the step length on the side that takes the shorter step[45]. Thus, adaptive gait training in stroke both generalizes beyond the learning environment and can lead to long-term improvements with repetitive practice.

1.4 Using real-time visual feedback for gait retraining

While adaptive training has proven effective for modifying interlimb coordination of gait (i.e. spatiotemporal deficits), it does not target intralimb parameters (i.e. kinematic deficits)[14]. Real-time visual feedback of gait kinematics has proven useful in altering targeted features of gait in healthy and neurological populations[46-51]. Visual feedback relies on the real-time measurement (via motion capture, electromyography, force plates, etc.) of a targeted parameter and providing quantitative information beyond what is typically available to the user. It allows for an individual to self-correct abnormal features of gait[52-53]. In a recent review of real-time biofeedback, feedback parameters of the 173 relevant studies included kinematics, kinetics, spatiotemporal, muscle activation, and physiological parameters with stroke patients consisting of the highest percentage of targeted clinical populations[54].

Cherry-Allen et al. used visual feedback of joint angles to individually alter peak knee angle while adapting to a split-belt treadmill perturbation in persons post-stroke[55]. Moreover, visual feedback has been effective in improving gait speed, stride length, and stride width in people post-stroke[56-58]. In healthy participants, visual feedback has been used to alter foot placement[48], knee or hip flexion angles[59], as well as lower-limb mechanics during long distance running[60-61].

A recent neurophysiological study demonstrated that acquiring a new gait pattern using visual feedback relies on enhanced motor planning[62]. Specifically, the authors used electroencephalography (EEG) to demonstrate a modulation in neural signal in motor and parietal regions with timing most consistent with transforming the visual cues into a new motor plan[64]. Parietal regions are implicated in encoding sensory stimuli and integrating multisensory information into a motor plan[63-64]. Thus, patient groups with intact parietal

regions stand to benefit from information provided by real-time visual feedback that allows them to correct aberrant features of gait.

1.5 Scope of dissertation

This dissertation focuses on how to more efficiently and effectively modify a gait pattern. The first two aims study various forms of learning mechanisms in healthy individuals to provide a framework for studying these principles in people post-stroke. The third aim studies a novel form of visual feedback in stroke that allows for the correction of multiple patient-specific deficits during training.

Aim 1: We can leverage the training structure of locomotor adaptive learning to achieve a high degree of performance while minimizing training sessions. Patients often face tight time and financial restrictions that limit their exposure to therapy. We know that adaptive learning requires repeated practice of the learning environment to achieve long-term effect[45]. Thus, it is crucial that we understand how to deliver therapy most efficiently so that patients may achieve the desired outcome with fewer training sessions.

The ability for the nervous system to store a motor memory is underscored by the motor learning phenomenon of savings—the faster relearning after initial exposure to a novel environment. Chapter 2 highlights how savings in healthy individuals progresses over five consecutive days of practice. We also investigate which specific elements of their walking pattern they adjusted to account for the split treadmill speeds from day-to-day and applied a state-space model to further characterize multiday locomotor savings.

We then explored methods of achieving comparable savings with less total training time. We studied people training only on Day 1, with either one extended split-

belt exposure, or alternating four times between split-belt and tied belt conditions rapidly in succession. Both of these single-day training groups were tested again on Day 5. Experiencing four abbreviated exposures on Day 1 improved the performance on Day 5 when compared to one extended exposure on Day 1. Moreover, this abbreviated group performed similarly to the group that trained for 4 consecutive days prior to testing on Day 5, despite only having one quarter of the total training time. These results demonstrate that we can leverage training structure to achieve a high degree of performance while minimizing training sessions.

Aim 2: Reducing the dimensionality of visual feedback allows for improved performance of a skilled walking task. Learning a skilled, coordinated movement often requires changing multiple kinematic features. Serial training is one common approach to learning a new movement pattern, where each feature is learned in isolation from the others. Once one feature is learned, we move on to the next. However, when learning a complex movement pattern, serial training is not only laborious but can also be ineffective. Often, movement features are linked such that they cannot simply be added together as we progress through training. Thus, the ability to learn multiple features in parallel could make training faster and more effective. When using visual feedback as the tool for changing movement, however, such parallel training may increase the attentional load of training and impair performance.

In Chapter 3, we investigate the utility of a novel visual feedback system that uses principal component analysis to weight four features of movement to create a simple one-dimensional 'summary' of performance. We used this feedback to teach healthy, young participants a modified walking pattern and compared their performance to those who

received four concurrent streams of visual information to learn the same goal walking pattern. We demonstrated that those who used the principal component-based visual feedback improved their performance faster and to a greater extent compared to those who received concurrent feedback of all features. These results suggest that our novel principal component-based visual feedback provides a method for altering multiple features of movement toward a prescribed goal in an intuitive, low-dimensional manner.

Aim 3: A novel principal-component based visual feedback to teach persons post-stroke to correct multiple patient-specific deficits. Chapter 4 discusses the use of the novel principal component-based visual feedback in a stroke population. This type of visual feedback offers two distinct advantages over traditional training with biofeedback: 1) it incorporates information from multiple features of gait and displays this to the user in a low-dimensional, intuitive manner and 2) it allows for individualized feedback such that the weights on each of the input dimensions are determined by a participant's baseline walking deficits.

For persons post-stroke, we established a walking goal consisting of bilateral hip and knee joint angles of an average 'healthy' gait. We compared this performance to a group of healthy, age-matched individuals who received an exemplar hemiparetic gait goal pattern. We investigated the use of the principal component-based feedback over two training sessions in which participants were first allowed to explore the correct solution using only the visual feedback and then allowed to hone in on the exact goal once instructed of the solution. We observed that both groups were able to bias their kinematics in the direction of the prescribed goal walking pattern. These results have important implications to rehabilitation as it offers a method for teaching multiple

features of gait in a personalized, patient-specific manner, thus allowing for more targeted, effective therapy.

1.6 Dissemination

Chapter 2 is described in a manuscript, "Accelerating locomotor savings in learning: compressing four training days to one" by Kevin A. Day, Kristan A. Leech, Ryan T. Roemmich and Amy J. Bastian published in *Journal of Neurophysiology*. Chapter 3 is described in a manuscript "Less is more: providing low-dimensional feedback of a high-dimensional movement allows for improved performance of a skilled walking task" by Kevin A. Day and Amy J. Bastian, which is in review at *Scientific Reports*. Chapter 4 is described in a manuscript "Individualized feedback to change multiple gait deficits in chronic stroke" by Kevin A. Day, Kendra M. Cherry-Allen, and Amy J. Bastian, which is submitted to *Journal of NeuroEngineering and Rehabilitation*.

Chapter 2 Leveraging training structure to increase the time efficiency of locomotor adaptive training

2.1 Introduction

Our ability to smoothly navigate our environment relies on the capacity to adapt our motor behavior to new environments and store a motor memory of the adapted movement. Consider the seemingly trivial transition of stepping from a boardwalk onto compliant sand. Transitioning between these walking environments poses a problem that the nervous system must solve for us to maintain balance and stay upright. When presented with predictable changes in the environment, the nervous system possesses the ability to change its motor output via motor adaptation—a process in which sensorimotor mappings update in response to systematic errors caused by new environmental demands [6,8-10]. Once these mappings are updated, it is equally crucial that the nervous system possesses the ability to store a motor memory of the new mapping so that it can be retrieved at a later point for successful navigation. Imagine if every time we step onto the sand, we have to adapt our walking pattern over the course of hundreds of steps as if we have never experienced anything similar before. The fact that we can smoothly transition from one walking environment to the next underscores the importance of storing a motor memory.

Prior work on motor adaptation in both reaching and walking has focused largely on adaptation over short timescales (e.g. learning within one session)[8-10,43]. While these studies are useful in uncovering the mechanisms underlying motor adaptation, we rarely come across truly novel environments in our everyday lives. More often than not, we rely on experience to re-adapt to the demands of previously encountered environments; alternatively, we are able to generalize previously learned movement patterns to new but similar environments. Just as a golfer can select from a number of clubs in his or her golf bag for a club best-suited for a given shot, we can call on an expansive collection of remembered movements to traverse a wide range of environments quickly and successfully. In the current study, we seek to understand how we can best incorporate a novel motor pattern into our repertoire of movements over multiple days of training.

Several studies have shown that people who have previously adapted to a perturbation can achieve faster learning when re-exposed to the same perturbation, a motor learning phenomenon termed 'savings'[34,35,37,65]. Savings has been well studied in the context of motor adaptation but these studies are often limited to 2 within-day training exposures[35, 66-69]. Previous studies show savings to be sensitive to the structure of training[35-37]. Specifically, savings in locomotor adaptation is driven by previous exposure to similar abrupt changes in the environment as well as the amount of exposure in the new environment[35]. Importantly, the balance of these two factors that leads to optimal savings across days has yet to be explored. Therefore, it is important that we understand how new movement patterns are learned over longer timescales (e.g., multiple days) and how different learning schedules affect the ability to store the newly learned pattern from day-to-day.

The ability to shape savings using the structure of training provides a promising tool for gait rehabilitation. Many patients face tight time and financial restrictions that limit their exposure to therapy, and thus it is critical that therapy is delivered as efficiently as possible. When training a new gait pattern, patients look to build on what was learned from the previous training sessions. Knowledge of how to prescribe rehabilitation schedules for fastest day-to-day learning could lead to more efficient therapy whereby patients achieve the desired outcome with fewer training sessions.

Here, we studied how altering the training schedule influenced savings of a split-belt walking pattern over multiple days. Specifically, we altered the frequency and duration of split-belt treadmill training within Days 1 to 4 of training and tested savings on Day 5. While some participants received extended split-belt training with continuous exposure to the split-belt environment, others received a condensed training schedule consisting of short bouts of training in which they switched between the split-belt and tied-belt environments. Furthermore, we varied the delivery of these training regimes across groups such that some participants only trained on Day 1 and returned to the lab for testing on Day 5 while others trained for four consecutive days before testing for savings on Day 5. We demonstrate that we can reduce the training load from four days to one day by implementing a switch training schedule and still achieve equivalent learning. Moreover, the savings observed following the switch training schedule followed a similar behavioral trajectory (i.e. altered kinematics) as that of savings observed following extended multiday training. Our findings indicate that we can leverage the structure of training to create an optimal training schedule that minimizes training time while still maintaining the integrity of the learned movement across multiple days.

2.2 Methods

2.2.1 Participants

Forty young, healthy adults were recruited for this experiment (12 male, 28 female; mean age ± SD: 22 ± 4 yrs). All participants provided written, informed consent prior to taking part in the experiment. The experimental protocol was approved by the Johns Hopkins Medicine Institutional Review Board. All participants were free of any neurological and musculoskeletal conditions. Leg dominance was determined by asking the participants which leg they would use to kick a soccer ball.

2.2.2 Split-belt treadmill

Adaptive learning was studied by having participants walk on a split-belt treadmill in which an independently-controlled belt was located under each foot (Woodway USA, Waukesha, WI). The two belts were controlled by custom MATLAB (MathWorks, Natick, MA) software and could move at the same speed (i.e. tied-belt) or at different speeds (i.e. split-belt). Participants were instructed to stand in the middle of the treadmill with one foot on each belt. They wore a safety harness that was suspended from the ceiling to protect against the risk of falling. The harness did not provide any body-weight support. Participants were not made aware of the speeds of the belts in subsequent trials and were given a handrail at the front of the treadmill to provide stability when the treadmill belts abruptly started. They were told to lift their hands off of the rail within the first few strides, walk with their arms across their chest, and avoid looking downward at the treadmill belts for the entirety of the experiment. Participants remained on the treadmill for the duration of each session.

2.2.3 Motion analysis

We recorded participants' kinematics as they walked using an Optotrak Certus motion capture system (Northern Digital, Waterloo, ON). Kinematic data were collected at 100 Hz from twelve infrared-emitting diodes placed bilaterally on the foot (fifth metatarsal head), ankle (lateral malleolus), knee (lateral joint space), hip (greater trochanter), pelvis (iliac crest), and shoulder (acromion process). Marker placement is displayed in Figure 2.1A.

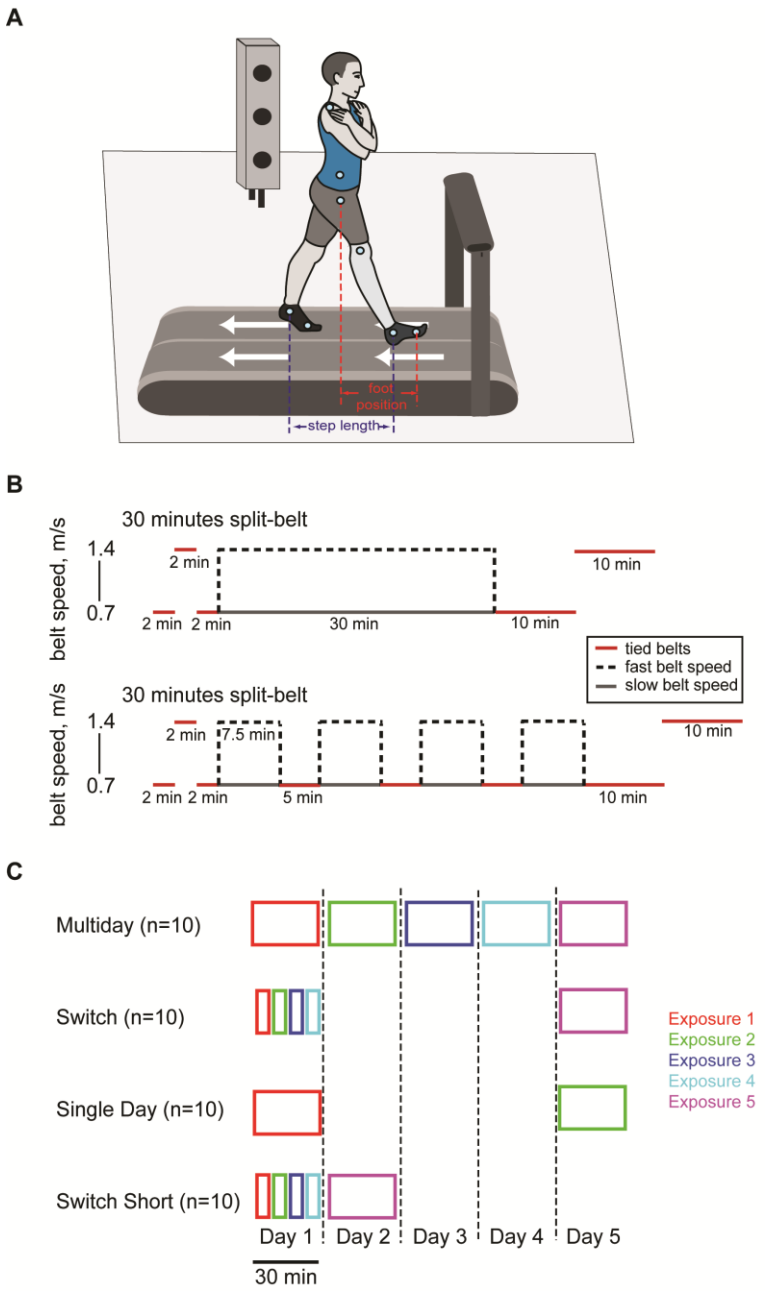

Figure 2.1 *Experimental paradigm.* **A)** General experimental setup in which participants walked with one foot on each independently controlled belt. Step length was calculated as the antero-posterior distance between ankle markers at heel strike. Foot position was calculated as the hip-centered antero-posterior coordinate of the toe marker. **B)** Experiment protocol diagrams for extended (top) and switch (bottom) training. Dashed and solid lines indicate the speeds of the fast and slow belt, respectively, while red solid lines indicate tied-belt walking. **C)** Split-belt exposure schedules for each condition. Each box indicates a separate split-belt adaptation block. The width of each box is proportional to the time spent walking with split-belts (i.e. a wide block denotes extended training, four abbreviated blocks denotes switch training). The colors of each exposure will remain consistent throughout subsequent figures.

2.2.4 Experimental paradigm

The goal of this study was to investigate how various perturbation schedules contribute to the accumulation of savings of a newly learned walking pattern over multiple days. To characterize this, participants were randomly assigned to one of four groups (n=10/group). The experimental paradigms are displayed in Figure 2.1B. All groups experienced the same baseline period in which they underwent tied belt walking for 2 min at 0.7 m/s, 2 min at 1.4 m/s, and then another 2 min at 0.7 m/s. The four groups differed in how the split-belt adaptation period was delivered over the multiday testing. Participants in the Multiday and Single Day groups were trained for 30 minutes of split-belt walking per day (abrupt 2:1 split-belt perturbation). Their self-reported dominant leg was placed on the 'slow belt' set to 0.7 m/s while the non-dominant leg was placed on the 'fast belt' set to 1.4 m/s. This was followed by a de-adaptation period which consisted of 10 min of walking with both belts set to 0.7 m/s followed by 10 min of walking with both belts set to 1.4 m/s. The Multiday group performed this protocol on 5 consecutive days whereas the Single Day group performed it only on Day 1 and Day 5, with no training on intervening days (Figure 2.1C).

To determine whether we could reduce the total amount of training time but still attain similar savings as in the Multiday group, we studied a switch training paradigm. On Day 1 of training, participants in the Switch and Switch Short groups experienced 4 bouts of 7.5 min adaptation periods (30 minutes total adaptation). Like previous groups, the perturbation was a 2:1 split with the dominant leg placed on the 'slow belt' set to 0.7 m/s and the non-dominant leg placed on the 'fast belt' set to 1.4 m/s. The four periods of adaptation were interleaved with 5 min de-adaptation blocks in which participants

experienced tied belts set to 0.7 m/s. The baseline periods and final de-adaptation blocks were identical across all 4 groups. After Day 1 switch training, we assessed learning in the Switch group on Day 5 with no training on intervening days, and in the Switch Short group on Day 2. These retests followed the same extended split-belt training paradigm (30 consecutive minutes of split-belt adaptation) as described above for the Multiday and Single Day groups. Importantly, the test paradigm to assess the effects of prior training was identical for all four groups (i.e. Day 5 for Multiday, Single Day, Switch; Day 2 for Switch Short).

2.2.5 Data analysis

The primary outcome measure used to quantify adaptation during split-belt walking was step length asymmetry. Step length asymmetry (SLA) was calculated by normalizing the difference in bilateral step lengths (SLF = fast belt step length, SLS = slow belt step length) to their sum:

$$\mathrm{SLA} = \frac{\mathrm{SLF} - \mathrm{SLS}}{\mathrm{SLF} + \mathrm{SLS}}$$

A step length asymmetry of zero therefore represents ‘perfect’ symmetry, while a positive step length asymmetry value indicates the right leg took a larger step than the left leg, and vice versa for negative values. During treadmill walking, step length was calculated as the antero-posterior distance between the ankle markers at heel-strike (Figure 2.1A). The heel strike and toe off events were determined using a custom Matlab program that extracted the gait events from the kinematic data. We targeted step length asymmetry for this experiment for two primary reasons. First, it is a parameter that has been shown to adapt during split-belt walking and results in aftereffects when the belts

are returned to the same speed[14]. Second, this normalized parameter allows us to fairly compare individuals of different height and stride length.

The rate of learning throughout the experiment was determined by measuring the step length asymmetry over key time periods in the experiment. For example, the size of the initial perturbation of each subject was defined as the average step length asymmetry of strides 1-5 during adaptation. Early change was defined as the average step length asymmetry of strides 6-30 during adaptation. Measuring the early change on different days allows us to determine the amount of savings from day to day and provides a measure of the rate of learning without assuming any stride-dependent relationship (i.e. exponential, double exponential) on step length asymmetry. The same trial epochs were used to quantify changes in unlearning during de-adaptation.

We know that step length asymmetry can result from differences in spatial control (i.e. where we place our feet), temporal control (i.e. the timing between foot-strikes), or the externally applied perturbation[29]. A model formulated by Finley et al. allowed us to separate the gait kinematics into spatial, temporal, and perturbation contributions to step length difference so that we could analyze how these features develop over exposures to the split-belt perturbation[29]. Similar to step length asymmetry, we use the early change epoch (strides 6-30) to quantify savings of each of these features across multiple exposures to the split-belt treadmill.

Finally, we investigated what spatial features of gait were being saved from one training session to the next using foot position and velocity. Foot position was defined as the hip-centered antero-posterior coordinate of the toe marker (Figure 2.1A). Thus, foot position was zero when directly below the hip marker, positive when the toe marker was

ahead of the hip marker and negative when the toe marker was behind the hip marker during the gait cycle.

2.2.6 Descriptive modeling of savings over multiple days

Several studies have aimed to derive computational models for savings in motor adaptation tasks. Of particular prevalence is the dual-rate state space model (SSM), composed of two linearly-independent hidden states that combine to give the total motor output[66]. These states are comprised of a fast state that learns quickly from error but is not retained well and a slow state that learns slowly from error but has high retention. Importantly, such a dual-rate SSM with time-invariant parameters cannot explain savings after prolonged washout, in which the hidden states have decayed to baseline values[70]. When modeling savings in locomotor adaptation, Mawase et al. demonstrated that a change in the learning parameters following initial learning can best explain savings observed during 2 within-day blocks of adaptive learning[34]. Within this framework, not only are the motor states updating trial by trial, but the learning parameters that govern the state updating rules are also updating with prior experience to the perturbation. Here, we apply this model to observe how learning parameters vary over multiple exposures to a split-belt perturbation over multiple days. The equations of the model are as follows:

$$x(n) = x_f(n) + x_s(n)$$

$$e(n) = p(n) - x(n)$$

$$x_f(n+1) = A_f(i) * x_f(n) + B_f(i) * e(n)$$

$$x_s(n+1) = A_s(i) * x_s(n) + B_s(i) * e(n)$$

$$0 < A_f(i) < A_s(i) < 1, \quad 0 < B_s(i) < B_f(i) < 1$$

On any trial n, x is the motor output, p is the external perturbation (0 for tied-belts, 1 for split-belts), and e is the error. The total motor output x is divided into a fast component, $x_{f,}$ and slow component, x_s. Each of these components updates trial-by-trial with a retention factor, A(i), and a learning factor, B(i). These retention and learning factors vary across exposure i to the split-belt perturbation.

We fit the model to individual symmetry change data[46]. Transforming step length asymmetry to symmetry change allowed us to convert our error signal (i.e. asymmetry) to a motor output form, which gradually updates in the presence of a perturbation and gradually returns to baseline from the adapted state once the perturbation is removed. We calculated symmetry change by shifting and normalizing step length asymmetry by each participant's maximal asymmetry during the adaptation block on exposure 1. That is, symmetry change data during adaptation is a measure between 0 and 1, where 0 indicates that symmetry is maximally perturbed and 1 indicates that symmetry has been restored. The converse applies to the de-adaptation block. As such, x(n) denotes what proportion of the perturbation p(n) has been restored on a given trial. We determined the parameters for individual subjects on each exposure by simultaneously fitting the entirety of adaptation and de-adaptation blocks.

2.2.7 Statistical analysis

To confirm there were no differences in baseline performance across groups, we ran one-way ANOVA of baseline step length asymmetry. Further, we performed one sample t-tests to confirm that the participants walked symmetrically (i.e. did not perform significantly differently from zero step length asymmetry). To measure if baseline performance or initial perturbation differed across days within a single group, we ran

repeated measures ANOVA and compared pairwise differences across days while correcting for multiple comparisons. To measure the rate of adaptation and de-adaptation, we used step length asymmetry during early change (strides 6-30). We performed a series of repeated-measures ANOVAs to observe any main exposure effects on early change measures in each group across exposures to the split-belt perturbation. Post-hoc analyses using the Studentized Range distribution (i.e. Tukey's test) to correct for multiple comparisons revealed any pairwise differences in savings between any two adaptation blocks. Repeated-measure ANOVAs were used throughout to assess main effect of exposure on our measures of learning (e.g. early change step length asymmetry, temporal/spatial contributions, fitted SSM parameters, etc.).

We used correlation analysis to determine the relationship between specific kinematic parameters within the gait cycle (e.g. heel strike/toe off position) and the rate of step length asymmetry adaptation. Correlation analyses were also used to help explain which parameters in the dual-rate SSM best explained our observed savings across days. Additionally, repeated-measures ANOVA were performed to investigate effects of exposure on heel strike/toe off locations as well as dual-rate SSM parameters. The α-level for all analyses was set at 0.05.

We were interested in how varying the training structure from Day 1 to Day 4 of training would influence savings on the testing day (i.e. Day 5). We performed a one-way ANOVA with the Day 5 step length asymmetry during early change of Multiday, Switch, and Single Day to measure a group effect of savings. We performed post-hoc analysis with Tukey's HSD correction for multiple comparisons to observe difference between any two groups. We used an independent sample t-test to confirm the time-decay

resistance of savings following extended split-belt training. To test for the time-decay resistance of savings following switch training, we used a similar independent sample t-test to compare exposure 5 step length asymmetry values. Additionally, we performed a mixed-design, repeated-measures ANOVA with group and exposure as factors to observe if savings differentially decayed between training and testing. For all repeated-measures ANOVA, we performed Mauchly's test of sphericity and used the Greenhouse-Geisser correction of degrees of freedom if sphericity was violated. All analyses were performed using SPSS 24.0 (IBM, Armonk, NY) and α-level was set at 0.05. All data are reported as mean ± standard error (SE).

2.3 Results

2.3.1 Multiday savings

In this experiment, we sought to determine how savings of a novel walking pattern developed over multiple days of training (30 minutes each day for 5 days; Figure 2.1C, top row), and how different kinematic components of the gait cycle contributed to savings. Figure 2.2A shows group data from this experiment. Day 1 baseline asymmetry (red) did not differ from zero (t_9=0.04, p=0.972), indicating participants walked symmetrically on the treadmill when belts were tied. Furthermore, baseline step length asymmetry on subsequent days did not differ from Day 1 baseline performance (all p>0.25), demonstrating that subjects were fully washed out from training on the prior day. Day 1 adaptation (red) showed the typical initial perturbation and learning curve, so that by the end of adaptation subjects showed near zero step length asymmetry. Day 1 de-adaptation showed the expected large aftereffect and subsequent error reduction, which eventually returned to baseline performance.

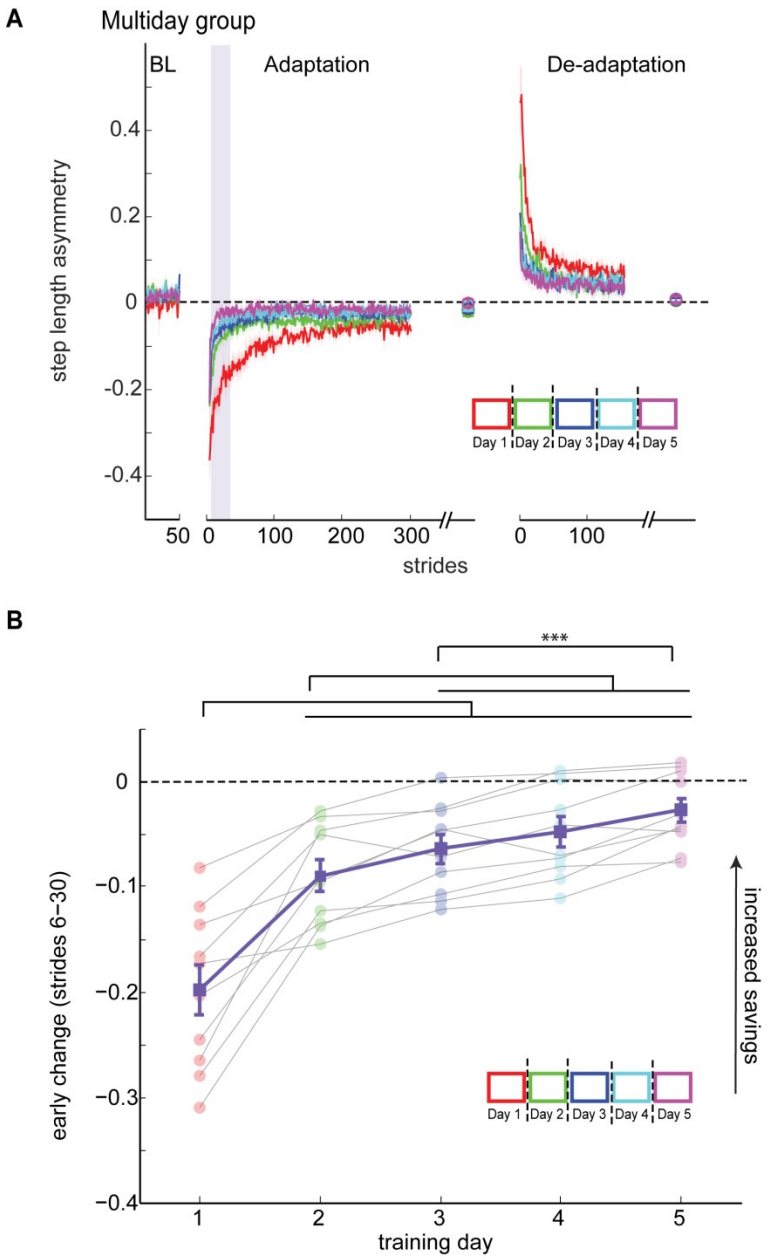

Figure 2.2 *Savings of locomotor adaptation over 5 days of training*. **A)** Comparison of step length asymmetry across all exposures for the Multiday group. Mean curves across participants denote mean ± SE. Baseline (BL; last 50 strides), adaptation, and de-adaptation mean curves are shown. Data points following adaptation and de-adaptation curves indicate mean plateau values (mean ± SE of last 50 strides) for each block. **B)** Early change step length asymmetry (mean ± SE of strides 6-30; shaded region in panel A) across all exposures of the Multiday group displayed in purple. Individual participant data is grayed in behind group mean with color indicating exposure number. *** denotes a significant difference between early change values with alpha-level set to 0.05 as determined by repeated-measures ANOVA, corrected for multiple comparisons.

Subject performance on the first stride during adaptation remained consistent across days (repeated-measures ANOVA; $F_{1.99, 17.92}$=1.54, p=0.242). However, performance on Days 2-5 showed progressively smaller step length asymmetry during the initial perturbation epoch (strides 1-5; $F_{2.00, 18.04}$=18.41, p<0.001) despite the fact that the split-belt parameters remained consistent across days. This is due to subjects' ability to more rapidly compensate for the treadmill perturbation within early strides (each stride takes ~ 1 second which allows for feedback control to partially change the walking pattern). Learning is more rapid in Days 2-5 compared to Day 1 and then reaches the same level at the end of adaptation. De-adaptation followed a similar pattern across days, with smaller aftereffects and a faster rate of unlearning.

Figure 2.2B shows our primary measure of savings across days (step length asymmetry during early change: mean of strides 6 to 30) for the entire Multiday group overlaid on individual subject performance. A decrease in mean asymmetry during early change suggests a faster rate of error reduction (i.e. savings). Our analysis revealed that savings increased across days ($F_{1.29,11.59}$=36.51, p<0.001) as participants performed extended split-belt training on five consecutive days. Participants reached the same level of learning at plateau in each of the days ($F_{4,36}$=2.19, p=0.090), indicating that while they learned at a faster rate from one day to the next, participants consistently reduced their errors to the same extent by the end of training on each day.

Following adaptation to the split-belt environment, the belts returned to the same speed to evaluate the presence of an aftereffect. The Multiday group showed a significant aftereffect on Day 1 (initial perturbation epoch; t_9=9.56, p<0.001). Similar to the savings demonstrated with learning to walk symmetrically in the split-belt environment, we also

found savings in un-learning when the belts were tied back to the same speeds. Analysis of the early change epoch revealed that participants reduced their error at a faster rate across successive days of training during de-adaptation ($F_{4,36}$=23.44, p<0.001). We focused the remainder of our analyses on the kinematic data during the adaptation block because we found the magnitude and rate of learning and unlearning to be similar. Specifically, a mixed methods repeated-measures ANOVA comparing absolute magnitude of early change in step length asymmetry during adaptation and de-adaptation blocks revealed no significant main effect of block ($F_{1,9}$=0.795, p=0.396) or block-exposure interaction ($F_{1.56, 14.06}$=1.88, p=0.192). This indicates savings in both adaptation and de-adaptation showed similar magnitude and time-course across days.

2.3.2 Spatiotemporal analysis

Spatial (i.e. where we step) or temporal (i.e. when we step) features of gait both contribute to step length asymmetry while walking on a split-belt treadmill[29,31]. We were interested in understanding how these spatial and temporal contributions changed across days as participants minimized their errors more quickly. As detailed in the Methods, we separated step length difference into spatial, temporal, and perturbation components[29]. Figure 2.3A displays each component during the adaptation block for each of the training days. Figure 2.3B shows the proportion of the perturbation corrected for by the spatial and temporal components during the early change epoch. Subjects showed savings in both the spatial and temporal contributions to step length difference: repeated measures ANOVA revealed a significant main effect of Exposure on proportion corrected for step length difference ($F_{1.47, 13.19}$=31.93, p<0.001), the spatial contribution ($F_{1.49, 13.37}$=17.10, p<0.001) and the temporal contribution ($F_{4, 36}$=11.65, p<0.001), with spatial providing a

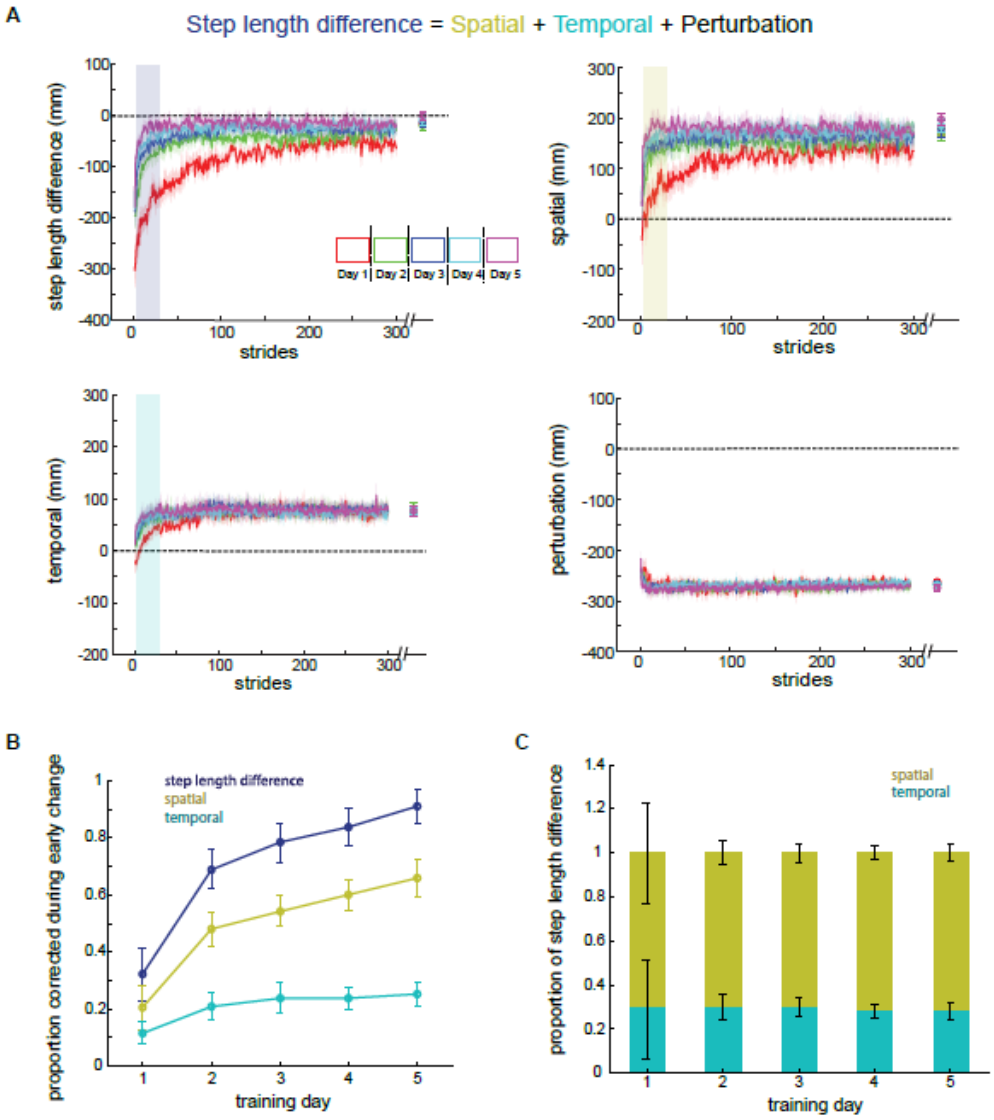

Figure 2.3 *Spatial and temporal contributions to step length difference over 5 days of training*. **A)** Comparison of motor adaptation parameters (step length difference, spatial contribution, temporal contribution, perturbation) across exposures in the Multiday group. Mean curves during adaptation are shown. Data points following the curves represent the mean plateau values during each exposure. All data are shown as mean ± SE. **B)** Proportion of the perturbation corrected for by step length difference, spatial contribution, and temporal components during the early change epoch (stride 6-30; shaded region in panel A) across training days. Note participants were able to reduce early change step length difference (i.e. error) across training days. **C)** Contribution of spatial (gold) and temporal (teal) features to step length difference across training days. Note that the spatial and temporal components scale equally with the reduction of step length difference. All error bars denote SE.

greater contribution than temporal ($F_{1,9}$=18.60, p=0.002). We performed further analysis to determine how the spatial and temporal components contributed to the corrected step length difference during the early change epoch. To do this, we normalized each participant's proportion corrected spatial and temporal contribution by the step length difference proportion corrected. Figure 2.3C demonstrates that although participants are able to correct a larger proportion of the perturbation, the proportion of spatial and temporal contributions scaled equally across days (approx. 70 and 30 percent, respectively). Repeated-measures ANOVA revealed no significant main effect of Exposure for either spatial or temporal proportion of step length difference ($F_{1.06, 9.58}$=0.01, p=0.940 and $F_{1.06, 9.56}$=0.01, p=0.945 respectively). In sum, the spatial and temporal components scale equally with savings of step length difference across days.

Since the spatial domain drives a majority (approx. 70 percent) of the correction in step length difference across days, we next analyzed specific spatial features of gait to observe what was saved across days. While the spatial contribution described above is an interlimb measure, we wanted to know how each leg's kinematics contributed to savings across days. Figure 2.4A displays the kinematic features in phase plane space (antero-posterior foot position and velocity) of an average gait cycle for each leg during the early change epoch of the adaptation block. Note that time is not represented in this phase plane space. Heel strike and toe off position were calculated as the maximum and minimum foot position of each leg relative to the hip. A full gait cycle (i.e. stride) on the split-belt treadmill is composed of two steps—one step when the leg on the fast belt leads and one step when the leg on the slow belt leads. Positive foot velocity indicates forward motion (i.e. swing) and negative foot velocity indicates backward motion (i.e. stance).

Heel strike and toe off locations occur approximately where foot velocity is zero. The leg cycles from stance to swing in a clockwise motion around this phase plane. Note that the overall shape of the trajectory for either leg is generally similar across days, though specific points change in a systematic manner.

We investigated which portion of the stride contributed to savings over days by investigating whether heel strike or toe off locations correlate with step length asymmetry savings. We found that the fast heel strike and slow toe off locations were most important to savings. This was tested by correlating matrices containing step length asymmetry and heel strike/toe off locations for the early change epoch (strides 6-30) across days. Separate analyses were done for these foot locations when the fast leg led (Figure 2.4A, squares) vs. when the slow leg led (circles). These locations are displayed schematically in treadmill space in the bottom half of Figure 2.4A. Our results indicate that the locations of heel strike and toe off when the fast leg leads significantly correlate with step length asymmetry ($r=0.81$, $p<0.001$; $r=-0.65$, $p<0.001$, respectively). That is, as participants adapted faster across days, the fast leg stepped further forward ($F_{4,36}=15.35$, $p<0.001$) and slow limb trailed further backward ($F_{4,36}=9.51$, $p<0.001$; Figure 2.4B, left). Conversely, the locations of slow leg heel strike and fast leg toe off did not correlate with step length asymmetry ($r=0.26$, $p=0.073$; $r=0.05$, $p=0.730$, respectively) across training days, and did not show a progressive change from day to day (Figure 2.4B, right). While ANOVA revealed a significant main effect of Exposure on slow limb heel strike location ($F_{4, 36}=3.19$, $p=0.024$, Figure 2.4B, right), this main effect was not a product of a progressive change in slow heel strike location from day to day. This measure did not change systematically with training day, as shown by a non-significant within-subjects

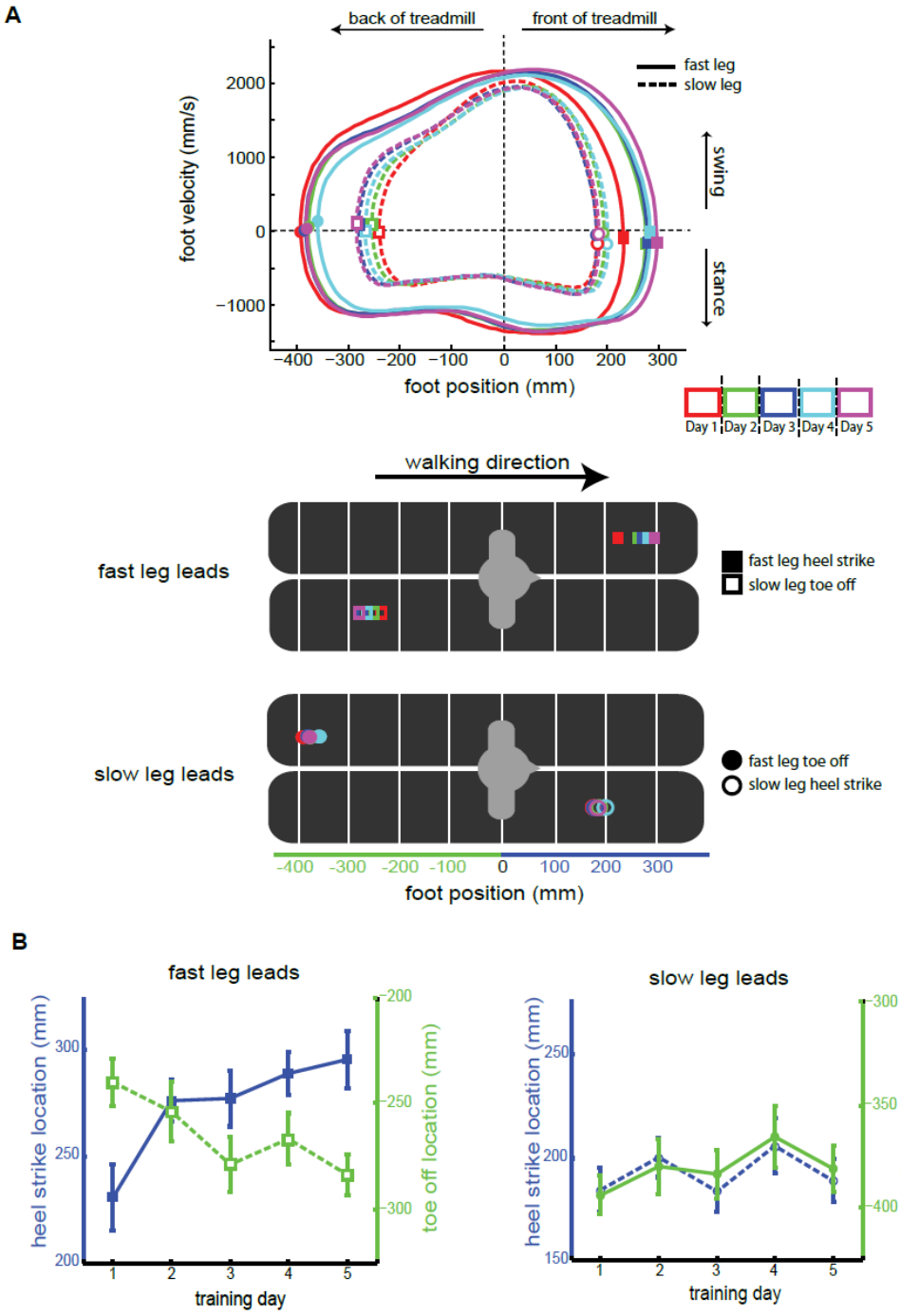

Figure 2.4 *Kinematic analysis of the Multiday group during the early change epoch of adaptation.* **A)** Average kinematics in phase plane (top) and treadmill (bottom) space. Phase plane plots average antero-posterior foot position and velocity during early change. Colors represent the exposure number shown in the split-belt schedule block diagram. Solid lines indicate the foot walking on the fast belt while dashed lines indicate the foot walking on the slow belt. Heel strike and toe off locations when the fast leg leads are marked with closed and open squares, respectively. Heel strike and toe off locations when the slow leg leads are marked with closed and open circles, respectively. The

treadmill schematic displays the progression of heel strike and toe off position across exposures. Fast heel strike (top row) denotes the portion of the gait cycle when the fast leg leads while slow heel strike (bottom row) denotes the portion of the gait cycle when the slow leg leads. Symbols and colors are consistent with the phase plane **B)** Summary plots of heel strike (blue lines; mean ± SE) and toe off positions (green lines; mean ± SE) during the early change epoch on each training day. Solid lines/closed points indicate the foot walking on the fast belt while dashed lines/open points indicate the foot walking on the slow belt. Note the change in heel strike and toe off locations during fast heel strike (left panel), indicating savings is a result of participants learning to take longer steps early on in adaptation when the fast legs leads.

linear contrast of days ($F_{1, 9}$=1.49, p=0.253). In total, these results demonstrate that savings from one day to the next is due to participants learning to take longer steps when the fast leg leads (via the fast leg stepping farther forward and the slow leg toeing off farther back).

While participants learned to take longer steps when the fast leg led from one day to the next, the velocity profile of their movement for either leg did not change significantly from day to day. ANOVA of maximum swing velocity during the early change epoch of adaptation revealed no significant main effect of Exposure for either the fast leg ($F_{4, 36}$=0.56, p=0.696) or the slow leg ($F_{1.87, 16.82}$=2.94, p=0.083). Because participants learned to take longer steps when the fast leg leads and swung their fast foot at equivalent rates across days, we can conclude that participants learned to spend increasing amounts of time in stance on the slow belt across days. This increased time spent standing on the slow belt allows for the fast leg to extend further out for heel strike and the slow leg to be pulled further back by the treadmill belts prior to toe off, thus normalizing step length asymmetry.

2.3.3 Effect of training structure on savings

We next investigated whether compressed training schedules could produce comparable savings to the Multiday group. Participants within the Switch group experienced four short bouts of split-belt adaptation on Day 1 and then returned on Day 5 to test for savings (Figure 2.1C). We also tested a Single Day group to observe whether switch training provided additional benefit over extended training while controlling for the four days between training and testing. Participants within the Single Day group experienced extended training on Day 1 and then returned on Day 5 to test for savings.

Note that regardless of the training structure, all participants experienced 30 total minutes of split-belt walking each day.

Figure 2.5 displays the group mean learning curves for the Switch (Figure 2.5A) and Single Day groups (Figure 2.5B). Naïve performance (i.e. Exposure 1, red) for either group did not differ from Day 1 of the Multiday group. Our analysis revealed no group differences in naïve performance across baseline values ($F_{2, 27}$=0.81, p=0.456), initial perturbation ($F_{2, 27}$=1.54, p=0.233), early change step length asymmetry ($F_{2,27}$=0.77, p=0.473), or aftereffect magnitude ($F_{2,27}$=1.58, p=0.224). Thus, similar to the Multiday group, participants in the Switch and Single Day groups showed typical adaptation behavior on Exposure 1; they walked symmetrically when belts were tied at baseline, experienced perturbed asymmetry when the belts were split, reduced their error during the course of the adaptation block and showed significant aftereffects during the de-adaptation block.

The Switch and Single Day groups both showed significant savings across subsequent exposures to the split-belt perturbation. Figure 2.5 displays the group mean of early change step length asymmetry overlaid on individual subject performance across exposures for Switch (Figure 2.5C) and Single Day groups (Figure 2.5D). Participants within the Switch group showed a significant main effect of Exposure on the early change measure ($F_{2.14,19.22}$=35.99, p<0.001), indicating that participants learned at a faster rate from one exposure of the split-belt perturbation to the next. Next, a comparison of early change on Day 1 to that of Day 5 in Single Day, revealed less step length asymmetry during early change on Day 5 ($F_{1,9}$=38.46, p<0.001), indicating significant savings following a single day of extended split-belt training.

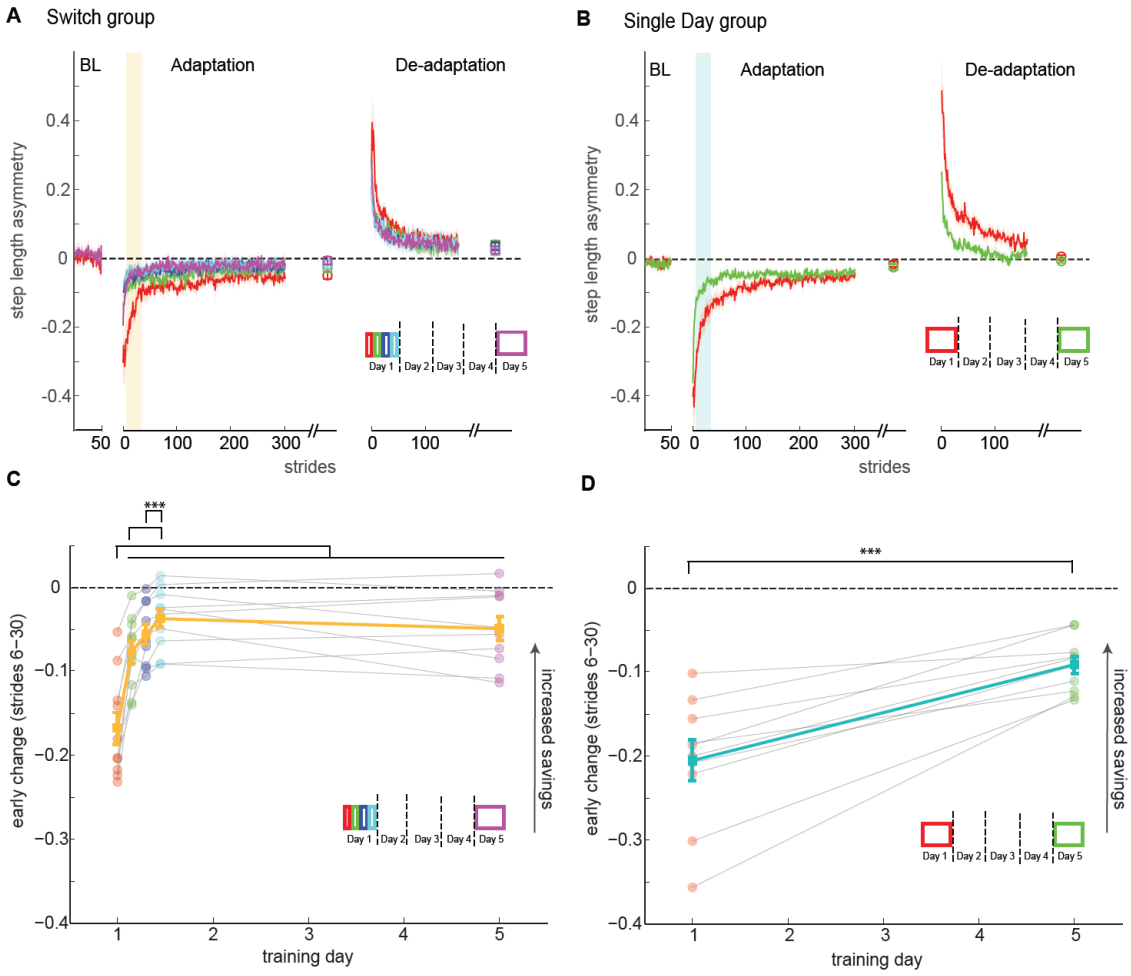

Figure 2.5 *Savings of locomotor adaptation over 5 training days using compressed training schedules*. **A)** Comparison of step length asymmetry across all exposures for the Switch group. Mean curves across participants denote mean ± SE. Baseline (BL; last 50 strides), adaptation (first 300 strides), and de-adaptation (first 150 strides) mean curves are shown. Data points following adaptation and de-adaptation curves indicate mean plateau values (mean ± SE of last 50 strides) for each block. **B)** Comparison of step length asymmetry across exposures for the Single Day group **C)** Summary of early change step length asymmetry (mean ± SE of strides 6-30; shaded region in panel A) across all exposures of the Switch group displayed in orange. Individual participant data are grayed in behind group mean with color indicating exposure number. **D)** Summary of early change step length asymmetry (mean ± SE of strides 6-30; shaded region in panel B) for the Single Day group. *** denotes significant difference between early change values with alpha-level set to 0.05 as determined by repeated-measures ANOVA, corrected for multiple comparisons when appropriate.

Next, we were interested in understanding how savings varied across groups on our test day (i.e. Day 5). Figure 2.6A displays Day 5 performance during the adaptation block for Multiday (purple), Switch (orange), and Single Day (teal) groups. Figure 2.6B displays how savings evolves across exposures for each group. Our measure of interest was early change step length asymmetry on our test day (i.e. Day 5) to observe whether training schedule influenced participants' ability to save over this time-span. A one-way ANOVA comparing step length asymmetry during early change on Day 5 for all three groups revealed a significant main effect of Group ($F_{2, 27}$=7.27, p=0.003). Post-hoc analysis with Tukey's HSD correction for multiple comparisons revealed greater savings in the Multiday and Switch groups on Day 5 compared to the Single Day group (p=0.002 and p=0.050, respectively) while Multiday and Switch experienced similar savings on Day 5 of testing (p=0.422). Notably, this Group effect ($F_{2, 27}$=13.78, p>0.0001) and post-hoc comparisons hold for the initial perturbation epoch (strides 1-5) of Day 5 adaptation as well (Figure 2.6A, inset).

Importantly, all groups were equally perturbed (i.e. Day 1 first stride; $F_{2, 27}$=0.66, p=0.523) and learned at the same rate when they were naïve to the split-belt perturbation (i.e. Day 1 early change; $F_{2,27}$=0.77, p=0.473). Additionally, analysis of step length asymmetry during the first stride of Day 5 adaptation revealed no difference in performance across conditions (one-way ANOVA; $F_{2, 27}$=3.16, p=0.058; see Figure 2.6A inset). Therefore, switch training provides a significant boost in savings over a 5-day span compared to a single day of extended training. Moreover, switch training can result in similar savings to that achieved over four consecutive days of training with just a quarter of the training load.

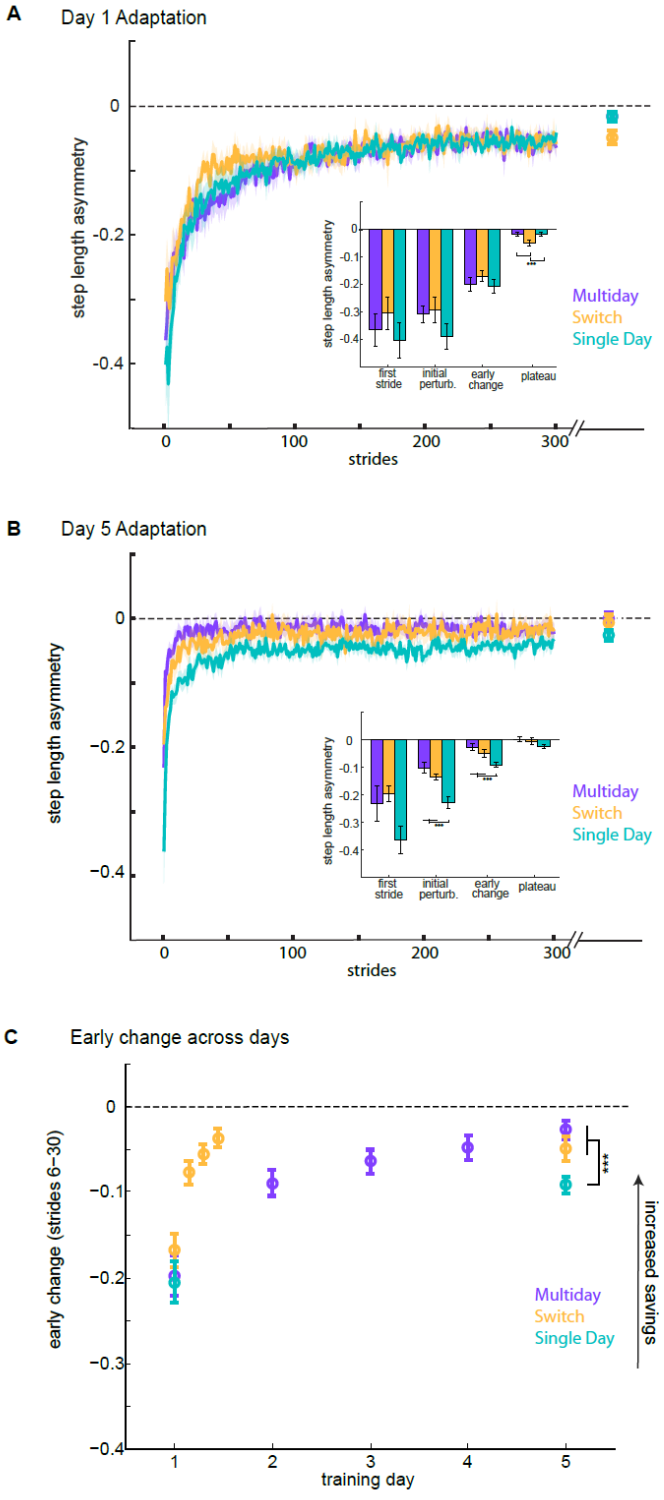

Figure 2.6 *Effects of training structure on savings over a 5-day span*. A) Comparison of step length asymmetry on Day 5 of training for Multiday, Switch, and Single Day groups. Mean curves during the adaptation block (strides 1-300) are shown. Data points following the curves represent the mean plateau values (last 50 strides) for each group.

The inset figure displays a summary of first stride, initial perturbation, early change, and plateau step length asymmetry across groups. B) Summary of early change (strides 6-30) step length asymmetry across all exposures for Multiday, Switch, and Single Day groups. Note the difference in savings between groups on Day 5 of training. The Switch group attains comparable savings as the Multiday group, despite having a quarter of the training time while both the Switch and Multiday group display greater savings than the Single Day group. *** denotes significant difference between early change values with alpha-level set to 0.05 as determined by one-way ANOVA, corrected for multiple comparisons.

To confirm that the Switch group learned a similar movement pattern over the course of training, we performed a similar kinematic analysis as we did in the Multiday group. That is, we compared the spatial and temporal components of gait[29] to ensure the integrity of the movement was maintained across training conditions. Indeed, in Day 5 of testing, Multiday and Switch had similar contributions from the spatial (t_{18}=0.90, p=0.381) and temporal (t_{18}=0.67, p=0.510) components to counteract the split-belt treadmill perturbation. Moreover, the proportions of spatial and temporal components toward the step length difference on Day 5 were equivalent in both groups (t_{18}=0.07, p=0.946; approx. 70 % spatial, 30 % temporal) indicating that the learned movement in Switch shared similar spatiotemporal characteristics to those observed in the Multiday group on Day 5 of training.

2.3.4 Time-resistance of savings

We observed similar savings in the Single Day group tested with a 4-day lag compared to that of the Multiday group on Day 2 with a 1-day lag (t_{18}=0.121, p=0.905; compare teal Day 5 to purple Day 2 in Figure 2.6B). Recall that in both of these groups Day 1 training structure was the same 30 minutes of split-belt walking. This comparison is important because it shows that this training protocol is resistant to time-decay over multiple days.

To observe if the time-resistance of savings was sensitive to the structure of training, we studied a new Switch Short group. The Switch Short group experienced four short bouts of split-belt adaptation on Day 1, and then returned on Day 2 to test savings (Figure 2.1C, bottom row). Figure 2.7A displays the Switch Short adaptation behavior and Figure 2.7B shows the early change in step length asymmetry. Similar to previous

groups, Switch Short showed a significant main effect of Exposure across five exposures to the split-belt perturbation on step length asymmetry during the early change epoch ($F_{1.77, 15.88}$=45.64, p<0.001; Figure 2.7B), indicating increasing savings from one exposure to the next.

We then compared the fifth exposure in Switch Short (collected on Day 2) to the fifth exposure of Switch (collected on Day 5) to observe the effects of additional days away from the lab on savings following a switch-training protocol (compare Figures 2.6 and 2.7). We found no significant difference in measures of savings between groups (t_{18}=-1.044, p=0.310), indicating that savings is also resistant to time-decay over multiple days following switch-training on Day 1. Analysis of exposure 4 and exposure 5 of Switch Short and Switch via a mixed-design, repeated-measures ANOVA yielded no significant main effects of Exposure ($F_{1, 18}$=1.49, p=0.238) or Group ($F_{1, 18}$=1.81, p=0.195, Figure 2.7B, inset) and no Exposure-Group interaction ($F_{1, 18}$=0.35, p=0.562). Additionally, early change differences between exposure 4 and exposure 5 in both Switch Short and Switch were not different from zero (t_9=-0.47, p=0.649 and t_9=-1.22, p=0.255 respectively). Our analysis shows both groups saved to a similar extent while the time between training and testing had no effect on the degree of savings we observed on our testing day (i.e. Day 2 or Day 5). Moreover, negligible savings were lost between training and testing for both groups.

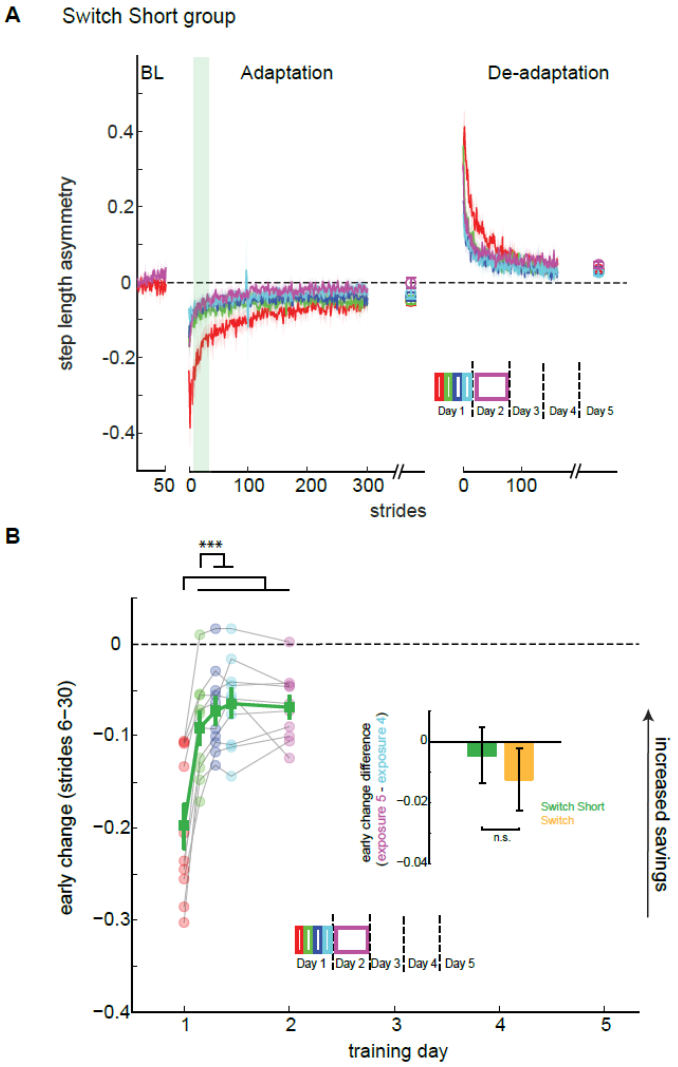

Figure 2.7 *Savings of locomotor adaptation for Switch Short group.* **A)** Comparison of step length asymmetry across all exposures for the Switch Short group. Mean curves across participants denote mean ± SE. Baseline (BL; last 50 strides), adaptation (first 300 strides), and de-adaptation (first 150 strides) mean curves are shown. Data points following adaptation and de-adaptation curves indicate mean plateau values (mean ± SE of last 50 strides) for each block. **B)** Summary of early change step length asymmetry (mean ± SE of strides 6-30; shaded region in panel A) across all exposures of the Switch Short group displayed in dark green. Individual participant data are grayed in behind group mean with color indicating exposure number. *** denotes significant difference between early change values with alpha-level set to 0.05 as determined by repeated-measures ANOVA, corrected for multiple comparisons. The inset figure displays the difference in early change step length asymmetry from exposure 4 to exposure 5, indicating savings following switch training is resistant to decay on this timescale. Note there is no savings lost for either the Switch or Switch Short group. n.s. denotes a non-significant difference as determined by mixed-design, repeated-measures ANOVA.

2.3.5 Dual-rate state space model of savings over multiple days

We used a dual-rate state space model to understand how savings developed in the Multiday group—did savings result from improved retention of what had been learned or faster relearning driven by increased sensitivity to error? We used a dual-rate state space model with time varying parameters similar to that used by Mawase et al. (2014)[34]. To observe how the model parameters evolved over subsequent exposures to a split-belt perturbation, we fit the four parameters (A_f, B_f, A_s, B_s) to individual participant symmetry change data for each day of split-belt learning and unlearning within the Multiday group. Conversion of step length asymmetry to symmetry change is displayed in Figure 2.8A and detailed in Methods. The fast state, which updates based on retention factor A_f and learning factor B_f, is characterized by a rapid learning rate and weak retention. The slow state, which updates based on retention factor A_s and learning factor B_s, is characterized by a slow learning rate and strong retention. Figure 2.8B summarizes the fitted parameter values across days for the Multiday group.

Our analysis showed that multiday savings was largely due to increased sensitivity to error in the fast state (i.e. B_f). Specifically, a repeated-measures ANOVA revealed no significant main effects of Exposure on A_f ($F_{1.65,14.86}$=2.27, p=0.144), As ($F_{1.16, 10.45}$=1.21, p=0.307), or B_s ($F_{1.21, 10.88}$=4.54, p=0.051). Meanwhile, ANOVA revealed a significant Exposure effect on B_f ($F_{4, 36}$=32.36, p<0.001). B_f increased from 0.091 ± 0.027 on Day 1 to 0.655 ± 0.053 on Day 5 (comparison of Day 1 to Day 5 fits in Figure 2.8C). Post hoc analysis on B_f revealed significant pairwise differences between Day 1 values and the values of Days 2-5 (all p<0.025). Furthermore, correlational analysis reveals B_f has the strongest correlation (r=0.70) with early change of step length

asymmetry (i.e. our measure of savings) compared to A_f, A_s, and B_s ($r = -0.09$, 0.07, and 0.37, respectively). These results suggest that the increase in B_f values can best explain the observed savings in the symmetry change data.

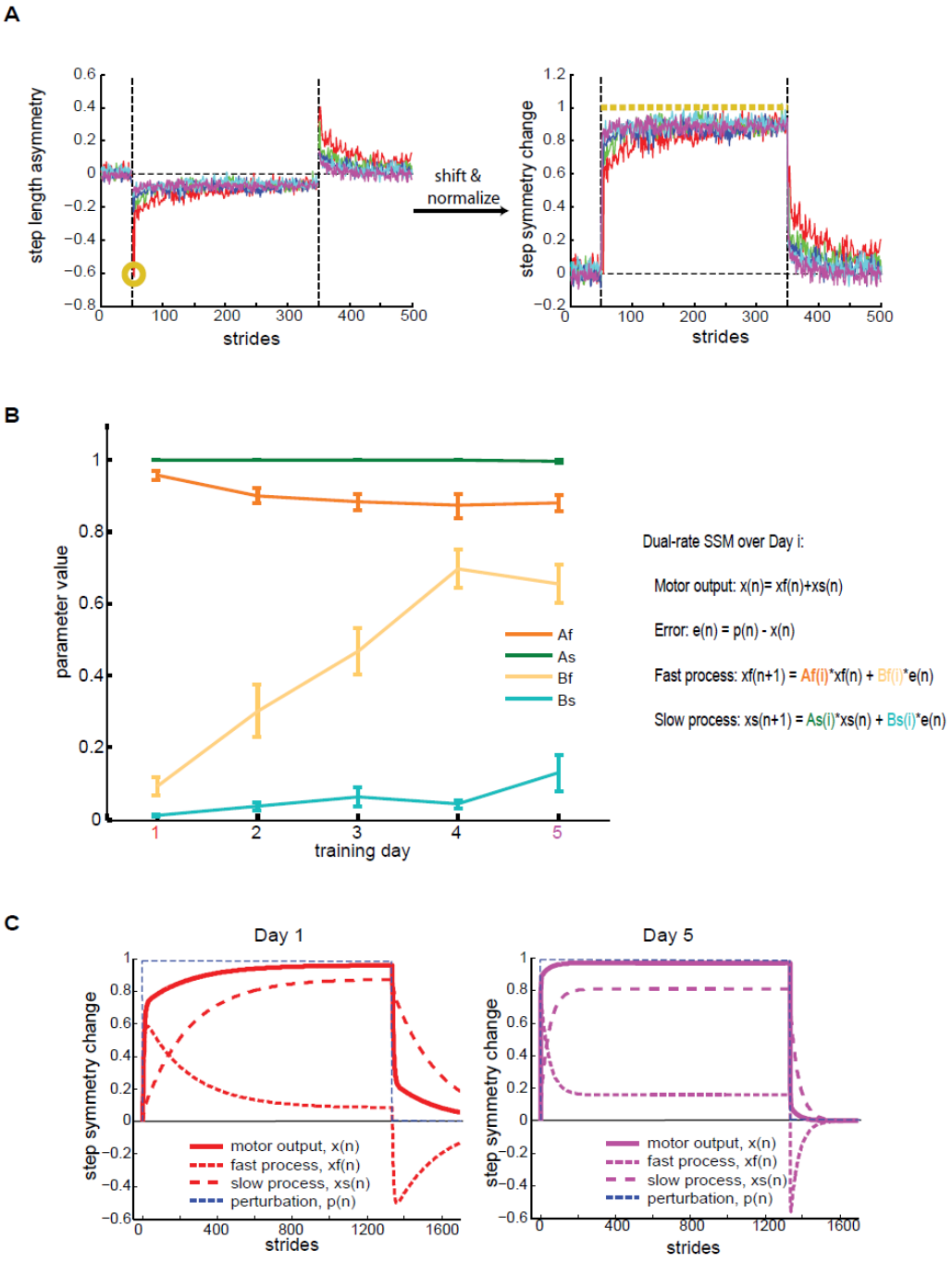

Figure 2.8 *Modeling savings in the Multiday group with a dual-rate state space model.* **A)** Conversion of step length asymmetry to step symmetry change for a representative subject. Individual step length asymmetry data (left) is shifted and normalized by the individual's maximal asymmetry during the adaptation block on exposure 1 (gold circle). Step symmetry change (right) is a measure where 0 indicates that symmetry is maximally perturbed and 1 (gold dashed line) indicates that symmetry has been restored during adaptation. **B)** Summary of dual-rate parameter values fitted to individual subjects across training days. A_f and B_f are the retention and learning factor for the fast process,

respectively. A_s and B_s are the retention and learning factor for the slow process, respectively. Each point represents mean ± SE. **C)** Comparison of model fits of step symmetry change on Day 1 (left) and Day 5 (right) for adaptation and de-adaptation to an abrupt perturbation using the mean parameters shown in (B) for the respective day. The motor output is calculated as the addition of the fast and slow processes.

2.4 Discussion

Learning a new movement pattern requires practice. For practice to be useful, it is crucial that we are able to remember what we learned from previous sessions. Whether learning a new golf swing or improving a dysfunctional gait pattern, training can be laborious and presents a significant time and financial burden. As such, coaches and clinicians often focus on how to get the greatest improvement in performance in the least amount of time. Here, we investigated how to manipulate the delivery of training of a novel walking pattern to increase the time efficiency of training.

We demonstrated that participants could learn a novel walking pattern over the course of five days such that they have minimal error when transitioning from novel (i.e. split-belt) to natural (i.e. tied-belt) environments. Participants achieved this level of learning via day-to-day savings such that they learned to counter the novel environment more rapidly across exposures. We also showed that we could induce similar savings by compressing a four day training regimen into a one day intervention with four abbreviated training exposures delivered in succession. Specifically, our Switch group displayed equivalent savings as our Multiday group despite having one quarter of the training time.

2.4.1 Multiday savings

This study aimed to determine how much savings could be induced during five consecutive days of split-belt training and what aspects of the motor pattern were being saved. Few studies have looked at multi-session savings of an adapted movement and most have focused on arm movements using visuomotor tasks[6,71,72]. Additionally, studies of savings during split-belt walking have been largely limited to just two exposures to the

training environment[34,35,72]. We were interested in how savings of a new walking pattern emerges on a longer timescale as split-belt training has proven to produce clinically meaningful improvements in pathological gait[45]. Interestingly, these lasting improvements were only observed following repeated practice[45] whereas effects following just one session of training quickly diminished[43]. Thus, a full understanding of the timescale of this learned pattern over repeated training sessions is needed to inform the most efficient and effective training of a novel walking pattern.

Our participants were able to save a substantial portion (approx. 85 percent; Figure 2.2B) of the split-belt adaptation task by Day 5 of training. Our analysis revealed that these savings accrued over days due to participants' ability to change both spatial (i.e. where they step) and temporal (i.e. when they step) elements of their gait pattern early on in the adaptation blocks. Globally, this allowed participants to more quickly increase the length of their steps when the fast leg led in order to counter the perturbation (i.e. step farther forward with the fast leg and trail farther back with the slow leg). These behavioral changes upon re-exposure reflect the nervous system's ability to retrieve a motor memory and adopt a set of kinematics best suited for a given environment.

From a clinical point of view, it is encouraging that people save both the spatial and temporal features of walking. Paretic gait in persons post-stroke has shown to be patient-specific, resulting from either deficits in spatial control, temporal control, or a combination of both[29,31]. Thus, the current work demonstrating that healthy individuals save both features bodes well for the possibility that stroke patients can do the same. It is important that the utility of multiday split-belt treadmill training is not limited to a subset

of patients, but has the potential to address all sources of paretic gait, regardless of whether the deficits are spatial or temporal.

Recent studies of reaching adaptation have suggested that savings is linked to conscious or strategic planning because it is abolished when preparation time is limited[68] and because savings can be accounted for by engaging an aiming strategy upon re-exposure[69]. Such findings are difficult to compare to savings in locomotor tasks because walking is a more automatic process and may not be as explicitly accessible as reaching. For example, we recently reported that the walking adaptation process is unaffected by explicit error correction[46]. Specifically, when subjects were given visual feedback of their stepping error, they could rapidly correct it. However, this correction was lost as soon as the feedback was removed and adaptation proceeded unaffected[46]. Thus, our interpretation is that locomotor adaptation operates in parallel to a more conscious correction process. Feedback of stepping error during adaptation also does not affect savings on a subsequent exposure to the split-belt perturbation[74]. Further, the current work demonstrates that savings of locomotor adaptation involves savings of temporal features of gait, which have previously been shown to be resistant to cognitive manipulations[30]. We therefore speculate that locomotor savings is less reliant on conscious or strategic processes compared to savings in reaching.

2.4.2 Improving the time efficiency of training

Our results indicate that we are able to shape the perturbation schedule to more efficiently train a novel walking pattern. By compressing training to four abbreviated bouts of adaptation, we induced similar savings to a training schedule consisting of four consecutive days of extended adaptation. Furthermore, one day of switch training

produced more savings than one day of extended training. Two factors have been previously shown to influence savings in locomotor tasks: 1) abrupt exposures to the adaptive environment and 2) time spent in the adapted state[35]. Here, we demonstrate that we can leverage these two factors to create a balance in our delivery of the perturbation that will more efficiently train the movement. That is, by maintaining the amount of abrupt exposures (i.e. four blocks) but reducing the total amount of time (i.e. reducing from four 30 minutes blocks to four 7.5 minute blocks), we did not lose any training effects when testing on Day 5, despite the reduced training time and the extended period between training and testing.

These results highlight the importance of early adaptation trials—and accompanying large errors—to the formation of a motor memory. Savings has been observed in both reaching and locomotor adaptation tasks as long as participants reach asymptotic performance during initial exposure[35,75]. Thus, experiencing a high frequency of these early adaptation trials (as did the Switch group) may strengthen the motor memory for subsequent exposures[36]. Although we aimed to control for the within-session time participants spend on split-belts (i.e. 30 minutes), it is feasible that with a higher frequency of switching in environments, we could reduce this within-session time and make training even more efficient. We anticipate, however, that decreasing the amount of time within a single adaptation block will eventually have diminishing or even counterproductive effects. Previous work suggests that repetition of the adapted movement at plateau is necessary for maximum savings[35,67]. Future work should aim at further characterizing this point of diminishing return.

It should be noted that savings during this locomotor task could be due to a combination of an immediate improvement in step symmetry within the first stride and a faster rate of improvement over subsequent strides. The present study reveals a trending difference ($p=0.058$) in first stride performance across training conditions. Considering that all training conditions were fully washed out prior to adaptation, this appears to be different than what is seen during reaching adaptation studies, where there is no immediate improvement in the first reach following a period of washout[65,67,69,76]. We think that difference is due to the nature of walking versus reaching tasks. Specifically, measurement of error during walking (i.e. step length asymmetry) is an interlimb measure that is collected stride-by-stride whereas the error in reaching (i.e. angular error) is a discrete measure observed following a relatively ballistic movement. As such, participants have a full walking stride (lasting approx. 1 sec) to make online corrections in their movements to counter the perturbation. We speculate that this observed (albeit trending) reduction in initial error could be a product of online feedback within the first stride and that we can assume that participants are equally perturbed across exposures and training conditions. Only during the initial perturbation epoch (strides 1-5) is a statistically significant difference realized across training conditions (Figure 2.6A, inset). Thus, while our training effect is largely driven by a faster stride-to-stride learning, it is possible that the training effects are two-fold: faster online correction within a stride accompanied by a faster stride-to-stride adaptation.

Alternatively, participants may be more effectively responding to the abrupt nature of the split-belt perturbation across exposures. Studies of slip-perturbations in walking have shown that repeated slip-perturbation training shifts the stability response

from a reactive (i.e. feedback) to a proactive (i.e. feedforward) control of center of mass[77-80]. Additionally, the training structure of the repeated slip-perturbation can alter the degree to which participants retain their slip response[81,82]. Thus, it is possible that participants in the present study are proactively shifting their center of mass as they become more familiar with the adaptation environment across exposures, resulting in less asymmetry during the first stride. Future work is needed to dissect the balance of feedforward/feedback control within the first stride of split-belt adaptation and the effect of multiple exposures on this response.

2.4.3 Dual-rate state space model of multiday savings

Recent results suggest that motor adaptation, in both locomotion and reaching, is a result of multiple learning processes operating on differing timescales to reduce error[34-36,65,66]. Savings represents our ability to form long term motor memories of a previously experienced environment[37] and has been explained computationally as a change in learning parameters following initial exposure[34]. Savings within a dual-rate SSM framework was thought to be the result of a residual slow state that has been retained from previous exposure[66]. Savings over multiple days, however, cannot be explained by such a mechanism[70]. Thus, if we model the multiday savings as a change in learning parameters across days, a change in the learning rate of the fast process best explains the data. It is also worth noting that the learning rate of the slow process trended toward changing across days ($p=0.051$). Thus, prior exposure to the perturbation may change how we respond to error on a trial-by-trial basis on subsequent exposures[35,65,76]. Moreover, our behavioral results indicate that these changes in our nervous system's ability to respond to error on subsequent exposures may be insensitive to time decay (e.g.

compare Multiday group day 2, versus Single Day group day 5), perhaps due to maintenance of increased learning rates. Indeed, the ability to save a locomotor task has been reported to be maintained over two months later[71], although participants were not washed out within-session in this prior work. This time invariance suggests that savings is not a result of a residual state that is governed by an invariant retention factor but rather a change in the updating rules that lasts for days and perhaps weeks following initial exposure.

2.4.4 Conclusion

We think these results have important implications for rehabilitation. By using switch training on Day 1 of testing, we were able to achieve equivalent learning to four consecutive days of extended training, thereby reducing the training time and sessions. Often, therapeutic approaches for gait rehabilitation focus on the amount of training as the manipulable factor for achieving improved rehabilitation outcomes, particularly in persons post-stroke[83-85]. We contend that how the training is delivered is of equal or possibly even greater importance than the amount of practice. The nervous system's ability to differentially respond to different parts of training (i.e. early training vs asymptotic performance) can allow us to tailor training regimes that can produce the most efficient and effective learning. Ultimately, we aim to apply these findings to inform training schedules for the rehabilitation of gait disorders so that we may achieve the desired rehabilitation outcome and maximize training efficiency.

Chapter 3 Reducing the dimensionality of visual feedback allows for improved performance of a skilled walking task

3.1 Introduction

Complex movements can be broken down into their constituent parts that vary over position and time in a coordinated manner. Whether it is the rotation of the shoulders, hips, and torso at specific times during a golf swing or the flexion/extension of the knee, shoulder, elbow, and wrist joints needed to execute a free throw shot in basketball, movements on a whole-body scale require coordination on the individual joint scale. A challenge when trying to alter these types of multi-jointed movements is that interactions between individual joints prevent us from manipulating one joint in isolation without impacting the others. Indeed, the principle 'the whole is greater than the sum of its parts' applies to complex movements, as a multi-jointed movement is not simply derived from the summation of the motor commands necessary to control individual joints[86-88]. When manipulating a walking pattern specifically, these principles must be taken into consideration as lower-limb sagittal plane kinematics (e.g. hip/knee angles) are closely coupled[89-91].

Previous studies have used visual feedback to allow healthy participants as well as orthopaedic and neurological patients to modify specific aspects of their walking patterns[54]. For example, visual biofeedback of kinematic/kinetic parameters has been

shown to be an effective tool for improving lower-limb mechanics in patients following total knee arthroplasty[92,93], anterior cruciate ligament reconstruction[94] and stroke[47,55,95,96]. Furthermore, healthy participants can use visual feedback to alter step length asymmetry[46], foot placement[48], and knee or hip flexion angles[59] while walking as well as improve lower-limb mechanics during long distance running[60,61]. Still, these studies provide feedback of just one aspect of gait and focus only on endpoint or peak measurements without prioritizing temporal specificity. Because gait deficits often involve multiple abnormalities that occur at specific points in the gait cycle, it is difficult to determine which would be the most effective to target for rehabilitation. Additionally, previous studies using visual feedback were not concerned with how the manipulation of one aspect of gait impacted walking kinematics globally. To constrain these interactions, it would be necessary to provide simultaneous visual feedback of multiple aspects of walking. Delivering additional streams of visual feedback, however, comes at the cost of added attentional load[97-99], which has been shown to hinder walking performance[101-103]. We investigated how we could more effectively deliver multiple channels of kinematic information to alter a walking pattern in a temporally-specific manner.

A series of studies has shown that people can use multiple dimensions of kinematic information to control a low-dimensional external device (e.g. visual cursor, wheelchair joystick, etc)[104-108]. Here, we look to utilize similar dimensionality reduction principles to change multiple facets of a walking pattern simultaneously. We have created a novel feedback system that uses principal component analysis (PCA) to weight multiple channels of kinematic information and display the participant's performance as a simple one-dimensional 'summary' of their walking pattern relative to a prescribed goal pattern.

We focused on sagittal ankle position trajectories such that participants had to alter their kinematics along the AP and vertical axes within each stride in order to match a prescribed goal stride. Thus, the feedback combined four dimensions of information (i.e. two for each ankle) to produce a one-dimensional summary of walking performance.

We investigated the rate and extent to which healthy participants could use the novel principal component-based visual feedback to learn a modified walking pattern. We compared the performance using the principal component-based visual feedback to participants who received four concurrent streams of one-dimensional, Cartesian-based visual feedback (i.e. one for each dimension) to learn the same goal pattern. Cartesian feedback is similar to conventional gait training in which a single stream of visual feedback contains information of one aspect of gait. We found that healthy, young participants could use the principal component-based visual feedback to learn a prescribed goal pattern at a faster rate than those who received concurrent feedback of all dimensions. Furthermore, participants were able to use the principal component-based feedback to more closely match the goal kinematics by the end of a single session of training than those who received feedback of each dimension.

These results suggest that this novel principal component-based visual feedback can be used as a straightforward summary of walking performance that enables us to alter multiple aspects of gait toward a given goal pattern. Our findings demonstrate that this novel approach could be promising for rapidly and intuitively teaching persons with pathological gait how to simultaneously correct multiple gait abnormalities.

3.2 Methods

3.2.1 Participants

Thirty young, healthy adults (10 per condition; PC feedback, Cartesian feedback, and PC match) were recruited for this experiment (15 men, 15 women; mean age ± SD: 23.5 ± 4.0 yr). All participants provided written, informed consent before taking part in the experiment. The experimental protocol was approved by the Johns Hopkins Medicine Institutional Review Board and all experiments were performed in accordance with relevant guidelines and regulations. All participants were free of any neurological and musculoskeletal conditions.

3.2.2 Motion analysis

We recorded participants' kinematics using an Optotrak Certus motion capture system (Northern Digital, Waterloo, ON) as they walked on a split-belt treadmill (Woodway, Waukesha, WI). The split-belts allowed us to detect right and left foot contacts via distinct force plates, but the belt speeds were equal throughout all experiments. Kinematic data were collected at 100 Hz from 12 infrared-emitting diodes placed bilaterally on the foot (fifth metatarsal head), ankle (lateral malleolus), knee (lateral joint space), hip (greater trochanter), pelvis (iliac crest), and shoulder (acromion process; Figure 3.1A).

3.2.3 Goal walking pattern calculation

The purpose of this study was to assess the use of different feedback types to instruct a new walking pattern. The desired walking pattern was calculated from each participant's baseline walking such that the vertical dimension of the ankle position was increased relative to baseline and the antero-posterior (AP) dimension of the ankle position was decreased relative to baseline (Figure 3.1C, D). All kinematics were

computed in a hip-centered coordinate system to ensure that any whole-body translation on the treadmill did not affect the output. We focused the goal kinematics on the swing phase (i.e. subjects had to take shorter, higher steps) rather than the stance phase because stance is largely constrained by the speed of the treadmill belts. To avoid discontinuities in the kinematics at the stance-swing transitions, the goal kinematics were calculated by applying a Gaussian weighted gain over the swing phase. The gains applied to the vertical and AP dimensions were 2.5 and 0.75, respectively.

This algorithmically generated goal was used in the first experiment to bias the participants' kinematics in the direction of the goal. We refer to the participants who received this walking goal and the principal component-based visual feedback as the PC feedback group. It should be noted that the algorithmically generated goal proved to be difficult to fully reach. In a second control experiment, we tested how participants performed if we gave them a more natural goal ankle trajectory instead of one that was generated algorithmically. The more natural goal was set as the average pattern of ankle kinematics that participants reached at the end of training in the first experiment. We refer to these participants as the PC match group. This allowed us to observe if participants could use the principal component-based feedback to match an exact set of goal kinematics that we have previously observed from another group of healthy, young participants.

3.2.4 Visual feedback

Participants received one of two forms of visual feedback designed to help them achieve a prescribed goal walking pattern: 1) principal component-based visual feedback that used PCA to combine four dimensions of kinematic information (Figure 3.1B, left)

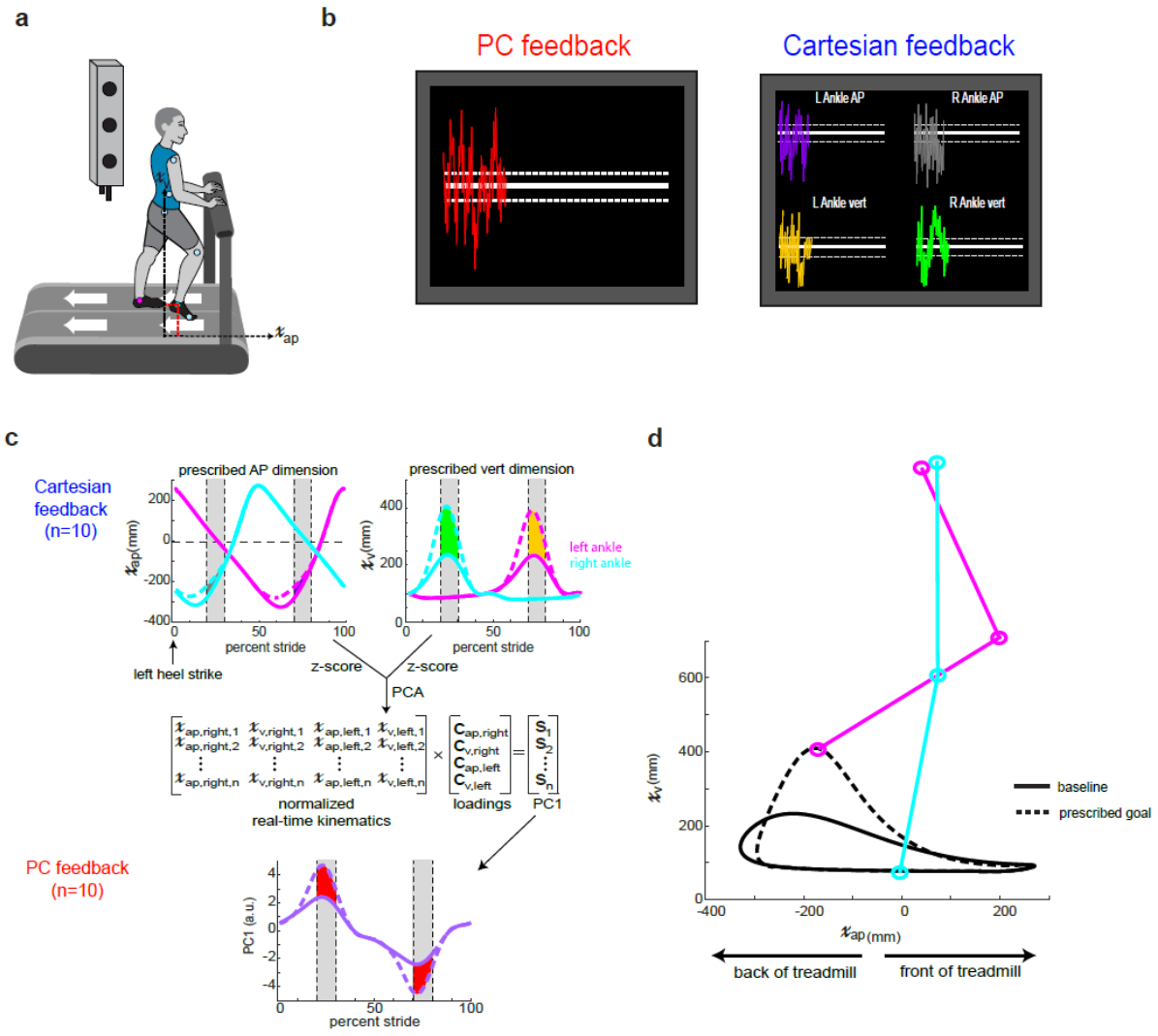

Figure 3.1 *Experimental set up and visual feedback display.* **A)** Marker placement and general set up for motion capture. Left and right ankle position was recorded in the sagittal plane. **B)** Visual display for PC feedback and Cartesian feedback. Participants were instructed to change their walking pattern so they minimized the distance from the target line(s). PC feedback had one target line while Cartesian feedback had four target lines (one for each kinematic dimension). Dashed lines around the target line correspond to the success zone. **C)** Calculation of the prescribed goal ankle kinematics. The pink trace denotes the left ankle while the cyan trace denotes the right ankle kinematics. AP and vertical dimensions were multiplied by Gaussian gains with maximum magnitudes of 0.75 and 2.5, respectively, over swing phase. Cartesian feedback displayed the difference between goal and real-time kinematics, displayed as the colored shaded regions during mid-swing on each leg. The gray shaded regions denote where this difference was averaged for visual feedback display (i.e. the rewarded time windows). We ran principal component analysis on the goal kinematics to calculate loadings. These loadings were used to calculated a goal PC1 for the PC feedback as well as a real-time PC1 using the normalized real-time kinematics. PC feedback displayed the difference between the goal

and real-time PC1, displayed as the red shaded region during mid-swing on each leg. **D)** Goal and baseline sagittal plane ankle kinematics for the left ankle. Participants had to take shorter, higher steps to improve performance in both dimensions. The right ankle had an identical goal pattern.

into a single stream of performance feedback or 2) four concurrent streams of Cartesian-based visual feedback (Figure 3.1B, right). Two groups (PC feedback and PC match) were tested using principal component based feedback while one group (Cartesian feedback) was tested using Cartesian-based feedback of sagittal plane ankle kinematics. Position of the left and right ankles in the AP and vertical axes were sampled from the Optotrak software and fed into a custom Python program at real-time. Visual feedback was displayed using a Vizard development environment (WorldViz, Santa Barbara, CA) and reflected the participants' step-by-step deviation from the desired pattern. This real-time information was displayed in a simple format, such as a trace that moves in and out of the prescribed goal zone(s) on a screen (Figure 3.1B). The feedback reflected the participants' deviation from a white 'target' line on the TV screen and we instructed subjects to change their pattern such that this deviation was minimized. The visual feedback was updated upon each heel strike (i.e. two new data points per stride) and tracked across the TV screen so that participants had information of their current and past performance.

For participants to use the visual feedback, it was necessary to standardize their stride time. This was because we needed to set a length of time for the goal stride from which to compare real time performance. Thus, we used a metronome to standardize the participants' walking cadence. Participants were instructed to heel strike in rhythm with the beat from the metronome. The goal stride time was calculated from each individual's average time between successive heel strikes during baseline walking (Figure 3.2A).

The principal component-based feedback contained one stream of performance feedback around one target line (Figure 3.1B, left). The position of the feedback relative

to the target line in the principal component-based feedback was the difference in the first principal component (PC1) of the normalized real time stride and PC1 of the goal stride. As such, a participant who matches the goal pattern exactly (i.e. difference of zero) would receive feedback on the white target line. Weights for the real time principal component were calculated by applying PCA to the z-scored goal stride. Importantly, these weights were kept constant across the entirety of the experiment so that the participants had a constant mapping between their change in kinematics and their feedback performance.

The Cartesian-based feedback contained four streams of performance feedback, each containing information specific to a given dimension, around four target lines (Figure 3.1B, right). The position of the feedback relative to each target line in the Cartesian-based feedback was determined by the difference between each of the z-scored dimensions in real time and their corresponding goal dimensions (i.e. vertical and AP ankle positions).

For both feedback types, these differences were calculated at approximately halfway through the swing phase of each leg and then displayed at heel strike. Thus, feedback given at right leg heel strike contained information from the preceding right leg swing and left leg stance phase, and vice versa for the feedback given at left leg heel strike. Visual feedback display and calculation are shown in Figure 3.1 (panels B and C).

3.2.5 Experimental paradigm

Participants walked on a custom-built treadmill which was also controlled through Vizard. Walking speed was set to 1 m/s for all walking trials (the belts were always tied at the same speed). Participants were instructed to stand in the middle of the treadmill

with one foot on each belt so that we could detect heel strikes from the force plates for visual feedback display. They wore a safety harness that was suspended from the ceiling to protect against the risk of falling. The harness did not provide any body weight support. While walking, participants were instructed to walk with their arms across their chest.

All groups experienced the same experimental paradigm that consisted of six blocks: 1) Baseline, 2) Familiarization, 3) No Feedback, 4) Feedback 1, 5) Feedback 2, and 6) Feedback 3 (Figure 3.2A). The groups differed by the type of visual feedback given (i.e. PC or Cartesian). During the Baseline block, participants walked at 1 m/s for 2 minutes. From this baseline walking, we calculated the goal stride and metronome cadence as detailed in 'Visual Feedback'. During the Familiarization block, participants walked with the visual feedback for 3 minutes to get accustomed to the visual display and metronome as they walked. The 'target' line(s) were set to the participants' baseline walking so that if they walked naturally, their visual feedback was close to the goal. Participants were informed that their performance did not matter during this block. Thus, they were free to explore the feedback and gain experience walking in beat with the metronome. During the No Feedback block participants were instructed to walk naturally in beat with the metronome. This block was designed to gather baseline performance. Next, participants experienced three identical, 5 minute Feedback blocks. During these blocks, participants responded to the visual feedback such that they had to alter their natural walking pattern to improve performance and progress their feedback closer to the target line(s). Participants were informed of the dimensions (AP and vertical positions of their ankles) that they could manipulate to alter their performance. For the principal

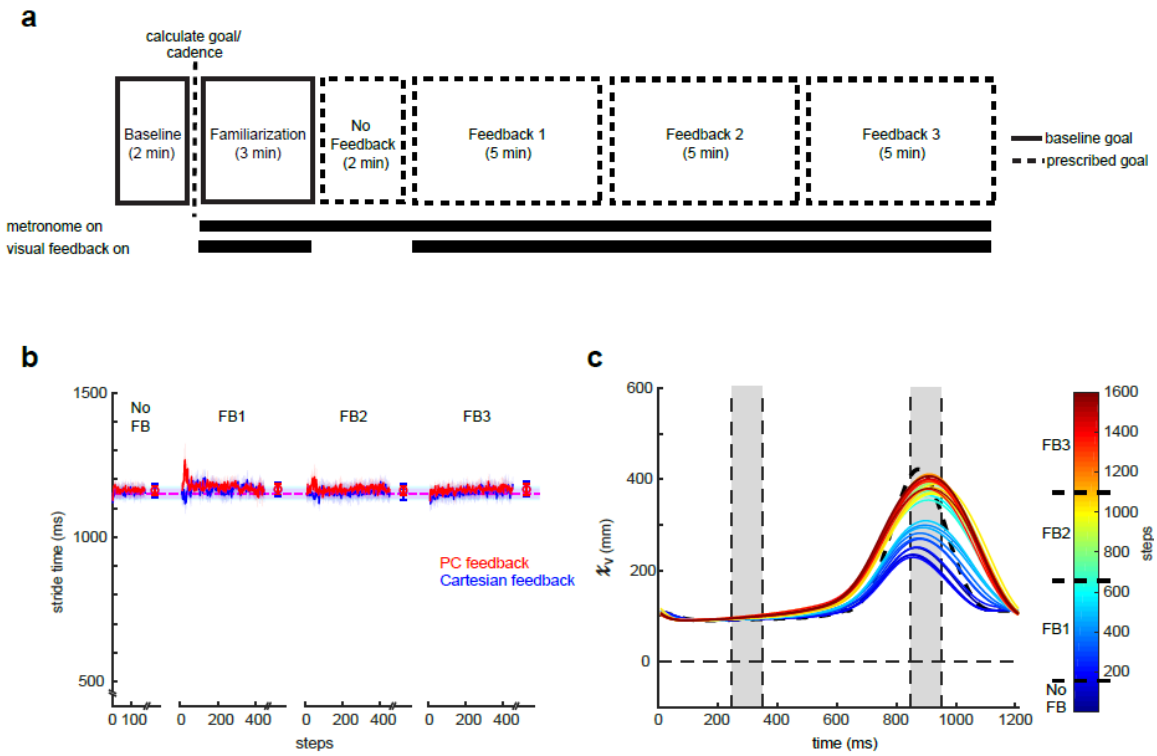

Figure 3.2 *Experimental paradigm.* **A)** Experimental paradigm for all conditions. We calculated the goal walking pattern and goal cadence from the 2 minutes of baseline walking at 1 m/s. Participants were given 3 minutes of familiarization were the goal 'target' line corresponded to their baseline walking. During No Feedback, participants were instructed to walk naturally in rhythm with the metronome but did not receive performance feedback. In Feedback 1-3, participants were instructed to minimize the deviation from the goal target line(s) by altering their walking pattern. The goal target line(s) corresponded to the modified walking pattern. Participants were instructed to walk in rhythm with the metronome during these blocks. Each feedback block was 5 minutes. **B)** Stride times for PC feedback (red) and Cartesian feedback (blue) across blocks. The dashed lines are the group average goal stride times provided by the metronome. Data points at the end of each block denote the group mean ± SEM of the last 50 steps within that block. All shaded regions denote SEM. **C)** Sample participant kinematics in the vertical dimension over training. Cold colors denote baseline/early training and hot colors denote late training. Participants had to use the feedback to incrementally change their kinematics toward the prescribed goal (dashed black line) over the course of training. The vertical shaded regions denote the rewarded time windows.

component-based feedback, participants were informed that it was some combination of these dimensions that determined their feedback performance. For the Cartesian-based feedback, participants were explicitly informed which dimension corresponded to which stream of visual information. Importantly, all participants were not informed of the goal pattern; therefore, improvement in feedback performance required the participant to explore alternative walking patterns and use the visual feedback to determine which patterns resulted in better or worse performance.

3.2.6 Data analysis

Our measure of performance can be mapped into two spaces—PC and Cartesian space—that can be linearly transformed from one to the other using the component loadings (Figure 3.1C). In each of these spaces, our primary outcome measure is the step-by-step difference between the current set of kinematics and the prescribed goal pattern. In PC space, this measure is a difference of principal components (measured in arbitrary units) while in Cartesian space, this measure is a difference of sagittal plane ankle position (measured in millimeters). These differences are calculated and averaged over the rewarded time window (100 millisecond windows centered approximately around mid-swing of each leg; displayed as vertical dashed lines between 20-30 and 70-80 percent stride in Figure 3.1C). As such a value of zero for these measures represents perfect performance in matching the prescribed goal pattern over these time windows. We use PC space as a measure of overall performance while we use Cartesian space to break out how individual dimensions evolve over the course of training. We ensured that participants were maintaining the cadence provided by the metronome by calculating stride time between consecutive left heel strikes.

Performance during the all blocks of the experiment was calculated by averaging over specific time periods in the experiment. For each of the feedback blocks, we averaged performance over the first and last 50 steps in each block to obtain a measure of early and late performance, respectively. Early performance was our measure of rate of increased performance while late performance was our measure of task proficiency at the end of each block.

To demonstrate that participants in PC match could exactly match the set of goal kinematics, we calculated the root mean squared error (RMSE) between the kinematics observed at the end of Feedback 3 and the goal and compared that to those of the PC feedback group.

3.2.7 Statistical analysis

To identify differences between groups in their ability to match the goal kinematics during training, we performed mixed design, repeated-measures ANOVA with 'block' (dimension 7) and 'group' (dimension 2) main factors. 'Block' was composed of performance during late No Feedback block and early and late performance from each feedback block. To observe differences between groups during specific blocks of training, we performed post-hoc analysis on the block-group interaction. Bonferonni correction for multiple comparisons was used when necessary. In addition, we used paired sample t-tests to determine which block subjects within each group reached the outer-bound of successful task performance (i.e. dashed lines in Figure 3.1B). These analyses were performed in both PC and Cartesian space. Similar mixed-methods repeated measures ANOVA design was used when analyzing group and dimension effects on loading values between PC and Cartesian as well as root mean squared error

values for PC and PC Match. For repeated-measures ANOVA, we performed Mauchly's test of sphericity and used the Greenhouse-Geisser correction of degrees of freedom if sphericity was violated. To ensure that participants remained within 60 ms (approx. 5 percent) of the prescribed stride cadence, we performed right-tailed, one-sample t-tests on the absolute difference between participants' baseline stride times and the metronome beat interval against a null hypothesis of mean 60. Because this task relies on exploration of alternative walking patterns to achieve task success, we considered that it might be possible that subjects did not explore beyond their natural walking pattern. Thus, we used outlier analysis to exclude participants from analysis who continued to walk naturally and did not improve their performance over the course of the three feedback blocks. This analysis eliminated one subject from each of the PC, Cartesian, and PC match groups. All analyses were performed using SPSS 25.0 (IBM, Armonk, NY) and α–level was set to 0.05.

3.3 Results

Figure 3.2B displays the stride times during all blocks of the experiment. Participants in the PC and Cartesian groups were able to stay within 60 ms of this prescribed walking cadence during the early and late epochs of all blocks of the experiment (all $p > 0.832$). Thus, we are confident that participants were able to follow instructions and complete the task.

3.3.1 Performance gains in a skilled walking task

To improve task performance, participants had to incrementally alter their walking pattern from their natural walking (example participant data for the vertical ankle movement shown in Figure 3.2C) and use the visual feedback to determine if their stride-

to-stride change resulted in improved or declined performance. Ultimately, participants were instructed to have their feedback as close to the target line(s) as possible and ideally within the outer-bounds of successful task performance (dashed lines in Figure 3.1B). Figure 3.3A displays our primary measure of performance (mean difference from goal PC1) for PC and Cartesian groups across all feedback blocks. Baseline performance did not vary between PC and Cartesian groups ($p = 0.976$; see Figure 3.3A, baseline late). For analysis, we binned performance into early and late epochs (first and last 50 steps) for each feedback block. Early epochs can be considered a measure of rate while late epochs can be considered a measure of plateau performance for each feedback block. These epochs, in addition to baseline measurements, were submitted to mixed-methods repeated-measures ANOVA with *block* and *group* main factors. Our analysis reveals that groups improved performance across feedback blocks ($F_{6, 96} = 60.89$, $p < 0.001$). Thus, participants were able to use the visual feedback (either PC or Cartesian) to approach the prescribed walking pattern.

Interestingly, PC and Cartesian groups' performance varied differently across time epochs as revealed by a significant *block*group* interaction ($F_{6, 96} = 3.23$, $p = 0.006$). We performed post-hoc analysis to observe which blocks drive the significant interaction. Analysis revealed that the PC group improved performance at a faster rate than the Cartesian group during Feedback 1 ($p=0.006$; see Figure 3.3A, FB1 early). Additionally, the PC group was closer to the goal at the end of Feedback 2 and 3 ($p = 0.013$ and $p = 0.020$, respectively; see Figure 3.3A, FB2 late and FB3 late). Furthermore, performance in the PC group did not differ from -0.25 a.u. (defined as the outer-bound of task success) while the Cartesian group was not able to reach task success ($t_8 = -5.28$, $p < 0.001$;

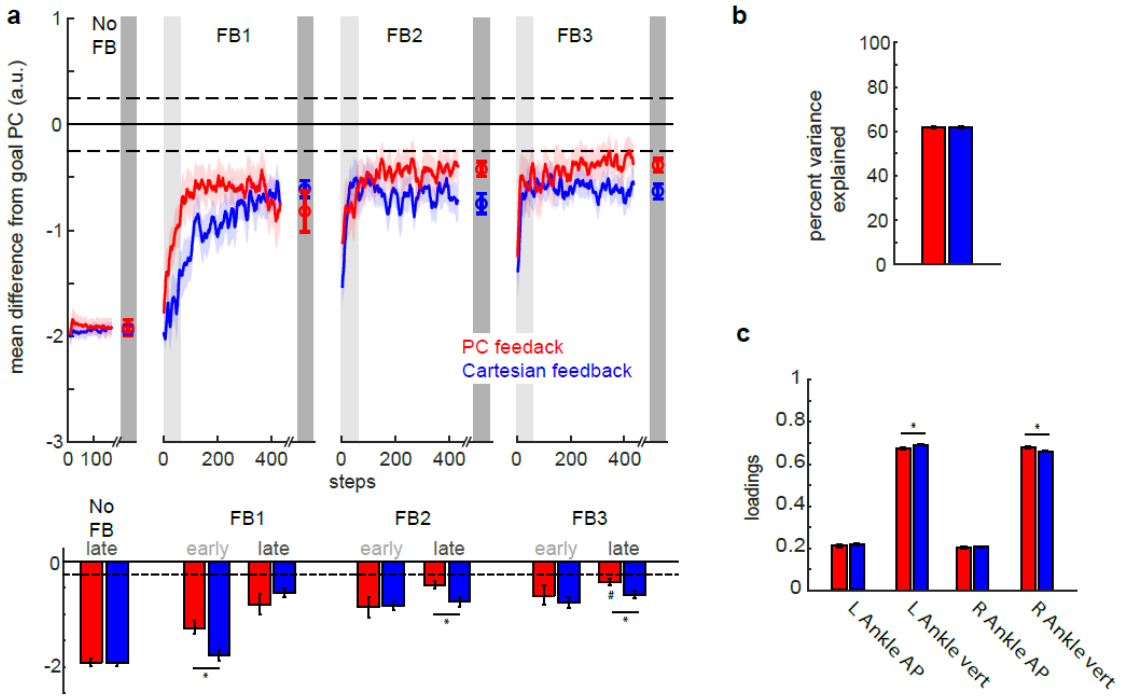

Figure 3.3 *Comparison of group performance in PC space.* **A)** Display of mean difference from goal PC across blocks. Differences were calculated during the rewarded time windows for each step (i.e. mid-swing). Perfect performance is reflected by a value of 0. Dashed lines correspond to the success zone (i.e. ± 0.25 a.u. from goal). Data points at the end of each block denote the group means ± SEM of the last 50 steps for the given block. The red traces denote performance for the PC feedback group while the blue traces denote performance for the Cartesian feedback group. Colored shaded regions denote standard error. Light and dark gray shaded regions denote early and late epochs consisting of the first and last 50 steps within that block. Mean performance during these early and late epochs are displayed in the bar graphs below the time series. * denotes a between-subject difference ($p < 0.05$) while # denotes a non-significant difference ($p > 0.05$) between performance during that epoch and the outer-bound of task success (i.e. 0.25 a.u.). **B)** Percent variance explained by the first principal component (i.e. goal PC1) for PC feedback (red) and Cartesian feedback (blue). **C)** Mean absolute loadings for each kinematic dimension for PC feedback (red) and Cartesian feedback (blue). These loadings were calculated from the normalized goal kinematics. * denotes a between-subject difference ($p < 0.05$) and all error bars denote SEM.

against a null hypothesis with mean -0.25). Therefore, participants using the PC feedback demonstrate faster and more complete learning of a prescribed goal pattern during one session of training.

Information on the first principal component (PC1) for each group is summarized in Figure 3.3B-C. Note that PC feedback actually received feedback of PC1 relative to the goal PC while these data were calculated for Cartesian feedback post-hoc from the goal stride kinematics. PC1 in both groups accounted for approximately 62 percent of the variance with no difference between the groups (Figure 3.3B; $t_{16} = 0.35$, $p = 0.750$). Meanwhile, group average absolute loadings for both groups were approximately 0.67 for vertical dimensions and 0.21 for AP dimensions (Figure 3.3C). Mixed-methods repeated-measures ANOVA with *dimension* and *group* main factors revealed no *group* effect on loadings ($F_{1, 16} = 0.68$, $p = 0.422$). Although there was a *dimension*group* interaction ($F_{1.98, 31.66} = 5.05$, $p = 0.013$), which is driven by significant pairwise differences between the vertical dimensions on both the right ($p = 0.006$) and left ($p = 0.005$) sides. Still, the mean pairwise difference of the loadings in these dimensions is only 0.019 and 0.016, respectively. The statistical significance is largely driven by the small standard error within these groups (~0.005). Given that these differences in loadings only weigh the respective dimensions by 1 to 2 percent differently, we were not concerned that this difference drove our performance effect in PC space (Figure 3.3A). Indeed, subsequent analysis of the kinematics reveals that these groups did differ in their walking pattern.

We were interested in understanding which dimensions were responsible for the difference in performance observed in PC space. Just as we transformed data from Cartesian group to perform analysis in PC space, we can also analyze the PC group in

Cartesian space. Figure 3.4 shows the deviation of each dimension from the prescribed goal kinematics for both groups over the course of the experiment. Of note, both groups performed the same at baseline for all dimensions (all $p > 0.62$). We separated the feedback blocks into early and late epochs and submitted each dimension to mixed-methods repeated-measures ANOVA with *block* and *group* main factors.

The observed difference in performance in PC space was largely due to the PC group's ability to correct their ankle trajectory in the vertical dimension more rapidly and completely than the Cartesian group. Analysis revealed a significant *block*group* interaction for the left vertical dimension (Figure 3.4A; $F_{6, 96} = 3.23$, $p = 0.006$). While analysis of the right vertical dimension did not yield a significant *block*group* interaction (Figure 3.4B; $F_{2.95, 47.15} = 1.36$, $p = 0.266$), we did observe some epoch-specific pairwise differences between groups that contributed largely to the effects seen in PC space. Specifically, we observed a difference in performance in the right vertical dimension during both FB1 early (Figure 3.4B; $p = 0.022$) and FB3 late ($p = 0.019$). These pairwise differences, along with the aggregate differences in other dimensions, are what led to the group differences observed during these epochs in PC space (Figure 3.3A).

We observed that participants receiving PC feedback were able to more closely match the goal kinematics in the AP dimensions throughout the experiment (Figures 3.4C and D). We observed several epoch-specific differences between groups in these dimensions. Specifically, PC showed improved performance relative to Cartesian for the left ankle AP dimension in FB1 late ($p = 0.029$), FB2 early ($p = 0.050$), and FB3 early ($p = 0.049$) (Figure 3.4C) as well as for the right ankle AP dimension in FB1 late ($p = 0.048$) (Figure 3.4D).

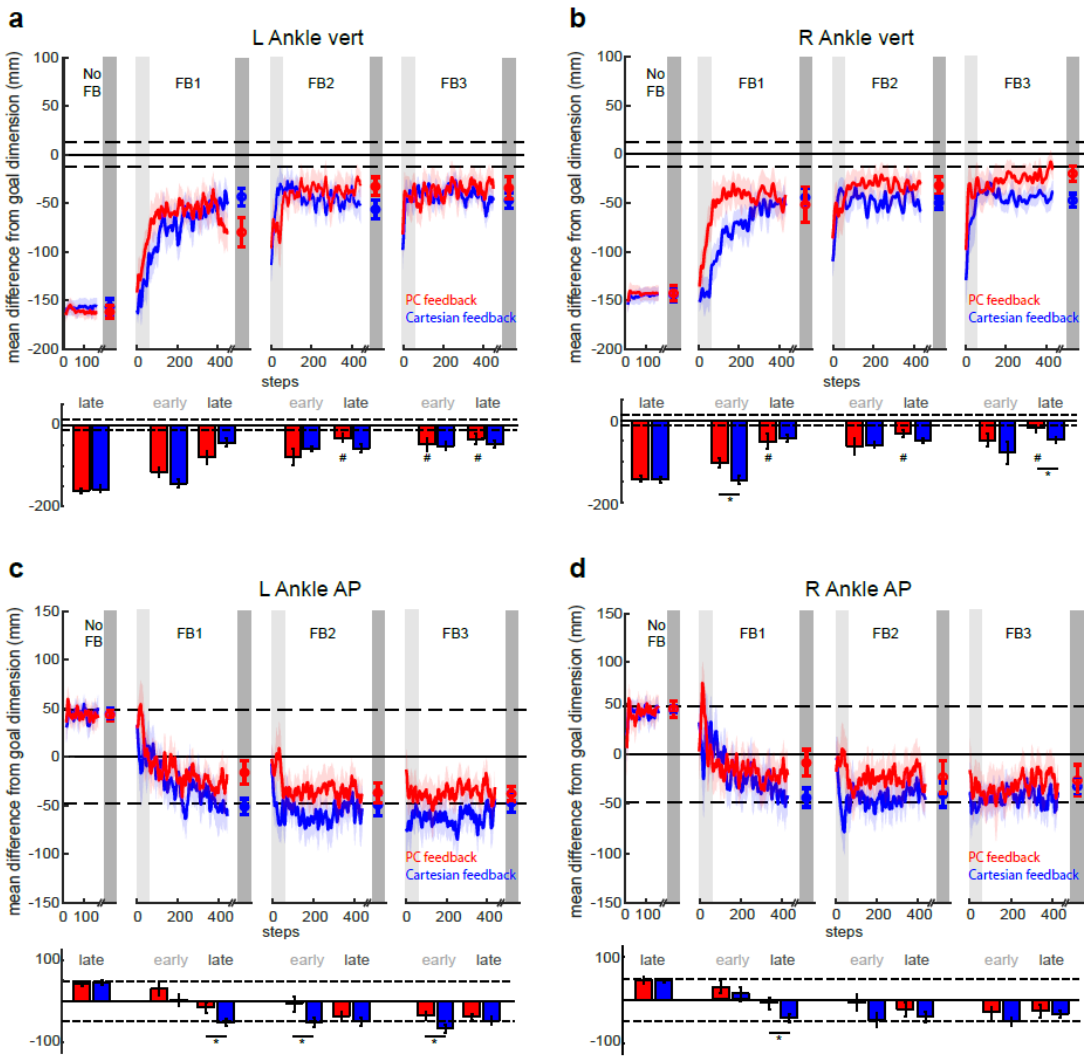

Figure 3.4 *Comparison of group performance in Cartesian space.* All panels show mean difference from the goal dimension for PC feedback (red traces) and Cartesian feedback (blue traces) where a value of 0 reflects perfect performance. Differences were calculated during the rewarded time windows for each step (i.e. mid-swing). Dashed lines around 0 denote the success zone for each kinematic dimension. Data points at the end of each block denote the group means ± SEM of the last 50 steps for the given block. Colored shaded regions denote standard error. Light and dark gray shaded regions denote early and late epochs consisting of the first and last 50 steps within that block, respectively. Mean performance during these early and late epochs are displayed in the bar graphs below the time series of each kinematic dimension. Data is displayed for **A)** left ankle vertical dimension, **B)** right ankle vertical dimension, **C)** left ankle AP dimension and **D)** right ankle AP dimension. * denotes a between-subject difference ($p < 0.05$) for a given dimension. For the vertical dimensions, # denotes a non-significant difference ($p > 0.05$) between performance during a given epoch and the outer-bound of task success; determined by a paired t-test between a given participant's outer-bound and performance during FB3 late. These are not displayed for the AP dimensions as performance is always within the success zone.

We then explored which dimensions of the task enabled the PC group to outperform the Cartesian group by the end of training. We tested if each group's performance was statistically different from the outer-bound of task success (dashed lines in Figure 3.4) using t-tests on the difference from the respective goal dimension. We interpreted a non-significant result as that group obtaining a level of performance that is statistically indistinguishable from the success zone that we provided (i.e. achieving task success). PC feedback's level of performance at the end of feedback 3 was statistically indistinguishable from the outer-bound of task success in all four kinematic dimensions.) The Cartesian group achieved task success in the AP dimensions, but did not achieve task success for the vertical dimension on both the left ($p = 0.002$) and right side ($p= 0.001$). Figure 3.5 displays sagittal left (panels A-C) and right (panels D-F) ankle kinematics at the end of training (FB3 late) for PC and Cartesian groups. The bolded regions of the trajectory in Figure 3.5A display the portion of the left ankle trajectory within the time window (i.e. mid-swing) in which the participants receive feedback of their performance. Individual dimensions within this time window are displayed in Figure 3.5B and C within the gray, shaded region between 70 and 80 percent stride. Similar information is conveyed in Figure 3.5D, E and F for the right ankle with right mid-swing located between 20 and 30 percent stride in Figures 3.5E and 3.5F. Notably, the PC group kinematics more closely match those of the prescribed goal pattern, particularly in the vertical dimensions. While both feedback types can be used to change a walking pattern, these results suggest that PC feedback is more effective than Cartesian feedback in teaching young healthy participants to achieve a new walking pattern within a single session.

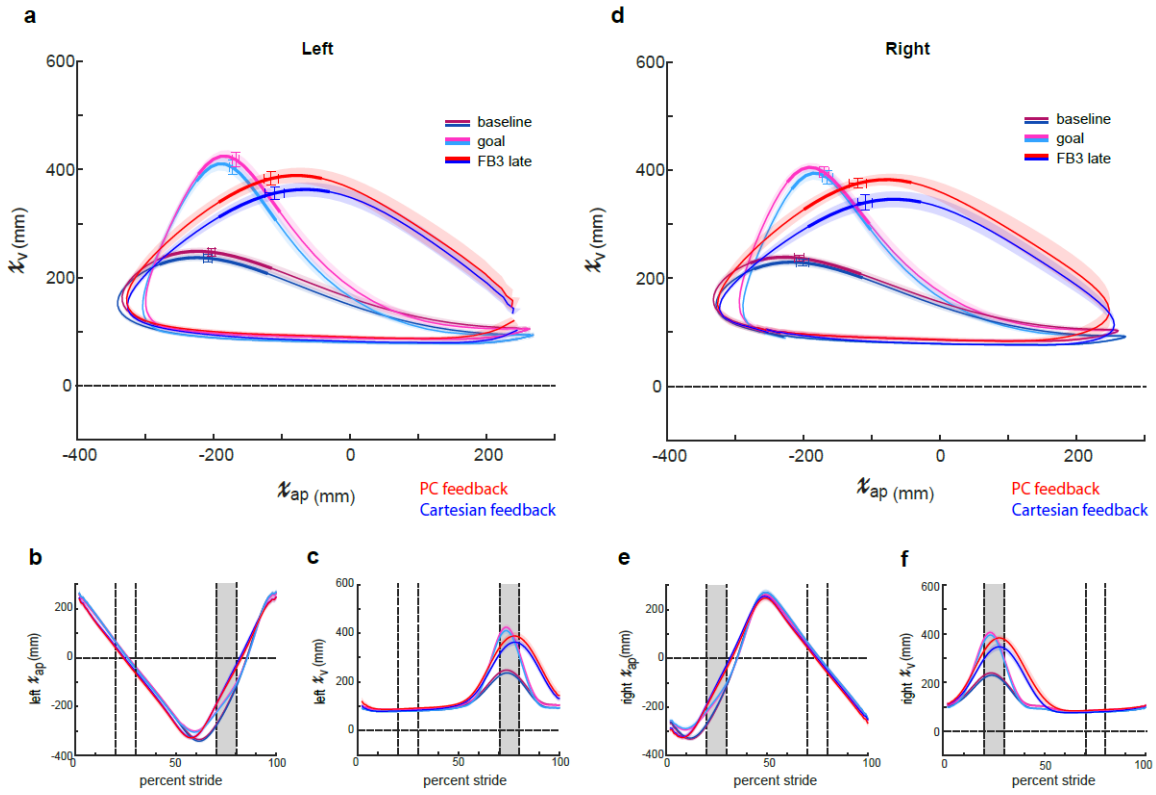

Figure 3.5 *Sagittal plane ankle kinematics during late training for PC and Cartesian feedback groups.* **A)** Left sagittal plane ankle kinematics for PC feedback (red shades) and Cartesian feedback (blue shades) during baseline and late training (FB3 late). Participants in both groups approach the goal kinematics (pink and cyan) by the end of training. The bolded region on each trace denotes the kinematics during the rewarded time window. Horizontal and vertical error bars within these bolded regions correspond to SEM during mid-swing in the AP and vertical dimensions, respectively. Shaded regions around each trace denote SEM in the vertical dimension. **B)** Time-series kinematics for the left ankle AP dimension. Kinematics are aligned to left heel strike (i.e. 0 percent stride). The gray shaded region corresponds to the rewarded time window during mid-swing for this dimension. **C)** Time-series kinematics for the left ankle AP dimension. The gray shaded region corresponds to the rewarded time window during mid-swing for this dimension. Panels **D**, **E**, and **F** contain the same information as A, B, and C but for the right ankle.

3.3.2 Is imperfect performance due to feedback or selected goal?

Although participants in the PC group were able to more closely match the goal kinematics by the end of training, we noticed that the trajectories did not perfectly match the given goal, particularly outside of the rewarded time window (compare red traces to pink traces in Figure 3.5). We considered that the original, algorithmically generated goal may have been too difficult to perform. Thus, we wanted to test if the imperfect performance in the PC feedback group was a product of the visual feedback itself or our selected goal walking pattern. Accordingly, we tested an additional group of participants—PC match—which received the identical feedback as PC but now had a goal pattern composed of the sagittal plane ankle kinematics observed in the PC group at the end of Feedback 3 (red traces in Figure 3.5). In contrast to the algorithmically calculated gained up/gained down goal used previously, we know that young healthy participants have and can achieve this exact set of kinematics on the treadmill.

To quantify differences over the entire gait cycle, we calculated the root mean squared error (RMSE) between the goal kinematics and the kinematics observed at the end of Feedback 3 for each group. These differences were computed by comparing the pink (i.e. goal) and red traces in Figure 3.6 for the PC group. For the PC match group, the red trace in Figures 3.5 and 3.6 was used as the goal and compared against the dark green trace in Figure 3.6 (i.e. late FB3 for PC match). We found that PC Match were able to use the PC feedback to more closely match their respective goal pattern than the PC group (Figure 3.6). Specifically, mixed-methods repeated-measures ANOVA revealed a significant between-subject effect of *group* ($F_{1, 16} = 16.97$, $p=0.001$) as well as a significant *group*dimension* interaction ($F_{1.60, 25.63} = 7.46$, $p = 0.005$) on RMSE (Figure

3.7). Post-hoc analysis revealed pairwise differences between groups' RMSE for the left vertical dimension ($p < 0.001$) and right vertical dimension ($p = 0.001$). These results suggest that the imperfect performance observed in the PC group was due to our selection of goal kinematics. Thus, given an appropriate goal, PC feedback can be used to teach an exact set of kinematics.

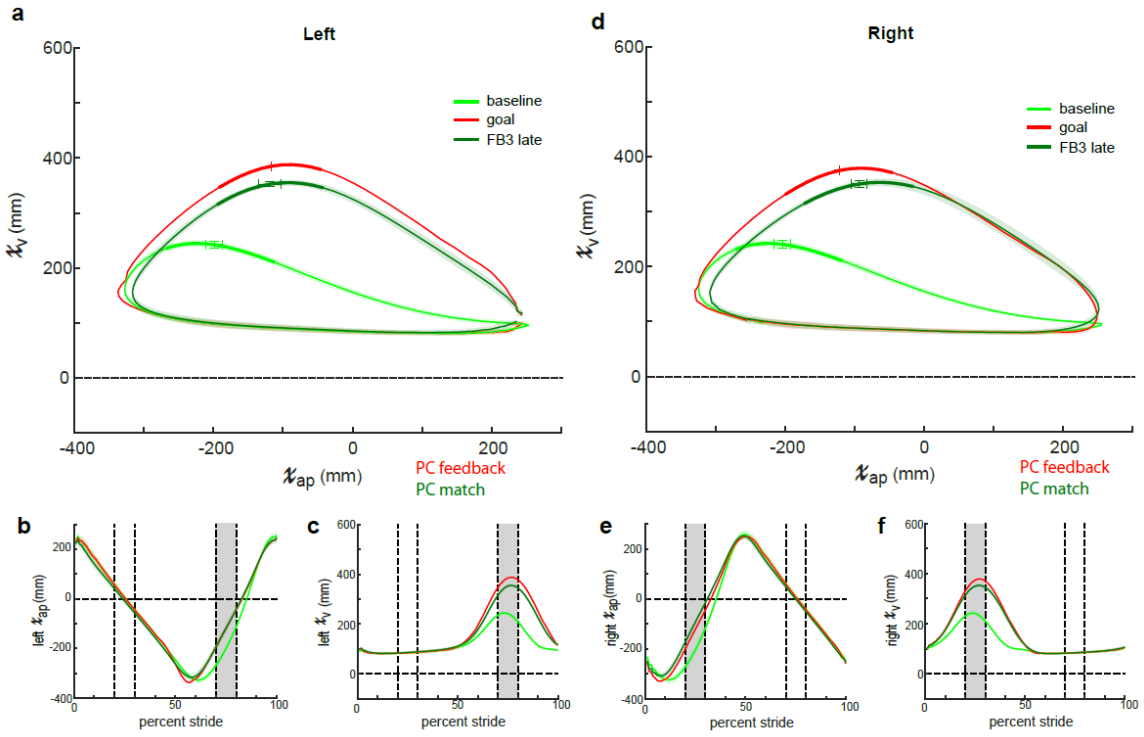

Figure 3.6 *Sagittal plane ankle kinematics during late training for PC match group.* **A)** Left sagittal plane ankle kinematics for PC match (green shades) during baseline and late training (FB3 late). Participants approach the goal kinematics (red; late training performance for PC feedback group displayed in Figure 3.5) by the end of training. The bolded region on each trace denotes the kinematics during the rewarded time window. Horizontal and vertical error bars within these bolded regions correspond to SEM during mid-swing in the AP and vertical dimensions, respectively. Shaded regions around each trace denote SEM in the vertical dimension. **B)** Time-series kinematics for the left ankle AP dimension. Kinematics are aligned to left heel strike (i.e. 0 percent stride). The gray shaded region corresponds to the rewarded time window during mid-swing for this dimension. **C)** Time-series kinematics for the left ankle AP dimension. The gray shaded region corresponds to the rewarded time window during mid-swing for this dimension. Panels **D**, **E**, and **F** contain the same information as A, B, and C but for the right ankle.

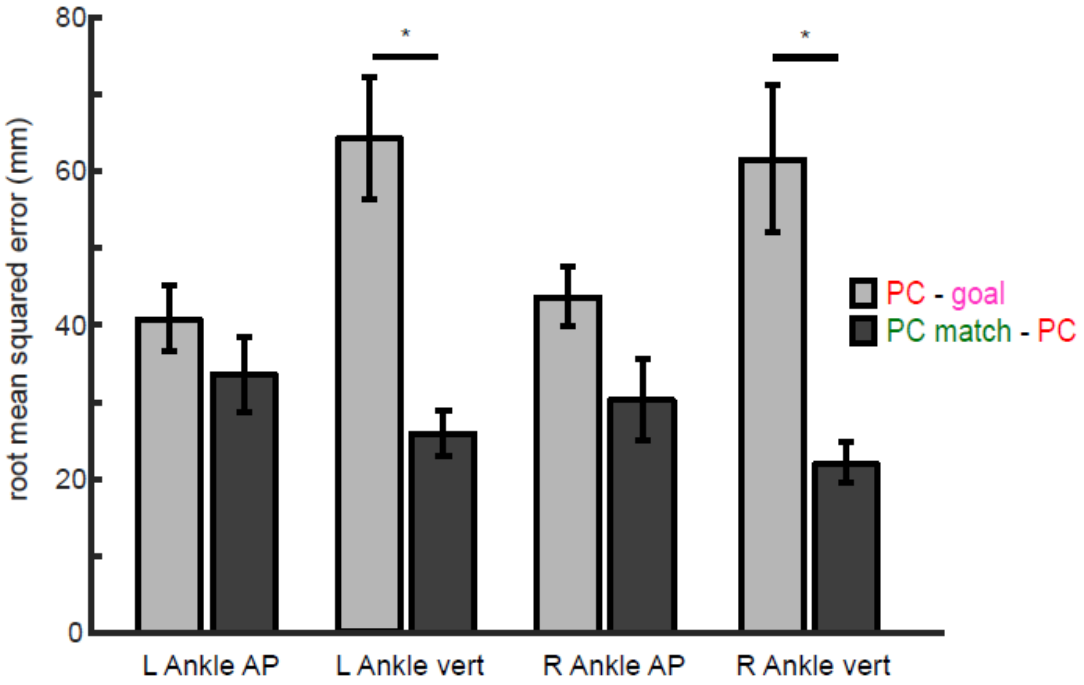

Figure 3.7 *Difference from goal walking pattern for PC and PC match groups.* Root mean-squared error between late training and goal kinematics for PC feedback (light gray) and PC match (dark gray) groups in each kinematic dimension. An error closer to a value of 0 corresponds to the participants more closely matching the goal kinematics. Color scheme in the legend corresponds to the colors of the kinematic traces displayed in Figure 3.5 and 3.6. Error bars denotes SEM. * denotes a between-subject difference ($p < 0.05$) for a given kinematic dimension.

3.4 Discussion

In this study, we have shown that more information is not necessarily better when using visual feedback to achieve a modified walking pattern. The participants in this study were able to use a single stream of PC information to change multiple features of their gait toward the prescribed goal pattern and outperformed those receiving Cartesian-based information. PCA is a commonly used algorithm when studying movement. For example, it has been used to characterize walking features[109-112] or map high dimensional movement to low-dimensional control of a device (i.e. body-machine interfaces)[104-108]. Here we used PC-weighted feedback to simultaneously teach participants multiple aspects of movement toward a prescribed movement pattern. This is novel as we are not aware of any work that has previously used this approach.

Performing a new walking pattern requires coordination of multiple aspects of lower extremity movement. This high dimensionality can be a challenge for gait retraining as it is difficult to determine which aspects to target with a given intervention. For example, traditional gait retraining using visual feedback focuses on altering a specific kinematic (e.g. peak knee flexion)[59] or kinetic parameter (e.g. push-off force)[113]. Often, however, multiple gait deficits are present concurrently. Addressing one deficit independently of the others may have unintended effects on the aspects of gait outside of what the intervention is targeting[59].

PC feedback offers specific advantages. Using PCA to reduce the dimensionality of visual feedback presents a solution to the high-dimensionality of learning a new walking pattern. Improved performance using this feedback requires concurrent improvement in multiple kinematic dimensions. For example, a subject that progresses

toward the goal pattern in one dimension but experiences an equal and opposite decline of performance in a different, equally-weighted dimension will not receive rewarding feedback for that particular set of kinematics. Thus, PC feedback constrains unwanted changes in kinematics while rewarding a change in walking pattern toward the prescribed goal on a whole-gait level. Additionally, PC feedback allows for simplicity of feedback such that participants can respond to an intuitive, low-dimensional form of feedback. They can simultaneously receive feedback of multiple aspects of their walking pattern without having the added attentional load of multiple streams of visual information. While both groups changed their walking pattern toward the prescribed goal pattern, the current results show participants receiving PC feedback displayed a faster and more complete change in performance than those receiving visual feedback containing four concurrent streams of kinematic information. Our primary measure of performance is the step-by-step difference from goal in PC space as this metric incorporates the aggregate performance from the individual weighted kinematic dimensions. This metric can be considered a standardized deviation from the prescribed goal pattern on a whole-gait level. We were able to see differences between PC feedback and Cartesian feedback when comparing single sessions of training. Thus, PC feedback has good potential for training a new set of walking kinematics more effectively than Cartesian feedback.

A key attribute of both feedback types in this study was temporal specificity of performance feedback. For participants to gain the most information from the visual feedback, we had to ensure that they could meaningfully assign a change in feedback performance to a change in their kinematics. For this reason, we chose to display two discrete measures of performance per stride (i.e. at left and right heel strikes) that

contained information during the most informative portion of the gait cycle needed to reach the goal pattern (i.e. mid-swing). As such, the visual feedback relayed the performance of the step immediately preceding its presentation. This temporal specificity introduces an additional constraint to participants' performance that most other gait retraining studies do not consider. A majority of studies using visual feedback to alter gait focus on scanning the entire gait cycle for either peak or endpoint kinematics[46,48,55,59,60,92,113]. While participants may be able to improve their performance using this feedback, gait deficits are often temporally specific within a given stride[114,115]. Thus, we wanted to address not only the extent to which they are adjusting their walking pattern but also constrain when they are making these adjustments.

The findings presented here also highlight the importance of selecting an appropriate goal pattern. In our first condition, we demonstrate that participants can use PC feedback to improve performance within the selected time-windows (Figure 3.3A and Figure 3.4). However, we observed imperfect performance in portions of the swing phase outside of the time-windows (Figure 3.5). Indeed, our original intention was to create an algorithmically generated goal to bias participants in the direction of the goal kinematics, not necessarily to achieve a perfect match. However, we contend that our original, algorithmically generated goal required coordination at the hip and knee joints that was not easily attained, which hindered achievement of the exact set of ankle kinematics over the entire stride cycle. To prove that the observed limit in performance in the original PC group was due to goal selection and not a product of the feedback, we observed a second condition in which our goal kinematics were adjusted to a more natural ankle trajectory (Figure 3.6). Subsequently, participants were able to use PC feedback to more closely

achieve the goal over the entire gait cycle (Figure 3.7). Thus, given an appropriate goal walking pattern, participants are capable of using PC feedback to match an exact set of kinematics.

A number of previous studies have used visual feedback to alter sagittal plane ankle trajectories[51,116-118]. The novelty of this study lies in the type of feedback used to bias the participants in the direction of the goal kinematics. We selected these kinematic features as a method for testing PC-based feedback in a healthy population. Ultimately, PC feedback can be used for any variety of kinematic features in any desired plane of movement. The only necessary ingredient is a goal template for the chosen kinematic features that differs from the current movement. Given the goal template, the feedback will algorithmically weight the most relevant features of movement and feedback the performance in an intuitive, summary format. We believe this feedback has applicability to a wide range of fields—from motor rehabilitation to athletic performance.

While this study reveals promise in PC feedback as a viable method for teaching multiple temporally-specific aspects of walking, there are some limitations. Because we did not test for participants' ability to retain the modified walking pattern, we are hesitant to term their improved performance 'learning'. Additionally, this study does not test for the generalization of this modified pattern to other walking patterns or other environmental contexts (e.g. overground). Many past studies have described using visual feedback to modify gait as skilled locomotor learning[49,51,117,119]. Our results and methodology compare favorably to these past studies; thus, we can best describe our task as a skilled motor task. While participants can use PC feedback to improve task performance, more studies are needed to test for the long-term retention and

generalization of the modified walking pattern for us to confidently conclude PC feedback induces learning. Indeed, our goal for this study was to use the feedback to increase performance using a variety of visual feedback types and compare performance across feedback types.

We think that these results have potential implications for both healthy and pathological movement. We have created a novel visual feedback system for teaching multiple aspects of modified walking pattern in an intuitive, low-dimensional way. The current results demonstrate how we can more effectively deliver multiple streams of kinematic information for the users to change their walking patterns toward a prescribed goal. Thus, if we have a high-dimensional, coordinated movement we would like to train, PC feedback can bias users toward that movement in a low-dimensional, digestible way. For healthy movement, this could mean training a more efficient running style, a modified golf swing, or altered free-throw shooting mechanics, among others. Furthermore, if we consider gait disorders that contain multiple kinematic abnormalities, PC-based feedback may present a viable method for teaching a new set of kinematics toward a more 'healthy' gait pattern. Consider, for example, a patient with stiff-knee gait following stroke. Beyond decreased knee flexion, stiff-knee gait typically presents with multiple kinematic abnormalities such as hip circumduction, vaulting, or pelvic tilt[24,25]. PC-based feedback offers a method for not only addressing the primary deficit (i.e. decreased paretic knee flexion) but also simultaneously addressing the accompanying deficits/compensatory movement. Ultimately, we aim to apply these findings to the rehabilitation of those with gait disorders.

Chapter 4 Persons post-stroke can use principal component-based visual feedback to bias multiple features of gait toward a prescribed walking goal

4.1 Introduction

Gait impairment following stroke often presents with multiple deficits. Some of the most common include decreased paretic leg knee flexion during swing, hip circumduction, step length asymmetry, pelvic tilt, and decreased ankle dorsiflexion[23-27]. Due to limited resources (e.g. patient time/finances, therapist time, etc), therapists are confronted with the challenge of prioritizing these deficits, using their judgment to select which is the most important to address in order to best improve walking function and independence. Not only does this process leave some deficits unaddressed, but addressing one deficit in isolation of the others may introduce unintended compensations that further impair gait. Thus, there remains a need for both the systematic prioritization of deficits and improvement in the efficiency of training so as to simultaneously address multiple patient-specific deficits.

Real-time visual feedback of gait kinematics has proven useful in altering targeted features of gait in healthy and neurological populations[46-51]. For example, Cherry-Allen et

al. used visual feedback of joint angles to individually alter peak knee angle while adapting to a split-belt treadmill perturbation in persons post-stroke[55]. Moreover, visual feedback has been effective in improving gait speed, stride length, and stride width in people post-stroke[56-58]. Still, protocols using visual feedback of kinematic gait parameters have two prominent issues when looking to improve individual patient deficits: 1) they are focused on altering one feature of walking while leaving others unconstrained and 2) they are predicated on the assumption that the targeted parameter is the priority deficit for an entire group of patients. Given the heterogeneity of deficits following stroke, it would be most beneficial to have a system that can accommodate a wide array of walking patterns.

We developed a novel method to generate individualized, yet simple, visual feedback for re-training walking on a treadmill. An innovative element of this process is the use of real-time principal component analysis (PCA) to display a simple 'summary' of a multi-dimensional movement pattern that continuously updates on a screen in front of participants as they walk. The question that we ask here is whether this novel visual feedback system can address multiple deficits simultaneously, as well as individualize the training to be specific to a patient's particular set of deficits. For stroke patients, we established a goal walking pattern that included four kinematic dimensions (bilateral hip and knee joint angles) of an average 'healthy' walking pattern. Each of the four kinematic dimensions was individually weighted based on a participant's baseline deficits (defined as the difference between baseline walking and the goal walking pattern). Thus, weights varied across participants and were specific to their deficit.

The primary objective of this study was to evaluate the efficacy of our novel visual feedback in altering gait post-stroke. Thus, to contrast performance of participants with chronic stroke who received a control goal walking pattern (i.e. stroke-to-control), we evaluated the performance of healthy, age-matched controls who receive a hemiplegic goal walking pattern (i.e. control-to-stroke) using the same visual feedback. This contrast allows us to further validate our method by investigating the extent to which performance in our participants with chronic stroke was limited by neurological injury compared to limitations imposed by the method itself. We hypothesized that participants in both groups would be able to use this summary visual feedback to simultaneously alter multiple aspects of their gait (albeit to varying extents depending on their impairment) toward the prescribed goal pattern while walking on a treadmill.

4.2 Methods

4.2.1 Participants

Ten adults with chronic stroke (3 female; age: 59.0 ± 7.4 yr) and ten group age-matched neurologically intact adults (7 female; age: 57.3 ± 6.8 yr) were recruited for this experiment. All participants with chronic stroke met inclusion and exclusion criteria (Table 4.1). All participants provided written, informed consent before taking part in the experiment. The experimental protocol was approved by the Johns Hopkins Medicine Institutional Review Board.

4.2.2 Clinical assessments

Participants with chronic stroke underwent clinical examination prior to the experiment. To quantify motor impairment we administered the lower extremity subscale of the Fugl-Meyer test (FM-LE)[120]. This test includes 17 items scored on an ordinal scale

(0-2) with 34 possible points and higher scores representing less impairment. We measured self-selected and fast over ground walking speeds by having participants walk two passes at each speed across a six-meter electronic walkway (Zeno Walkway, ProtoKinetics, Havertown, PA). Baseline knee and hip flexion angles, used to determine study eligibility, were measured using motion capture while participants walked on the treadmill at their self-selected speed. Participants who customarily wore an ankle-foot orthosis continued using these items throughout the study.

We also tested for sensory impairment in participants with chronic stroke. For proprioception testing, participants were supine with their eyes closed. The examiner stabilized the proximal joint segment and passively moved the distal segment to a position above or below the neutral starting position (neutral position was midway through the joint's range of motion). The participant reported whether the position of the specified joint was above or below the starting position. Paretic hip, knee, and ankle joints were each tested at six different positions (18 total probes). Participants with stroke also completed The Star Cancellation Test, a screening tool that detects the presence of unilateral spatial neglect[121]. Scores less than 44/54 stars cancelled is suggestive of unilateral spatial neglect.

We assessed cognitive function in both participants with chronic stroke and control participants using the Montreal Cognitive Assessment (MoCA)[122]. Scores greater than 26/30 possible points reflect normal cognitive function.

Inclusion criteria	Exclusion criteria
1. Diagnosis of ischemic or hemorrhagic stroke*	1. Neurological condition or injury other than stroke $^{\Delta}$
2. Ambulatory with or without an assistive device $^{\Delta}$	2. Uncontrolled hypertension (>190/110 mmHg)
3. Persistent lower extremity hemiparesis with a score of <34 on the lower extremity subscale of the Fugl-Meyer	3. Cerebellar signs or evidence of cerebellar involvement*
4. Gait speed > 0.40 m/s	4. Pregnancy $^{\Delta}$
5. Paretic leg peak knee flexion < 55 degrees	5. Orthopedic or other medical condition that could compromise walking performance$^{\Delta}$
	6. Unable to give informed consent
	7. Unilateral spatial neglect (Star Cancellation Test score <44/54)

Inclusion and exclusion criteria were determined through standard clinical examination procedures as described in the methods, unless otherwise indicated. *information confirmed by a neurologist and/or magnetic resonance imaging (MRI) reading; Δ information determined by self-report

Table 4.1 *Inclusion and exclusion criteria for stroke patient population.*

4.2.3 Motion analysis

We recorded participants' kinematics using an Optotrak Certus motion capture system (Northern Digital, Waterloo, ON) as they walked on a split-belt treadmill (Woodway, Waukesha, WI). The split-belts allowed us to detect right and left foot contacts via distinct force plates, but the belt speeds were equal throughout all experiments. Kinematic data were collected at 100 Hz from 12 infrared-emitting diodes placed bilaterally on the foot (fifth metatarsal head), ankle (lateral malleolus), knee (lateral epicondyle), hip (greater trochanter), pelvis (iliac crest), and shoulder (acromion process; Figure 4.1A).

4.2.4 Experimental design

The study included 2 groups of participants (stroke-to-control and control-to-stroke). Stroke-to-control consisted of participants with stroke who received a control goal walking pattern (Figure 4.1B). Control-to-stroke consisted of neurologically intact participants who received a stroke goal walking pattern (Figure 4.1C). Both groups participated in two sessions at least 3 days apart (time between session: 46 ± 45 days for stroke-to-control, 30 ± 10 days for control-to-stroke) and received the same type of visual feedback (explained below in *Visual Feedback* subsection). During session 1 (visual feedback + exploration, Figure 4.2), participants did not receive information about the goal walking pattern and were instructed to use the visual feedback to explore ways in which to improve their performance. During session 2 (visual feedback + instruction, Figure 4.2), participants were instructed of what to change from their baseline walking in

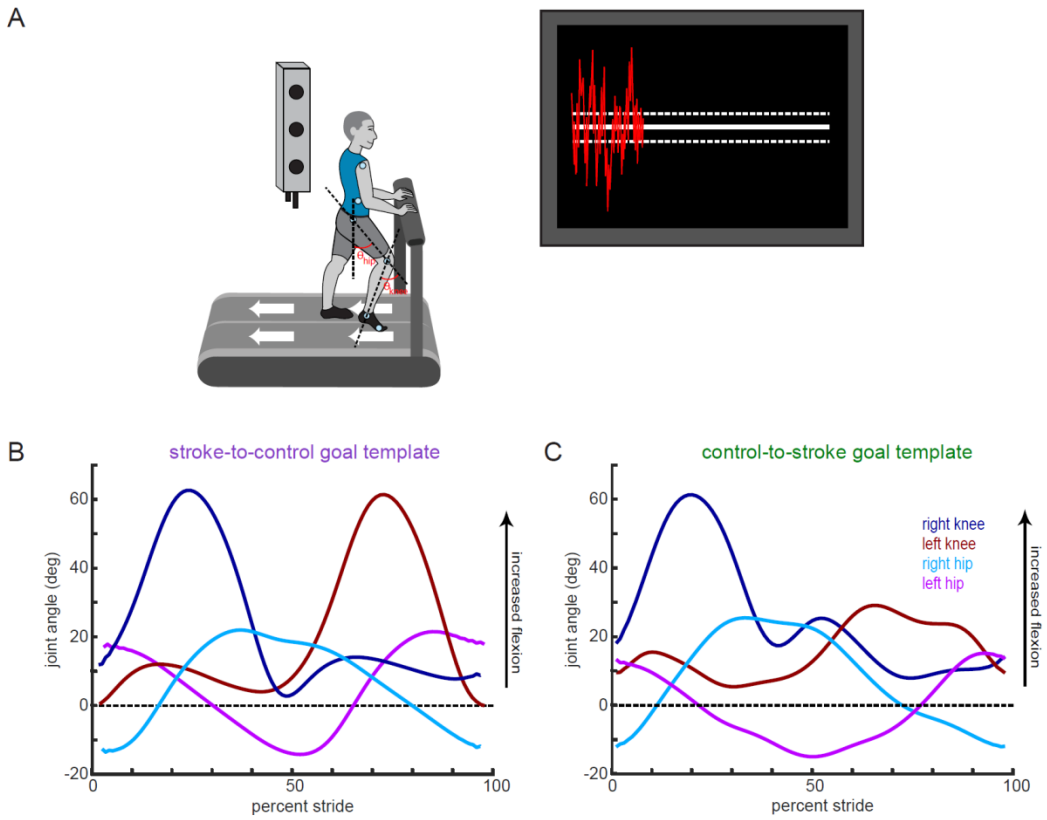

Figure 4.1 *Experimental set-up, visual feedback display and goal walking patterns*. **A)** Marker placement and general set up for motion capture. Bilateral, sagittal-plane hip and knee angles were calculated from the marker positions in real-time. These angles were fed into an algorithm to condense the information into a single dimension. The visual display that participants received is displayed on the left. Participants were instructed to minimize the deviation between their feedback performance (red trace) and the center white target line. Dashed lines around the target line correspond to the success zone. **B)** Stroke-to-control goal template consisting of the bilateral hip and knee angles of an average control participant while walking. Persons post-stroke improved their performance using the visual feedback by more closely matching this set of kinematics. **C)** Control-to-stroke goal template consisting of the bilateral hip and knee angles of an exemplar patient post-stroke with hemiparetic gait affecting the left side. Control participants improved their performance using the visual feedback by more closely matching this set of kinematics.

order to progress toward the goal walking pattern and improve their performance using the visual feedback. Session 2 was intended to investigate 1) if participants' Session 1 performance was limited by incomplete exploration and 2) if the visual feedback offered additional improvement over verbal instruction.

4.2.5 Goal walking pattern calculation

Participants in the stroke-to-control group received a control goal walking pattern while participants in the control-to-stroke group received a stroke goal walking pattern. These goal walking patterns consisted of the sagittal plane knee and hip angles for both legs. We defined knee angle as the angle between the vector connecting the hip and knee marker and the vector connecting the knee and ankle marker (Figure 4.1A). We defined hip angle as the angle between the vector connecting the hip and knee marker and a vertical vector (Figure 4.1A). The control goal walking pattern was obtained by averaging the baseline walking of 10 neurologically intact individuals who did not take part in this study (Figure 4.1B). This control goal walking pattern was collected at 1 m/s. The stroke goal walking pattern was obtained by taking the baseline walking of an exemplar participant with stroke who displayed decreased paretic leg knee and hip flexion during swing (Figure 4.1C). This participant was walking at his self-selected speed (0.885 m/s).

We chose to focus on altering kinematics during swing on each leg because kinematics during stance are largely constrained by the speed of the treadmill belts. Therefore, we set the goal during stance for each individual to the kinematics observed during their baseline walking. To obtain the individualized goal during swing, we

resampled the goal templates over the stride time of the particular individual (Figure 4.3B-C).

4.2.6 Visual feedback

All participants received the same visual feedback over the two sessions. This feedback consisted of a principal component-based visual feedback in which information from the four kinematic dimensions (bilateral knee and hip angles) was condensed to a one-dimensional summary of performance.

Bilateral lower limb marker positions were sampled from the Optotrak software and fed into a custom Python program in real-time. From these positions, we calculated sagittal plane hip and knee angles over the stride cycle. Visual feedback was displayed using a Vizard development environment (WorldViz, Santa Barbara, CA) and reflected the participants' step-by-step deviation from the desired pattern. This real-time information was displayed in a simple format, such as a trace that moves in and out of the prescribed goal zone on a screen (defined as ± 0.25 a.u., Figure 4.1A). The feedback reflected the participants' deviation from a white 'target' line on the TV screen and we instructed subjects to change their pattern such that this deviation was minimized. As such, a participant who matches the goal pattern exactly (i.e. difference of zero) would receive feedback on the white target line. The visual feedback was updated upon each heel strike (i.e. two new data points per stride) and tracked across the TV screen so that participants had information of their current and past performance.

The principal component-based feedback individually weighted each of the input kinematic dimensions. These loadings were calculated from baseline walking by submitting the difference between baseline and goal kinematics (i.e. the deficit) to the

PCA (Figure 4.3A). Thus, real-time performance in PC space could be calculated by a vector multiplication of the real-time deficit (i.e. difference between current kinematics and goal) and the loadings (Figure 4.3A). Loadings were kept constant across all sessions so that the participants had a constant mapping between a change in their kinematics and their feedback performance.

While using the visual feedback, locking stride time was necessary as we had to set a length of time for the goal stride from which to compare real-time performance. Thus, we used a metronome to standardize the participants' walking stride time. Participants were instructed to heel-strike in rhythm with the beat from the metronome. The metronome pacing was calculated from each individual's average stride time during baseline walking.

4.2.7 Experimental paradigm

Participants walked on a custom-built treadmill which was also controlled through Vizard. For stroke-to-control, walking speed was set to participants' self-selected walking speed for all walking trials (the belts were always tied at the same speed). For control-to-stroke, walking speed was set to the selected speed in which the exemplar stroke kinematics were collected (0.885 mm/s). Participants were instructed to stand in the middle of the treadmill with one foot on each belt so that we could detect heel strikes from the force plates for visual feedback display. They wore a safety harness that was suspended from the ceiling to protect against the risk of falling. The harness did not provide any body weight support. All participants were allowed to hold on to a handrail in front of them (Figure 4.1A).

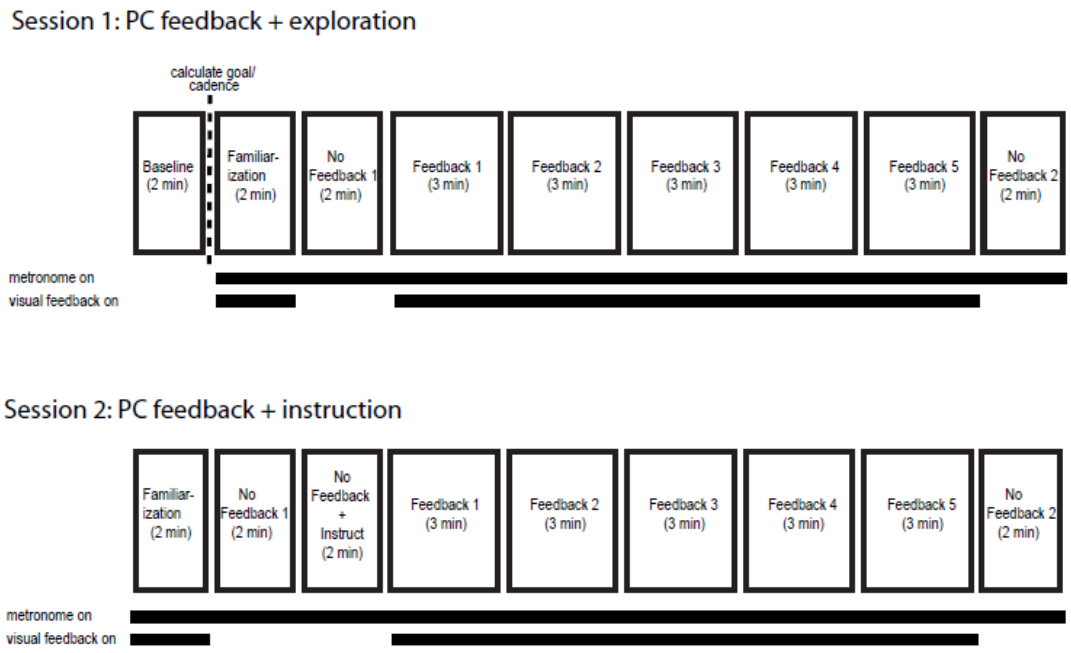

Figure 4.2 *Experimental paradigm*. Participants completed two sessions using PC feedback. During session 1, participants were instructed to use the visual feedback to explore ways in which they could more closely match the goal kinematics. During session 2, participants were explicitly instructed of how they must alter their walking pattern in order to more closely match the goal kinematics. Participants received 5 three-minute blocks of visual feedback in each session.

Session 1 (PC feedback + exploration) consisted of 9 walking blocks (Figure 4.2). *Baseline*: 2 minutes of walking naturally. From this block, we calculated the goal walking pattern and goal stride time. *Familiarization:* 2 minutes of walking with the visual feedback and metronome. The goal walking pattern was set to each individual's baseline kinematics and participants were informed that performance during this block did not matter and they were free to explore using the feedback. *No Feedback 1:* 2 minutes of walking naturally to the beat of the metronome. Participants did not receive performance feedback. This block served as our measure of baseline performance. *Feedback 1-5:* 5 identical, 3 minute blocks of walking while responding to the visual feedback. Participants were instructed to change their walking pattern to get as close to the target line as possible. Importantly, participants were not informed of the goal walking pattern and were instructed to use the visual feedback to determine which walking patterns improved their performance. Participants were free to take rests (either sitting or standing) in between blocks. *No Feedback 2:* 2 minutes of walking without the visual feedback but still in rhythm with the metronome. Participants were instructed to replicate the walking pattern that maximized their performance during the preceding feedback blocks. This block served as our measure of retention of performance.

Session 2 (PC feedback + instruction) was similar to Session 1 with the exception of an included *No Feedback + Instruct* block following *No Feedback 1* (Figure 4.2). During this block, participants were explicitly told how to change their walking to more closely match the goal kinematics. For example, control-to-stroke was told to stiffen their left leg (i.e. keep their hip and knee more extended during swing) while walking naturally with their right leg. Instructions for the participants in stroke-to-control depended on the

individual deficit and were directional in nature (i.e. more, less, faster, slower, etc). For example, a participant with deficits in paretic leg flexion and no deficits on the nonparetic leg would be instructed to keep their nonparetic leg constant while bending their paretic knee more and bringing their paretic hip through faster during swing. The *No Feedback + Instruct* block was intended to measure the influence of solely verbal instruction on participants' performance. Thus, participants did not receive visual feedback during this block. For *Feedback 1-5,* participants were reminded of the instruction prior to each of these feedback blocks and were instructed to use the visual feedback to hone in on the exact goal walking pattern we were instructing. Session 2 was designed to observe whether incomplete exploration had limited performance during Session 1.

4.2.8 Data analysis

Our primary measure of performance is the mean difference from goal in PC space (measured in arbitrary units) over the course of training. This measure gives a standardized step-by-step difference between the current performance and the prescribed goal pattern and is calculated as a linear transformation from the real-time kinematics using the individualized loadings (Figure 4.3A). These differences are calculated and averaged over the rewarded time window (100 millisecond windows centered approximately around mid-swing of each leg; displayed as vertical dashed lines between 20-30 and 70-80 percent stride in Figure 4.3B-C). A value of zero represents perfect performance in which the current kinematics exactly match the goal walking pattern within the rewarded time windows. We calculated the difference between *No Feedback 1* and *Feedback 5* as our measure of training and the difference between *Feedback 5* and *No Feedback 2* as our measure of retention of performance. Two participants in stroke-to-

control did not experience a *No Feedback 2* block so our retention measure for session 1 was calculated for the remaining eight participants. We were able to collect all blocks for all participants in control-to-stroke. For session 2, we calculated the difference between *No Feedback 1* and *No Feedback + Instruct* to measure the effect of verbal instruction on performance. We also included a measure of training beyond instruction (difference between *No Feedback + Instruct* and *Feedback 5*) and a measure of retention (difference between *Feedback 5* and *No Feedback 2*). Due to travel restrictions, one participant from stroke-to-control was not able to return for Session 2. All participants in control-to-stroke were able to return for Session 2.

In addition, we measured specific kinematic features over the course of training. Specifically, we observed the hip and knee flexion angles within the rewarded time window. For clarity in reporting, we refer to the control participants' left leg as the 'paretic' leg and right leg as the 'nonparetic' leg as these terms correspond to the goal set of kinematics they are trying to match for the exemplar stroke walking pattern. We were also interested if training increased the amount of ankle clearance present in the stroke-to-control group. As such, we calculated the average step-by-step vertical dimension of the ankle marker during late swing of the paretic foot (defined as mid-swing to heel strike).

To better understand how participants were changing their kinematics during training, we conducted an analysis to calculate the percentage of steps taken outside of their natural walking variability. We defined this measure as *percent exploration*. To define each participant's natural walking variability, we calculated the paretic hip and knee flexion during mid-swing of each step within No *Feedback 1* and fit a 95 percent

confidence ellipse to those joint angles. For subsequent training blocks, we calculated what percentage of steps were both outside of this baseline confidence ellipse and resulted in improved performance (i.e. closer to the PC goal). This allowed us to obtain a single measure that quantified a participant's change in kinematics beyond their baseline walking for a given feedback block.

Participants were instructed to walk in rhythm with the metronome. We calculated stride time as the time between successive heel strikes (measured in milliseconds).

4.2.9 Statistical analysis

To identify differences between groups demographics (e.g. age, MoCA score, etc.) we used independent samples t-tests. When comparing loading values within and across groups, we used mixed-method, repeated-measures ANOVA with *dimension* and *group* main factors. A linear least squares regression was used to relate loading values to the deficit for individual kinematic dimensions in stroke-to-control. To ensure that participants remained within 60 ms (approx. 5 percent) of the prescribed stride time, we performed right-tailed, one-sample t-tests on the absolute difference between participants' stride times during all blocks of the experiment and the metronome beat interval against a null hypothesis of mean 60. As detailed in 'Data Analysis', we were interested in specific *a priori* performance measures in PC space across blocks (i.e. training, retention for session 1; instruction, training beyond instruction, and retention for session 2). We performed one-way t-tests on each of these measures to observe our performance changes.

When comparing each kinematic dimension across training in session 1 (i.e. *No Feedback 1* to *Feedback 5)*, we used paired sample t-tests. When performing this analysis for session 2 (now with *No Feedback 1, No Feedback + instruct,* and *Feedback 5* blocks included), we used repeated-measures ANOVA with a *block* main factor. To compare changes in joint angles across groups, we used mixed-method, repeated-measures ANOVA with *joint* and *block* within-subject factors and a *group* between-subject factor. To observe how these joint angle changes affected the end effecter (i.e. ankle) over training, we used a linear least squares regression on the ankle clearance during late swing over trials of training.

To compare *percentage exploration* across blocks and groups, we used mixed-method, repeated-measure ANOVA with *block* and *group* main factors. We performed a separate ANOVA for each session. For all repeated-measures ANOVA, we performed Mauchly's test of sphericity and used the Greenhouse-Geisser correction of degrees of freedom if sphericity was violated. We used a Bonferonni correction of multiple comparisons when performing our post-hoc analysis. All analyses were performed using SPSS 25.0 (IBM, Armonk, NY) and α–level was set to 0.05.

4.3 Results

Table 4.2 summarizes the demographic data for the stroke-to-control group. Participants in the control-to-stroke group were recruited to be group average age-matched to participants within the stroke-to-control group (t_{18}=-0.53, p=0.600). To test cognitive function, we collected MoCA scores for participants in both groups. Average scores for stroke-to-control were 23 ± 2.9 while average scores for control-to-stroke were

	1	2	3	4	5	6	7	8	9	10	Group
Age (years)	57	51	48	68	61	53	62	55	65	70	59.0 ± 7.4
Gender (male/female)	M	F	M	F	M	F	M	M	M	M	7/3
Time post stroke (months)	78	35	84	101	75	11	94	29	93	57	65.7 ± 31.1
Dominant side (right/left)	R	R	R	R	R	R	R	R	R	R	10/0
Paretic side (right/left)	L	L	L	R	L	L	R	L	L	L	2/8
Self-selected gait speed (m/s)	0.885	0.739	1.175	0.736	0.514	0.510	0.741	0.426	0.641	0.700	0.707 ± 0.214
Baseline paretic knee flexion (degrees)	41.1	33.5	49.3	34.4	35.4	48.9	36.5	9.3	28.4	31.4	34.8 ± 11.3
Baseline paretic hip flexion (degrees)	22.0	20.5	20.1	19.5	23.8	15.6	16.2	9.9	10.9	16.9	17.5 ± 4.6
LE-FM score	25	26	25	26	21	22	31	29	30	24	25.9 ± 3.3
Proprioception (intact/impaired)	+	-	+	+	+	+	+	-	+	+	8/2
MoCA score	26	26	30	30	21	27	27	23	23	27	26.0 ± 2.9
Return for session 2 (y/n)	y	y	y	y	y	y	y	n	y	y	9/1

Demographic data for individual subjects. Group data are means ± SD or counts. M: male, F: female; R: right, L: left; P: paretic, NP: non-paretic; LE-FM: Lower extremity subscale for the Fugl-Meyer; out of 34, higher is less impairment. Proprioception: out of 18 total responses (6 probes at 3 joints); +: intact indicates that all responses were correct, - : impaired indicates at least one response was incorrect. MoCA: Montreal Cognitive Assessment; out of 30, higher is less impairment.

Table 4.2 *Individual demographic information for stroke-to-control group.*

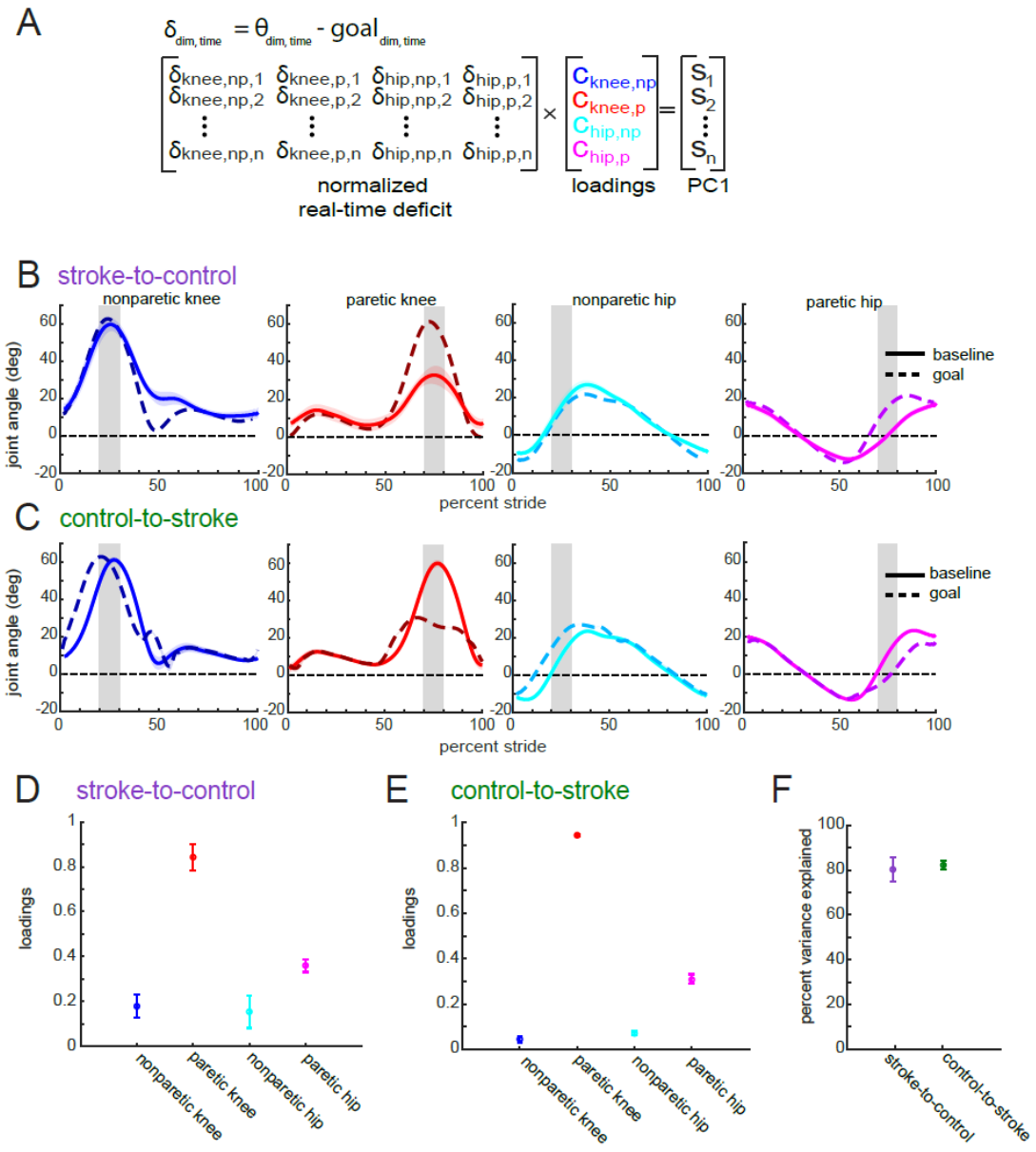

Figure 4.3 *Inputs for the calculation of real-time principal component for visual feedback display*. **A)** Loadings for each dimension were calculated by submitting each individual's baseline deficit principal component analysis (PCA). These loadings were used to calculate a real-time principal component (PC1) which is a vector multiplication of the normalized real-time deficit (defined as the difference between the z-scored real-time kinematics and the prescribed goal kinematics) and the loadings. **B)** Stroke-to-control group average baseline kinematics (solid traces) plotted against goal kinematics (dashed traces) for the four input dimensions. The shaded gray regions denote the rewarded time window during swing phase for that particular dimension **C)** Control-to-stroke group average baseline kinematics (solid traces) plotted against goal kinematics (dashed traces) for the four input dimensions. The shaded gray regions denote the rewarded time window during swing phase for that particular dimension. **D)** Stroke-to-

control group average loadings for the four input dimensions. **E)** Control-to-stroke group average loadings for the four input dimensions. **F)** Percent variance explained by the first principal component. All shaded errors and error bars denote SEM.

28.1 ± 1.0. Formally, MoCA scores in stroke-to-control were lower than those observed in our age-matched controls (t_{18}=2.14, p=0.047).

The goal of this experiment was to evaluate the use of principal component-based visual feedback to bias participants in the direction of a prescribed goal walking pattern. The feedback contained four input kinematic dimensions (bilateral hip and knee angles, Figure 4.3A). Notably, participants in both groups experienced the largest deficits in paretic knee and hip flexion (Figures 4.3B-C). On average, stroke-to-control needed to increase the amount of flexion during the rewarded time windows to approach the goal (Figure 4.3B) while control-to-stroke needed to decrease the amount of flexion observed during the rewarded time window (Figure 4.3C).

4.3.1 Patient-specific weighting of input dimensions

These general directional goals for each group are reflected in the loading values (Figure 4.3D-E). The loadings reflect the amount that each dimension is weighted when calculating the principal component (Figure 4.3A). A loading value of 1 corresponds to a highly-weighted dimension while a value of 0 corresponds to a dimension that is unweighted. Both the stroke-to-control and control-to-stroke groups are most heavily loaded on the paretic knee and paretic hip. Nonparetic knee and nonparetic hip are less heavily loaded for both groups. Specifically, a mixed-methods repeated-measures ANOVA with *dimension* and *group* main factors reveals a significant *dimension* effect ($F_{1.31,\ 23.56}$ = 183.27, p<0.001) in which post-hoc analysis shows the paretic knee is more heavily loaded than the nonparetic knee (p<0.001) and the paretic hip is more heavily loaded than the nonparetic hip (p<0.001). Additionally, the paretic knee is more heavily loaded than the paretic hip (p<0.001). Both groups have similar loadings across

dimensions as revealed by a nonsignificant *dimension x group* interaction ($F_{1.31, 23.45}$ = 1.78, p=0.193). These loadings produce a principal component that account for approximately 80 percent of the variance for both stroke-to-control and control-to stroke (t_{18}=-0.35, p=0.731; Figure 4.3F).

Determining the loadings based on the deficit for each input dimension allows for individualization of the visual feedback based on patient-specific deficits. Figure 4.4 displays the positive relationship (R^2=0.684, p<0.001) between the magnitude of a participant's deficit in a given dimension and the corresponding PC loading. Thus, participants in stroke-to-control who display varying levels of deficits in their baseline walking will receive higher loadings on the dimensions in which there exists greater discrepancy between baseline walking and the goal pattern. This patient-specific weighting provides an advantage when providing visual feedback in a stroke population, in which the deficits tend to be very heterogeneous.

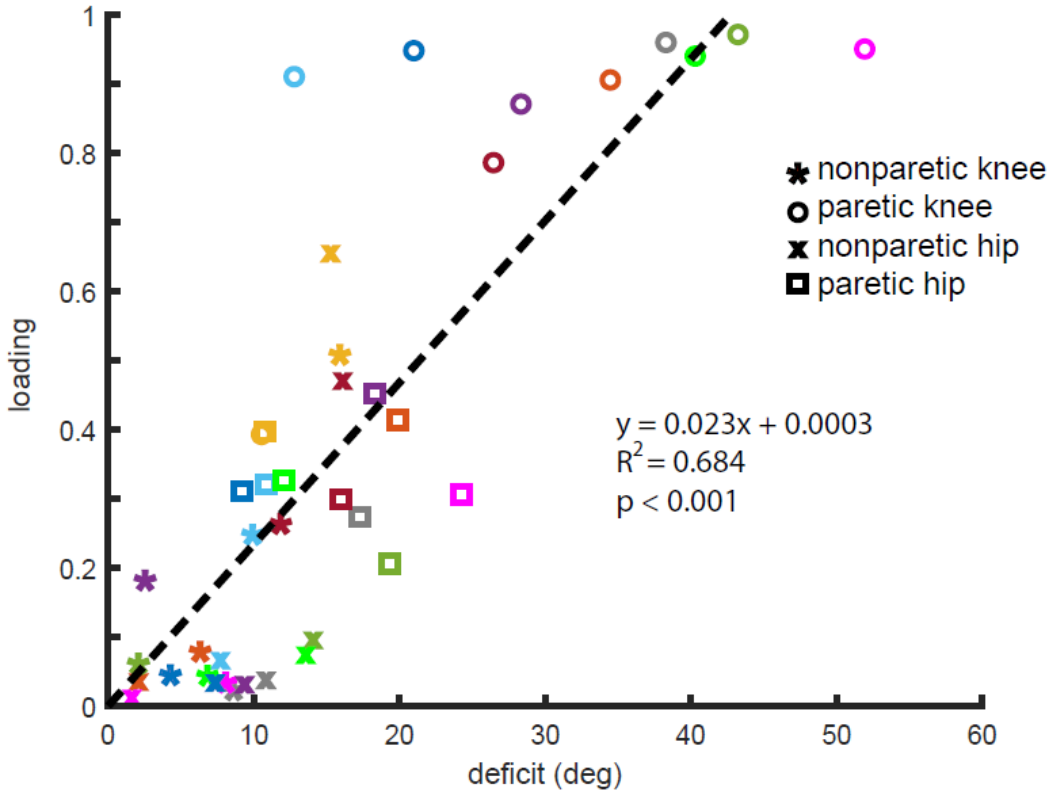

Figure 4.4 *Individualization of visual feedback based on baseline walking deficits in stroke*. Each participant is denoted by a separate color with different symbols corresponding to one of the four input dimensions. The dashed line corresponds to a best-fit linear relationship determined by least-squares linear regression. Note, the larger the deficit in a given dimension, the more heavily weighted it is when calculating the PC feedback.

4.3.2 Session 1 performance

Figures 4.5A and 4.5B display the stride times during all blocks of session 1 for stroke-to-control and control-to-stroke, respectively. Participants in both groups were able to stay within 60 ms (approx. 5 percent) of this prescribed walking cadence during all blocks (all $p>0.937$ for stroke-to-control, Figure 4.5A; all $p>0.065$ for control-to-stroke, Figure 4.5B). Thus, we are confident that participants were able to step in rhythm to the metronome beat while performing the task.

Our primary measure of performance was the stride-by-stride difference from the goal principal component (measured in a.u., Figure 4.5C, 4.5D). This measure is a composite of all weighted input dimensions. Thus, values closer to zero correspond to improved performance in this task. We were first interested in the effect of the feedback on performance (i.e. training) and used the difference in performance between *No Feedback 1* and *Feedback 5* to quantify this effect. Both stroke-to-control (t_9=4.16, p=0.003; Figure 4.5E) and control-to-stroke (t_9=-2.67, p=0.026; Figure 4.5F) showed significant improvement in performance due to training with the visual feedback. When comparing the absolute improvement across groups, we observed that the control-to-stroke group demonstrated a larger improvement in this measure than stroke-to-control (t_{18}=2.94, p=0.009). Both groups displayed similar absolute levels of performance at baseline (i.e. *No Feedback 1*; t_{18}=0.77, p=0.451).

We were also interested if participants in both groups were able to retain their level of performance when the visual feedback was turned off. During *No Feedback 2*, participants were instructed to replicate the walking pattern that allowed them to achieve their best performance while using the visual feedback. We used the difference in

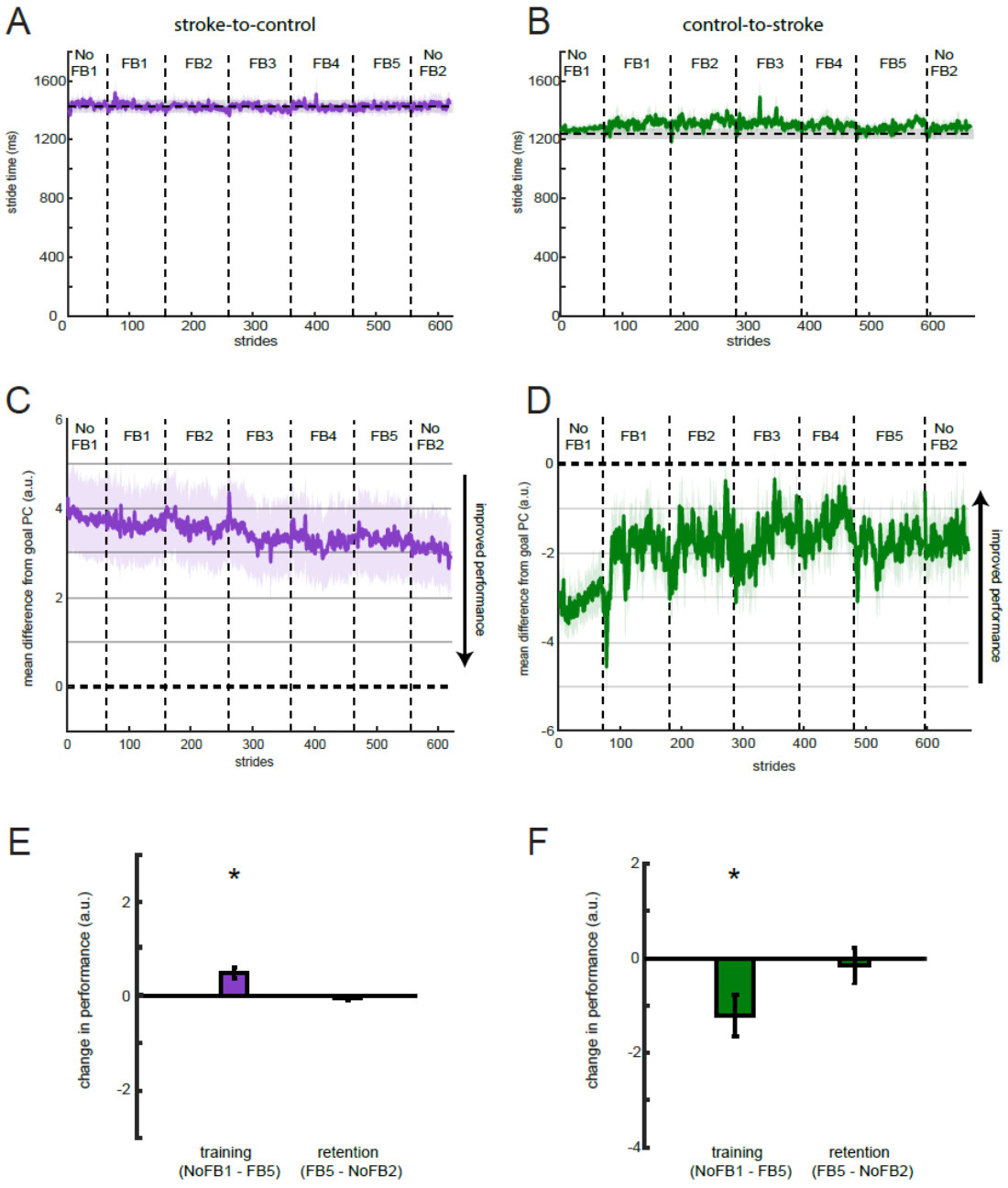

Figure 4.5 *Performance during session 1*. Stride times across blocks for **A)** stroke-to-control and **B)** control-to-stroke groups. The horizontal shaded dashed line corresponds to the group average ± SEM stride time provided by the metronome. Group performance in PC space for **C)** stroke-to-control and **D)** control-to-stroke groups. . Differences were calculated during the rewarded time windows for each step (i.e. mid-swing). Perfect performance is reflected by a value of 0. Measures of performance change are displayed for **E)** stroke-to-control and **F)** control-to-stroke groups. * denotes a significant change between blocks ($p<0.05$).

performance between *Feedback 5* and *No Feedback 2* to quantify this effect. Interestingly, performance did not deteriorate between blocks for either stroke-to-control (t_7=-1.40, p=0.203; Figure 4.5E) or control-to-stroke (t_9=-0.40, p=0.700; Figure 4.5F). Thus, both groups of participants were able to maintain performance despite the removal of visual feedback.

To observe which walking features participants were modifying during training, we analyzed each kinematic dimension separately. Figure 4.6 displays the kinematics over training for the paretic knee and paretic hip for both groups. To improve in the task, participants in the stroke-to-control group were required to increase flexion during swing in these dimensions while participants in the control-to-stroke group were required to decrease flexion during swing in these dimensions. We observed that participants were indeed able to adjust their kinematics toward the goal walking pattern over the course of training (Figure 4.6A-B). When comparing mean joint angles between *No Feedback 1* and *Feedback 5*, we observed that participants in the stroke-to-control group trended toward increasing flexion in their paretic hip (t_9=-2.08, p=0.067; Figure 4.6D) and showed a robust increase in flexion in their paretic knee (t_9=-4.13, p=0.003; Figure 4.6C). Participants in control-to-stroke demonstrated decreased flexion in the paretic knee (t_9=2.96, p=0.016; Figure 4.6C) but not the paretic hip (t_9=1.21, p=0.258; Figure 4.6D). Overall, we were able to demonstrate that PC feedback was successful in driving kinematics toward the respective goal for each group during a single session. That is, stroke-to-control tended to increase flexion in paretic hip and knee angles while control-to-stroke tended to decrease flexion in paretic hip and knee angles. Specifically, mixed-

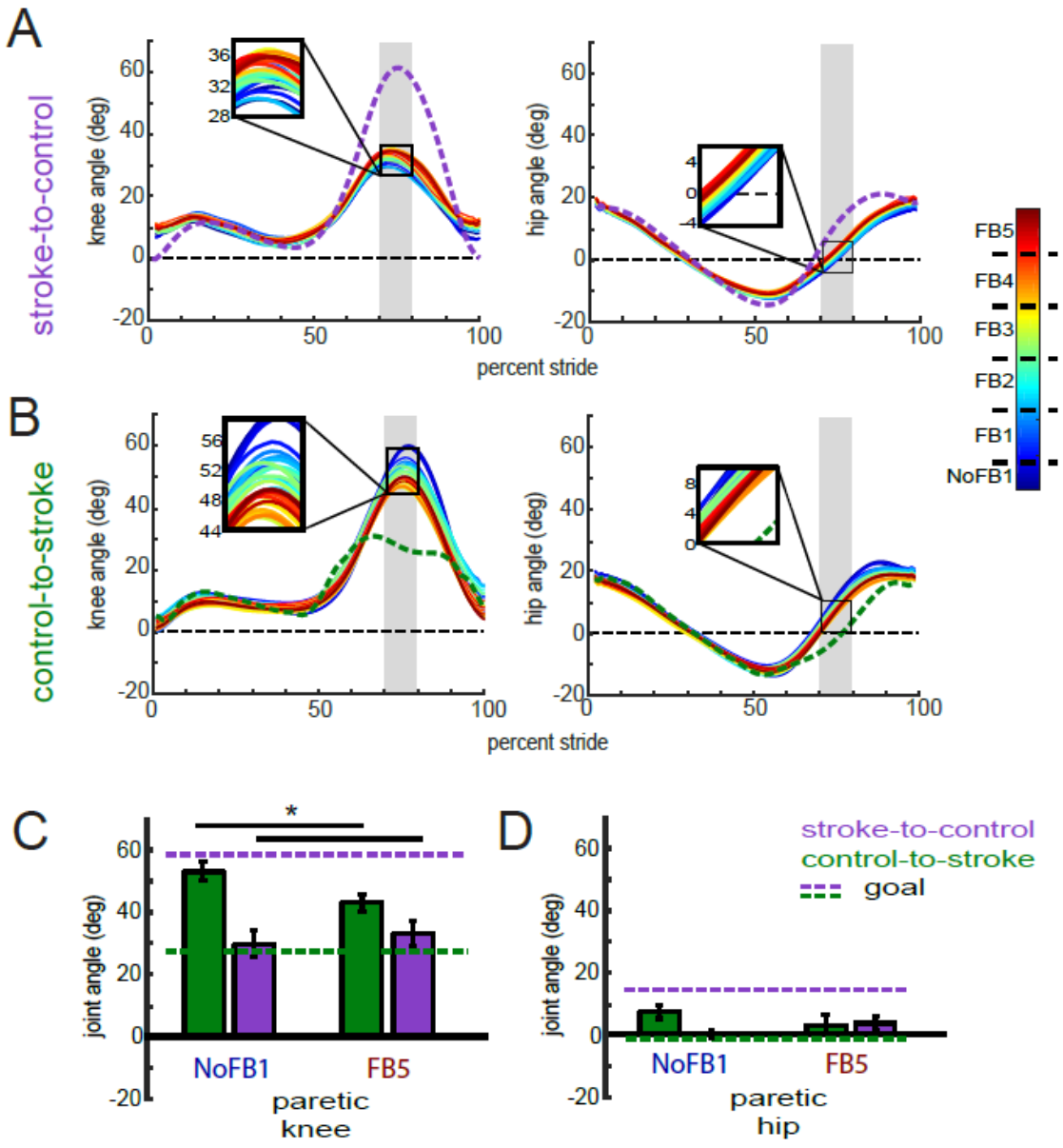

Figure 4.6 *Paretic leg kinematics during session 1*. **A)** Paretic knee (left) and hip (right) kinematics for stroke-to-control group. **B)** Paretic knee (left) and hip (right) kinematics for control-to-stroke group. Cold colors denote early training while warm colors denote late training. The shaded gray region denotes the rewarded time window during mid-swing. Insets display magnified kinematics during this time window. Colored dashed lines correspond to the goal kinematics for that given dimension. **C)** Group average paretic knee flexion angles within the rewarded time window during *No Feedback 1* and *Feedback 5* blocks. **D)** Group average paretic hip flexion angles within the rewarded time window during *No Feedback 1* and *Feedback 5* blocks. Colored dashed lines correspond to the goal for that given dimension (purple for stroke-to-control, green for control-to-stroke). * denotes a between-subject difference ($p < 0.05$) and all error bars denote SEM.

methods repeated-measures ANOVA with *block* and *joint* within-subject factors and a *group* between-subject factor revealed a *block x group* interaction ($F_{1,18}$ =9.28, p=0.007). Thus, participants in each group displayed directional bias in their kinematics toward their respective goal while using the feedback.

The combination of increased flexion in the paretic hip and paretic knee joints during swing can lead to an increase in the amount of vertical ankle clearance participants achieve over one session of training (Figure 4.7A shows example participant). Often, people with paretic gait experience decreased clearance during swing on their affected side (approx. 151 mm prior to training; Figure 4.7B), which can increase the risk of tripping. Here, ankle marker clearance is defined as the average vertical distance from the treadmill belt during late swing (i.e. mid-swing to heel strike). We chose ankle clearance instead of toe clearance because our visual feedback did not directly target ankle plantar/dorsiflexion; thus, the ankle is the end effecter for this particular training. Figure 4.7B shows that training using the PC visual feedback allows for participants to a gradual linear increase (R^2=0.447, p<0.001) in the vertical clearance of their ankle during late swing (0.158 mm/trial; 1 trial is 30 seconds of walking containing approx. 25 strides).

4.3.3 Session 2 performance

Figures 4.8A and 4.8B display the stride times during all blocks of session 2 for stroke-to-control and control-to-stroke, respectively. Similar to session 1, participants in both groups were able to stay within 60 ms (approx. 5 percent) of this prescribed walking cadence during all blocks (all p>0.316 for stroke-to-control, Figure 4.8A; all p>0.764 for control-to-stroke, Figure 4.8B).

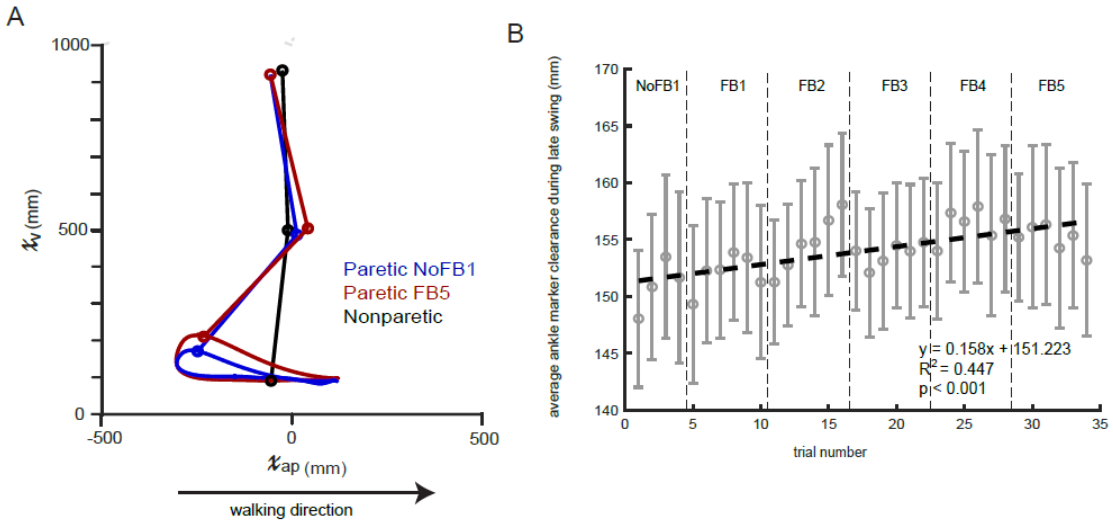

Figure 4.7 *Ankle clearance over training during session 1*. **A)** Sagittal plane ankle trajectory of example stroke patient prior to training (*No Feedback 1*, blue) and during late training (*Feedback* 5, red). Nonparetic leg is drawn in black. Notice the increased clearance during mid-swing as well as the cleaner heel strike during late training **B)** Average ankle marker clearance (defined as the mean vertical position of the ankle from mid-swing to heel strike) over training. The dashed black line is a linear fit calculated by a least-squares linear regression. Each trial on the x-axis corresponds to 30 seconds of walking (approx. 25 strides).

During session 1, participants were not explicitly told how to improve performance while using the feedback. They were told to rely on the feedback to explore walking patterns that progressed them closer to the goal. During session 2, we wanted to remove the potential limitations on performance due to exploration. Therefore, we provided instruction of the goal walking pattern and details of how participants could alter their baseline walking to improve their performance using the feedback. Figures 4.8C and 4.8D display performance in PC space during session 2 for stroke-to-control and control-to-stroke, respectively. As a measure of effect of verbal instruction on performance, we calculated the difference in PC space between *No Feedback 1* and *No Feedback + Instruct* blocks. Interestingly, stroke-to-control was not able to improve their performance over baseline (t_8=1.27, p=0.241, Figure 4.8E) while control-to-stroke experienced a large change in performance (t_9=-6.14, p<0.001, Figure 4.8F) and actually overshot the target, given the instruction. When given visual feedback to improve performance beyond the level observed due to solely verbal instruction, the stoke-to-control group was again unable to alter performance (t_8=-0.157, p=0.879, Figure 4.8E) while the control-to-stroke group was able to hone in on the goal pattern and use the visual feedback to improve their performance beyond instruction (t_9=3.24, p=0.010, Figure 4.8F). Once the visual feedback was turned off in *No Feedback 2* and participants were instructed to replicate the walking pattern that produced the best performance, participants in the control-to-stroke group were able to maintain the performance observed during *Feedback 5* (t_9=-2.15, p=0.06, Figure 4.8F) albeit performance actually trended toward the goal target (Figure 4.8D).

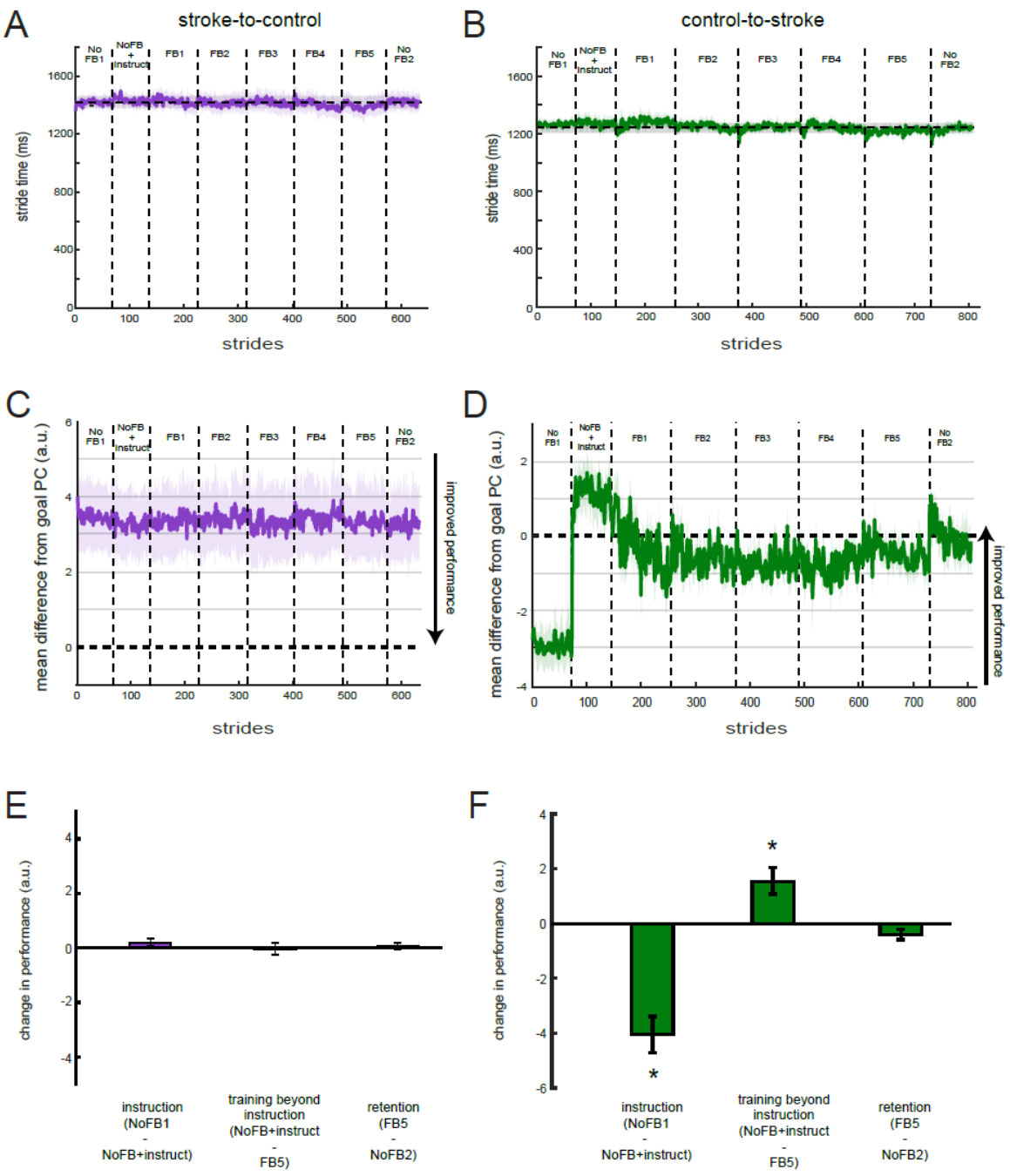

Figure 4.8 *Performance during session 2*. Stride times across blocks for **A)** stroke-to-control and **B)** control-to-stroke groups. The horizontal shaded dashed line corresponds to the group average ± SEM stride time provided by the metronome. Group performance in PC space for **C)** stroke-to-control and **D)** control-to-stroke groups. . Differences were calculated during the rewarded time windows for each step (i.e. mid-swing). Perfect performance is reflected by a value of 0. Measures of performance change are displayed for **E)** stroke-to-control and **F)** control-to-stroke groups. * denotes a significant change between blocks ($p<0.05$). All error bars denote SEM.

Notably, stroke-to-control was unable to alter performance beyond baseline during Session 2 (Figure 4.8B). We considered if this was perhaps due to participants within this group reaching a performance ceiling during session 1. Interestingly, baseline performance (i.e. *No Feedback 1*) during session 2 did not differ from performance observed at the end of training (i.e. *Feedback 5*) during session 1 (t_8=-1.83, p=0.104). We also considered the possibility that the one participant who could not return for session 2 (subject 8, Table 4.2) was responsible for driving the training effect observed during session 1. When removing this subject from analysis for session 1, we still observed a significant effect of training (t_8=3.88, p=0.005). Thus, it is possible that the lack of improvement during session 2 is due to a performance ceiling following session 1.

To gain additional insight into each group's performance during session 2, we analyzed the paretic hip and paretic knee angles over blocks of training (Figure 4.9A-B). We observed that while stroke-to-control was not able to change their paretic knee flexion ($F_{2,16}$=0.002, p=0.998; Figure 4.9C), they were able to increase their paretic hip flexion during swing ($F_{2,16}$=5.03, p=0.020; Figure 4.9D). Post-hoc analysis revealed that stroke-to-control experienced greater paretic hip flexion in *Feedback 5* than *No Feedback 1* by approximately 4.75 degrees (p=0.039; Figure 4.9D). Control-to-stroke experienced both a change in paretic knee ($F_{2,16}$=29.35, p<0.001; *NoFB1* vs *FB5* p<0.001; *NoFB1* vs *NoFB+instruct* p<0.001; *NoFB+instruct* vs *FB5* p=0.039; Figure 4.9C) and paretic hip angles ($F_{2,16}$=16.23, p<0.001; *NoFB1* vs *FB5* p=0.260; *NoFB1* vs *NoFB+instruct* p=0.001; *NoFB+instruct* vs *FB5* p=0.014; Figure 4.9D) across blocks. Indeed, participants within the control-to-stroke group overshot the goal walking pattern when

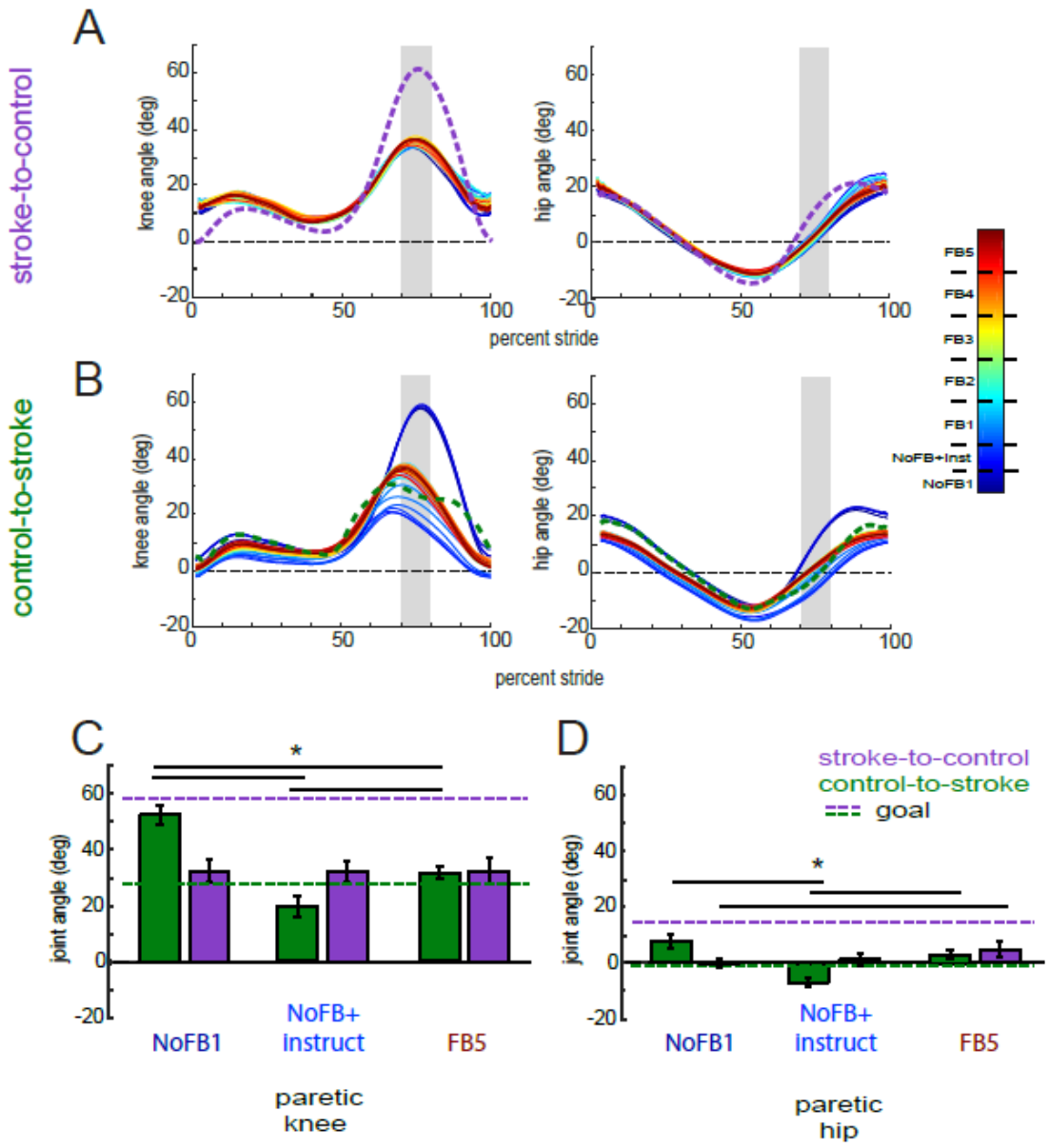

Figure 4.9 *Paretic leg kinematics during session 2*. **A)** Paretic knee (left) and hip (right) kinematics for stroke-to-control group. **B)** Paretic knee (left) and hip (right) kinematics for control-to-stroke group. Cold colors denote early training while warm colors denote late training. The shaded gray region denotes the rewarded time window during mid-swing. Colored dashed lines correspond to the goal kinematics for that given dimension. **C)** Group average paretic knee flexion angles within the rewarded time window during *No Feedback 1, No Feedback + Instruct,* and *Feedback 5* blocks. **D)** Group average paretic hip flexion angles within the rewarded time window during *No Feedback 1, No Feedback + Instruct,* and *Feedback 5* blocks. Colored dashed lines correspond to the goal for that given dimension (purple for stroke-to-control, green for control-to-stroke). * denotes a between-subject difference ($p < 0.05$) and all error bars denote SEM.

given solely verbal instruction and then were able to use the visual feedback to approach the goal in both the knee and hip (Figure 4.9B). When comparing stroke-to-control to control-to stroke performance using mixed-method repeated-measures ANOVA with *joint* and *block* within-subject factors and a *group* between-subject factor, we observed a significant *block x group* interaction ($F_{2,16}$=16.00, p<0.001). Therefore, we can conclude that groups differentially vary their joint angles over training during session 2.

4.3.4 Biasing movement outside of baseline walking

The purpose of the visual feedback was to bias participants away from their baseline walking pattern in the direction of the goal walking pattern. Thus, we wanted to quantify the percentage of steps in which participants were outside of their normal walking pattern during training using the *percentage exploration* metric. This metric describes the percentage of steps each participant experienced that was outside of their baseline variability for both paretic knee and hip flexion during mid-swing (defined as a 95 percent confidence ellipse from steps taken during *No Feedback 1*; blue ellipse, Figure 4.10A) as well as demonstrating improved performance in PC space relative to the mean performance seen during *No Feedback 1*. Figure 4.10A displays this calculation over training for an example participant from the stroke-to-control group. Each symbol represents flexion values from the paretic hip (x axis) and knee (left y axis) during mid swing for each step. The teal lines represent the combination of paretic hip and knee flexion angles that would represent the same deviation from the goal PC (right y axis). Recall that the goal, noted here as a pink dot, can be represented in joint angle or PC space—this figure displays it in both ways. This was done to highlight the fact that the PC goal is simply a linear combination of the joint angles. Recall that the mean difference

from goal PC was calculated with four input dimensions. Here, we focus on the paretic side joint angles. To condense this four dimensional calculation onto two dimensions for display, nonparetic flexion angles were set equal to the goal flexion angles. In this two-dimensional space, locking the nonparetic flexion angles would only result in a parallel shift in the teal performance lines and does not alter this analysis. The inset shows how we obtain our metric—steps both outside of baseline variability *and* closer to the goal PC (i.e. improved performance) are marked by an 'x' and steps within baseline variability or farther from the goal PC (i.e. diminished performance) are marked by an 'o'. The percent exploration is the proportion of improved performance steps over the total number of steps multiplied by 100.

Figure 4.10B displays group averages for *percent exploration* over the course of the session 1 of training. Although both groups were able to increase their percentage exploration over blocks during session 1, control-to-stroke was able to do so to a greater extent than stroke-to-control. Specifically, a mixed-method, repeated-measures ANOVA revealed a significant *block* effect ($F_{1.37,21.96}$=24.31, p<0.001), *group* effect ($F_{1,16}$=5.62, p=0.031), and *block x group* interaction ($F_{1.37,21.96}$=4.78, p=0.030). Blocks included in this analysis were *No Feedback 1, Feedback 5,* and *No Feedback 2.* Interestingly, post-hoc analysis revealed that stroke-to-control was able to reach a similar level of percent exploration compared control-to-stroke by the end of training (*Feedback 5*, p=0.056). However, a pairwise difference emerged during *No Feedback 2* (p=0.021).

Figure 4.10C displays group averages for *percent exploration* over the course of the session 2 of training. A similar mixed-method, repeated-measures ANOVA again

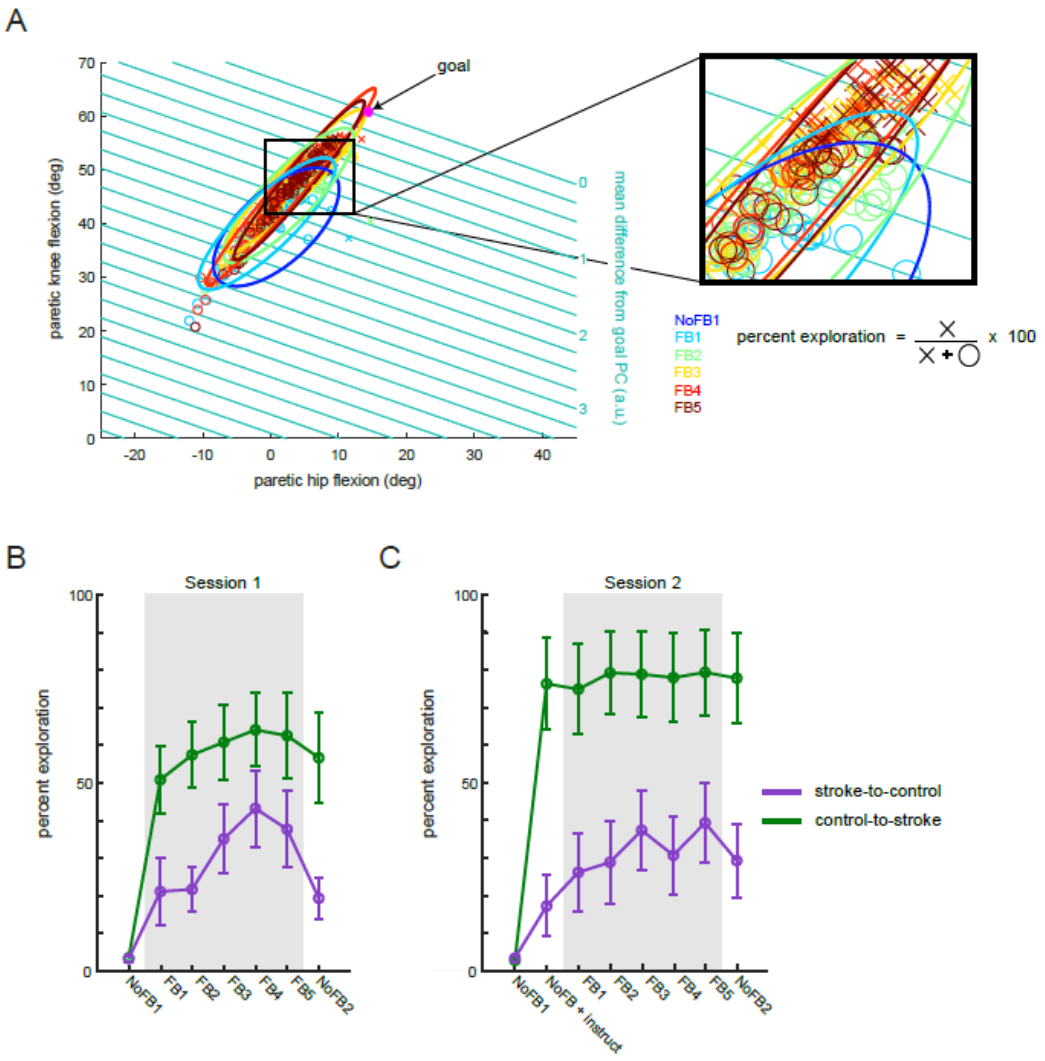

Figure 4.10 *Percentage of steps taken outside of baseline walking pattern*. **A)** Calculation of percent exploration metric for sample stroke patient. Blue ellipse corresponds to a 95 percent confidence ellipse for baseline (*No Feedback 1)* paretic hip and knee flexion angles. Parallel teal lines denote combinations of paretic hip and knee flexion angles that represent the same deviation from the goal PC. Steps in subsequent training blocks are marked with an 'x' if outside of the baseline ellipse and closer to the goal PC. Steps in subsequent training blocks are marked with an 'o' if inside of the baseline ellipse or further from the goal PC. The inset displays steps around the border of the baseline ellipse to highlight this separation. **B)** Percent exploration for stroke-to-control (purple) and control-to-stroke during session 1 of training. **C)** Percent exploration for stroke-to-control (purple) and control-to-stroke during session 2 of training. Shaded regions in B) and C) correspond to blocks in which participants received visual feedback while walking. Error bars denote SEM.

revealed a significant *block* effect ($F_{1.98,33.68}$=31.06, p<0.001), *group* effect ($F_{1,17}$=10.94, p=0.004), and a *block x group* interaction ($F_{1.98,33.68}$=8.07, p=0.001). Blocks included in this analysis were *No Feedback 1, No Feedback + Instruct, Feedback 5,* and *No Feedback 2*.Of note, control-to-stroke was able to reach a higher level of exploration during the *No Feedback + instruct* (p=0.001), *Feedback 5* (p=0.023), and *No Feedback 2* (p=0.007) than stroke-to-control. Still, stroke-to-control demonstrated an improved ability to explore beyond their baseline performance during *Feedback 5* (p=0.036). Interestingly, participants within stroke-to-control were not able to improve their percent exploration given solely verbal instruction (i.e. *No Feedback + instruct* vs *No Feedback 1*; p=1.000). Thus, stroke-to-control was able to improve the quality of their steps beyond baseline only once they were given additional training with the visual feedback during session 2.

4.4 Discussion

These results demonstrate that principal component-based visual feedback is effective in simultaneously improving multiple features of walking in people with stroke. Moreover, the improvements were specific to each individual's baseline walking deficits. Specifically, we found that people post-stroke were able to use the visual feedback to increase their paretic knee and hip flexion angles toward a more 'healthy' walking pattern. Additionally, a group of age-matched control participants were able to decrease their knee and hip flexion angle on a particular side to more closely match the goal kinematics of a hemiparetic walking pattern. This experiment investigated the use of the PC visual feedback when subjects were both unaware (Session 1) and explicitly aware (Session 2) of the goal walking pattern. Interestingly, while both groups were able to

improve their performance when using purely exploration to find a more correct solution to the task, only the healthy controls were able to take advantage of the explicitly provided instruction to further improve performance. People post-stroke were unable to improve their performance once given information of the goal walking pattern.

4.4.1 Patient-specific weighting of input dimensions

A key component of this novel visual feedback is its ability to individualize the performance feedback based on baseline deficits. Stroke often results in multiple deficits that negatively affect walking. Abnormal gait arises both from the direct consequences of neurological injury (e.g. decreased knee flexion due to paresis or spasticity[24-25]) or compensations that arise to mitigate the primary impairment (e.g. hip hiking or circumduction to compensate for decreased knee flexion during swing) [18]. This feedback algorithmically weights deficits in the inputted dimensions and is agnostic to whether they are due to impairment or compensation. Thus, the feedback guides participants to change multiple faulty features of their movement, whether from impairment or compensation, in order to achieve improved task performance. Figure 4.4 highlights this feature of the visual feedback in which the dimensions that show greater deficits tend to be weighted higher when calculating feedback performance. For example, we can contrast the subject labeled with gold symbols who displays baseline deficits in all four input dimensions to the subject labeled with pink symbols who displays significant baseline deficits in only the paretic joint angles. The gold subject will be prompted to change aspects of walking within both the nonparetic and paretic step while the pink subject will be prompted to change aspects of walking only within the paretic step in order to attain improved feedback performance. Note that the y-intercept of the best fit

line is near zero, indicating that dimensions which do not display deficits will not be weighted using this feedback.

4.4.2 Using PC feedback to alter multiple features of walking in people with stroke

We chose walking goals that necessitated each group to move in opposite directions so that we could demonstrate if the feedback led to differential changes in joint kinematics between groups. Indeed, we observed that the stroke-to-control group improved performance by increasing flexion angles while control-to-stroke group improved performance by decreasing flexion angles.

The group of control participants experienced a larger improvement in performance than the group of people with stroke. This is not unexpected due to the presence of neurological pathology in our stroke-to-control group. Not only did they display baseline kinematic deficits due to either impairment or compensation, we also observed a difference in baseline cognitive function between groups. Stroke-to-control had lower MoCA scores (23 ± 2.9), compared to those of control-to-stroke (28.1 ± 1.0). Indeed, previous research has shown that cognitive decline impairs participants' ability to improve in motor skill tasks[123-126]. Additionally, the 'deficits' imposed on the healthy control participants were due to our selected hemiplegic goal, which purposefully differed from healthy walking. Thus, healthy participants possessed a wider dynamic range to modify their walking pattern as they did not have the neurological constraints present in our stroke population. Although not explicitly tested, neurological damage following stroke places a limit on the capacity of some individuals to perform certain movements (e.g. achieve 60 degrees of paretic knee flexion while walking). Still, the

intention of the 'healthy' walking goal was to bias the patients with stroke toward a healthier walking pattern within their capacity and not necessarily to achieve perfect performance. Therefore, decreased relative performance by the stroke-to-control group could have been due to motor impairment, cognitive impairment, or most likely a combination of both.

Interestingly, both groups displayed immediate retention of the modified walking pattern when the visual feedback was removed (Figure 4.5). In the *No Feedback* 2 block, participants were instructed to continue walking in a way that allowed them to achieve their best performance during the preceding feedback blocks. This retention of performance demonstrates that participants had some level of explicit awareness of how they were modifying their walking patterns to achieve improved performance. These results highlight the utility of visual biofeedback. It allows participants to form an explicit connection between a desired outcome and their current motor output, beyond what is naturally available to them[52]. With this awareness, participants can self-correct aberrant features of gait. More work is needed to investigate retention over a longer time period and the effect of repeated, prolonged exposure to this type of visual feedback.

4.4.3 Adding movement-related instruction to PC feedback hinders performance in people with stroke

Control-to-stroke was extremely responsive to instruction (Figure 4.8D, F). In fact, they overshot the goal following an instruction to walk with a hemiplegic gait (i.e. stiff knee and hip). Subsequently, they were then able to use the visual feedback to hone in on the goal until their performance was near-perfect (Figure 4.8D). These results

demonstrate that this novel PC feedback is effective in training an exact set of kinematics for a multi-dimensional walking pattern.

The stroke-to-control group was unresponsive to instruction and was unable to improve their performance during Session 2 (Figure 4.8C,E). When observing the kinematics, stroke-to-control was unable to increase their knee flexion beyond baseline levels. They were, however, able to increase their hip flexion by the end of training (Figure 4.9D). Because the hip tended to be weighted less than the knee (Figure 4.3D), these increases in flexion angle did not translate as much to performance in PC space as would an increase in knee flexion.

These results are surprising to us as conventional therapy heavily relies on instruction (e.g. bend knee more during swing, bring hip through faster, etc) to alter features of gait[127]. Verbal cues have been shown to increase muscle activity in paretic muscles in walking post-stroke[128]. In this same study, however, verbal cues did not have an effect on restoring symmetrical gait[128]. Therefore, it is possible that patients were co-contracting and making more effortful movements in response to instruction but not actually changing the movement itself.

Perhaps, the inclusion of joint-based instruction in Session 2 shifted the participants' focus from external (i.e. improve performance using the visual feedback) to internal (i.e. try harder to bend my knee). In people post-stroke, verbal movement-related instructions has been shown to hinder motor performance compared to verbal task-related instruction[129]. Indeed, physical therapists tend to use more externally focused instruction during gait rehabilitation in stroke[127] as it has consistently shown to result in improved motor performance in healthy and pathological populations[130-132]. It appears that the shift

to internal focus limited performance in this skilled walking task in people post-stroke. While future studies with a cross-over design are needed to confirm this hypothesis, it is worth considering where focus is directed when delivering therapy to patients post-stroke.

4.4.4 People with stroke can use PC feedback to improve the quality of their steps during practice

Our analysis of percent exploration revealed that stroke-to-control was able to take a larger percentage of steps outside of their baseline walking during Session 1 and Session 2 (Figure 4.10B,C). This suggests that patients are able to increase the quality of their practice while using the visual feedback. That is, approximately 30-40 percent of their steps are closer to a healthier walking pattern than they experienced when walking naturally. Moreover, persons post-stroke appear able to maintain this higher quality of practice when the visual feedback is removed.

Previous work suggests that the greater repetition of high quality movements results in improved rehabilitation outcomes[133,134]. From a motor learning perspective, a greater proportion of improved steps represents promise for engaging mechanisms—namely use-dependent plasticity (UDP) and reward-based learning—that could lead to long term changes in the motor repertoire. UDP refers to the process in which movement history biases subsequent movements toward the repeated movement[135] and has shown to increase with the learning of skilled motor task[136]. Reward-based learning occurs when different movements are associated with varying task outcomes[5]. Subsequent movements are biased toward the previously rewarded movement[67]. In the context of this task, the patients are not only experience repetition of a 'better' walking pattern during training

but they are also being rewarded for that improved pattern (i.e. via improved performance feedback). Both UDP[137] and reward-based learning[138] mechanisms have been shown to be present after stroke, thus providing promise for using visual feedback as a tool for long-term gait rehabilitation. Although we attribute improvements in this short-term study to improved performance, it is possible that with increased repetition and longer-term training that we can engage these learning mechanisms.

4.4.5 Conclusion

Overall, these results suggest that our novel PC feedback is an effective tool for people post-stroke to correct multiple features of gait and attain repetition of higher quality steps during training. Moreover, the PC visual feedback described here allows for individualization of performance feedback. Even in a group of ten participants with chronic stroke, we observed a heterogeneous set of deficits. This algorithmic feedback accommodated this heterogeneity by weighting each walking feature accordingly to target patient-specific deficits. While long-term studies are needed to evaluate the use of PC feedback to more permanently alter gait, we believe these findings show promise for PC feedback as a tool for improving multiple patient-specific features of gait following stroke.

Chapter 5 General Conclusions

This work provides insight into how we can more efficiently alter a walking pattern. In Chapter 1, we investigated how we could deliver a novel perturbation to induce the most efficient storage of a motor memory over a 5-day training period. We introduced healthy participants to a split-belt treadmill environment, which induced adaptive learning mechanisms that result in a restoration of walking symmetry. We were able to characterize the storage (i.e. savings) of this modified walking pattern over five consecutive days of extended split-belt training. Previous work has demonstrated that savings of an adapted walking pattern is sensitive to both the abrupt introduction of the learning environment as well as the extended exposure to that environment[35]. The nervous system's ability to differentially respond to different parts of training (i.e. early training vs asymptotic performance) can allow us to tailor training regimes that can produce the most efficient learning. Here, we alter the balance of these two factors to condense training to a single day. We show that a training schedule that introduces four short bouts of adaptive learning on Day 1 yields equivalent savings on Day 5 as that of the original 5-day extended training group. Moreover, the savings demonstrated from quickly switching between adaptive and deadaptive environments on Day 1 produced greater savings on Day 5 than if the adaptive environment was delivered for one extended block on Day 1. These results underscore the influence of the initial large errors when the perturbation is first introduced on locomotor savings. By repeatedly introducing short bouts of the adaptive environment, we were able to take advantage of the nervous system's responsiveness to these large errors. In this condition, we observed equivalent

savings as daily, extended practice with just one-fourth of the training time over a 5-day span. Ultimately, we want to apply these findings to the rehabilitation of gait so that patients and therapists may achieve the desired rehabilitation outcome while maximizing training efficiency.

In Chapter 3, we investigated how we can most efficiently deliver visual feedback to modify multiple kinematic features of gait. We developed a novel visual feedback system that uses principal component analysis (PCA) to reduce the information from four kinematic dimensions to a single stream of summary visual feedback. We contrasted performance using this novel visual feedback to the performance of participants who received four concurrent streams of information for each of the included kinematic dimensions. Healthy participants who received the summary principal component-based feedback were able to attain a modified walking pattern more rapidly and completely than those who received four concurrent streams of visual information. These results demonstrate how we can more efficiently train a multi-dimensional movement in an intuitive, low-dimensional manner.

We believe these results have implications to healthy and pathological movement. Traditional motor training using visual feedback often targets one feature without constraining the entire movement. When training complex, multi-dimensional movements, the inclusion of multiple dimensions within the visual feedback could prove beneficial. However, introducing multiple streams of visual information may hinder performance due to the increased attentional load. Our novel visual feedback provides a method for incorporating weighted information from the relevant kinematic dimensions into a single stream of visual information. Indeed, this method leads to more rapid and

effective learning of a skilled walking task in healthy individuals. The algorithmic nature of this visual feedback allows for the inputted dimensions to be varied as long as we have a goal template for that dimension. PCA will weigh each of the dimensions such that the most information is retained for performance feedback. Therefore, we can envision PC feedback having application to a wide range of field in which we seek to alter complex movement (e.g. motor rehabilitation, sports, etc).

In Chapter 4, we demonstrated that our novel principal component-based visual feedback was effective in biasing multiple features of movement toward a prescribed walking goal in participants with chronic stroke. Visual feedback was individualized for each patient based on their baseline walking deficits. Because walking deficits post-stroke are heterogeneous in nature, this patient-specific targeting of deficits offers a distinct advantage over traditional visual feedback training. Often traditional visual feedback interventions are best suited for a particular set of patients with particular deficits, depending on the targeted parameter. This feedback circumvents the need of a 'one size fits all' visual feedback system and can accommodate the heterogeneity of gait deficits post-stroke.

We observed utility of PC-based visual feedback in allowing participants post-stroke to experience a larger proportion of steps that are closer to a 'healthy' walking pattern. We believe that using this visual feedback to bias participants in the direction of a selected movement goal offers a method for persons post-stroke to experience higher quality practice. While more investigation is needed to determine the long-term effects of this practice, we have demonstrated that persons post-stroke are able to use this novel feedback to alter multiple aspects of their walking pattern within a single session of is

flexible for any kinematic feature in any plane of movement, given a suitable goal movement template. Ultimately, we believe that principal component-based feedback is a promising tool for altering a wide array of patient-specific gait abnormalities in persons post-stroke and should be tested further for clinical viability.

Bibliography

1. Roemmich R.T. & Bastian A.J. Closing the loop: from motor neuroscience to neurorehabilitation. *Annu. Rev. Neurosci.* **41**, 415-429 (2018).
2. Kitago T. & Krakauer J.W. Motor learning principles for neurorehabilitation. *Handb. Clin. Neurol.* **110**, 93-103 (2013).
3. Krakauer J.W., Hadjiosif A.M., Xu J., Wong A.L., & Haith A.M. Motor learning. *Compr. Physiol.* **9**, 613-663 (2019).
4. Bastian A.J. Understanding sensorimotor adaptation and learning for rehabilitation. *Curr. Opin. Neurol.* **21**, 628-633 (2008).
5. Haith A.M. & Krakauer J.W. Model-based and model-free mechanisms of human motor learning. *Adv. Exp. Med. Biol.* **782**, 1-21 (2013).
6. Martin T.A., Keating J.G., Goodkin H.P., Bastian A.J., & Thach W.T. Throwing while looking through prisms. II. Specificity and storage of mulitple gaze-throw calibrations. *Brain*. **119**, 1199-1211 (1996).
7. Weiner M.J., Hallet M., & Funkenstein H.H. Adaptation to lateral displacement of vision in patients with lesions of the central nervous system. *Neurology*. **33**, 766-772 (1983).
8. Shadmehr R.& Mussa-Ivaldi F. Adaptive representation of dynamics during learning of a motor task. *J. Neurosci.* **14**, 3208-3224 (1994).
9. Mazzoni P. & Krakauer J.W. An implicit plan overrides an explicit strategy during visuomotor adaptation. *J. Neurosci.* **26**, 3642-3645
10. Tseng Y.W., Diedrichsen J., Krakauer J.W., Shadmehr R., & Bastian A.J. Sensory

prediciton errors drive cerebellum-dependent adaptation of reaching. *J. Neurophysiol.* **98**, 54-62 (2007).

11. Verghese J., LeValley A., Hall C.B., Katz M.J., Ambrose A.F., & Lipton R.B. Epidemiology of gait disorders in community-residing older adults. *J. Am. Geriatr. Soc.* **54**, 255-261 (2006).

12. Guralnik J.M., Ferrucci L., Simonsick E.M., Salive M.E., & Wallace R.B. Lower-extremity function in persons over the age of 70 years as a predictor of subsequent disability. *N. Engl. J. Med.* **332**, 556-561 (1995).

13. Studenski S. et al. Gait speed and survival in older adults. *JAMA*. **305,** 50-58 (2011).

14. Reisman D.S., Block H.J., & Bastian A.J. Interlimb coordination during locomotion: what can be adapted and stored? *J. Neurophysiol.* **94**, 2403-2415 (2005).

15. Morton S.M. & Bastian A.J. Cerebellar contribution to locomotor adaptations during splitbelt treadmill walking. *J. Neurosci.* **26**, 9107-9116 (2006).

16. Oviagele B. & Nguyen-Huynh M.N. Stroke epidemiology: advancing our understanding of disease mechanisms and thearpy. *Neurotherapeutics*. **8**, 319-329 (2011).

17. Goldie P.A., Matyas T.A., & Evans O.M. Deficit and change in gait velocity during rehabilitation after stroke. *Arch. Phys. Med. Rehabil.* **77**, 1074-1082 (1996).

18. Olney S.J. & Richards C. Hemiparetic gait following stroke. Part I: characteristics. *Gait & Posture*. **4**, 136-148 (1996).

19. Tang A. & Rymer W.Z. Abnormal force-EMG relations in paretic limbs of

hemiparetic human subjects. *J. Neurol. Neurosurg. Psychiatry*. **44**, 690-698 (1981).

20. Bourbonnais D. & Vanden Noven S. Weakness in patients with hemiparesis. *Am. J. Occup. Ther.* **43**, 313-319 (1989).

21. McComas A.J., Sica R.E.P, Upton A.R.M., & Aguilera N. Functional changes in motoneurones of hemiparetic patients. *J Neurol. Neurosurg. Psychiatry.* **36**, 183-193 (1973).

22. Dietz V. & Berger W. Interlimb coordination of posture in patients with spastic hemiparesis. *Brain*. **107**, 965-978 (1984).

23. Patterson K.K., Parafianowicz I., Danells C.J., et al. Gait asymmetry in community-ambulating stroke survivors. *Arch. Phys. Med. Rehabil*. **89**, 304-310 (2007).

24. Kerrigan D.C., Frates E.P., Rogan S., & Riley P.O. Hip hiking and circumduction: quantitative definitions. *Am. J. Phys. Med. Rehabil.* **79**, 247-252 (2000).

25. Sulzer J.S., Gordon K.E., Dhaher Y.Y., Peshkin M.A., & Patton J.L. Preswing knee flexion assistance is couple with hip abduction in people with stiff-knee gait affter stroke. *Stroke*. **41**, 1709-1714 (2010).

26. Lewek M.D., Osborn A.J., & Wutzke C.J. The influence of mechanically and physiologically imposed stiff-knee gait patterns on the energy cost of walking. *Arch. Phys. Med. Rehabil.* **93**, 123-128 (2012).

27. Blazkiewicz M., Wiszomirska I., Kaczmarczyk K., Brzuszkiewicz-Kuzmicka G., & Wit A. Mechanisms of compensation in the gait of patients with drop foot. *Clin. Biomech. (Bristol, Avon)*. **42**, 41-49 (2017).

28. Vasudevan E.V. & Bastian A.J. Split-belt treadmill adaptation shows different functional networks for fast and slow human walking. *J. Neurophysiol.* **103**, 193-191 (2010).

29. Finley J.M., Long A., Bastian A.J., & Torres-Oviedo G. Spatial and temporal control contribute to step length asymmetry during split-belt adaptation and hemiparetic gait. *Neurorehabil. Neural Repair*. **29**, 786-795 (2015).

30. Malone L.A. & Bastian A.J. Thinking about walking: effects of conscious correction versus distraction on locomotor adaptation. *J. Neuorphysiol.* **103**, 1954-1962 (2010).

31. Malone L.A. & Bastian A.J. Spatial and temporal asymmetries in gait predict split-belt adaptation behavior in stroke. *Neurorehabil. Neural Repair.* **28**, 230-240 (2014).

32. Vasudevan E.V.L, Torres-Oviedo G., Morton S.M., Yang J.F., & Bastian A.J. Younger is not always better: development of locomotor adaptation from childhood to adulthood. *J. Neurosci.* **31**, 3055-3065 (2011).

33. Statton M.A., Vasquez A., Morton S.M., Vasudevan E.V.L., & Bastian A.J. Making sense of cerebellar contributions to perceptual and motor adaptation. *Cerebellum*. **17**, 111-121 (2018).

34. Mawase F., Shmuelof L., Bar-Haim S., & Karniel A. Savings in locomotor adaptation explianed by changes in learning parameters following initial adaptation. *J. Neurophysiol.* **111**, 1444-1454 (2014).

35. Roemmich R.T. & Bastian A.J. Two ways to save a newly learned motor pattern. *J. Neurophysiol.* **113**, 3519-3530 (2015).

36. Malone L.A., Vasudevan E.V.L., & Bastian A.J. Motor adaptaation training for faster relearning. *J. Neurosci*. **31**, 15136-15143 (2011).

37. Shadmehr R. & Brashers-Krug T. Functional stages in the formation of the human long-term motor memory. *J. Neurosci.* **17**, 409-419 (1997).

38. Yanagihara D. & Kondo I. Nitric oxide plays a key role in adaptive control of locomotion of cat. *Proc. Natl. Acad. Sci.* **93**, 13292-13297 (1996).

39. Forssberg H., Grillner S., Halbertsma J., & Rossignol S. The locomotion of the low spinal cat. ii. Interlimb coordination. *Acta physiologica Scandinavica*. **108**, 283-295 (1980).

40. Hsu A.L., Tang P.F., & Jan M.H. Analysis of impairments influencing gait velocity and asymmetry of hemiplegic patients after mild to moderate stroke. *Archives of physical medicine and rehabilitation*. **84**, 1185-1193 (2003).

41. Lamontagne A. & Fung J. Faster is better: impliciations for speed-intenstive gait traning after stroke. *Stroke*. **35**, 2543-2548 (2004).

42. Olney S.J., Griffin M.P., & McBride I.D. Temporal, kinematic, and kinetic variables related to gait speed in subjects with hemiplegia: a regression approach. *Physical Therapy*. **74**, 872-885 (1994).

43. Reisman D.S., Wityk R., Silver K., & Bastian A.J. Locomotor adapation on a split-belt treadmill can imrpove walking symmetry post-stroke. *Brain*. **130**, 1861-1872 (2007).

44. Reisman D.S., Wityk R., Silver K., & Bastian A.J. Split-belt treadmill adaptation transfers to overground walking in persons poststroke. *Neurorehabilitation and Neural Repair*. **23**, 735-744 (2009).

45. Reisman D.S., McLean H., Keller J., Danks K.A., & Bastian A.J. Repeated split-belt treadmill training improves poststroke step length asymmetry. *Neurorehabilitation and Neural Repair.* **27**, 460-468 (2013).

46. Roemmich, R.T., Long, A.W. & Bastian, A.J. Seeing the errors you feel enhances locomotor performance but not learning. *Curr. Biol.* **26,** 2707-2716 (2016).

47. Yang, Y.R. *et al*. Effects of interactive visual feedback training on post-stroke pusher syndrome: a pilot randomized controlled study. *Clin. Rehabil.* **29,** 987-993 (2015).

48. Long, A.W., Roemmich, R.T. & Bastian, A.J. Blocking trial-by-trial error correction does not interfere with motor learning in human walking. *J. Neurophysiol.* **115,** 2314-2318 (2016).

49. Qaiser, T., Chisholm, A.E. & Lam, T. The relationship between lower limb proprioceptive sense and locomotor skill acquisition. *Exp. Brain Res.* **234,** 3185-3192 (2016).

50. Krishnan C., Ranganathan R., Kantak S.S., Dhaher Y.Y, & Rymer W.Z. Active robotic training improves locomotor function in a stroke survivor. *J. Neuroeng. Rehabil.* 9-57 (2012).

51. Marchal-Crespo, L., Tsangaridis, P., Obwegeser, D., Maggioni, S. & Riener, R. Haptic error modulation outperforms visual error amplification when learning a modified gait pattern. *Front. Neurosci.* **13,** 61 (2019).

52. Stanton R., Ada L., Dean C.M., & Preston E. Biofeedback improves activities of the lower limb after stroke: a systematic review. *J. Physiother.* **57**, 145-155 (2011).

53. Genthe K., Schenck C., Eicholtz S., Zajac-Cox L., Wolf S., & Kesar T.M. Effects of real-time gait biofeedback on paretic propulsion and gait biomechanics in individuals post-stroke. *Top. Stroke. Rehabil.* **25**, 186-193 (2018).

54. van Gelder, L.M.A., Barnes, A., Wheat, J.S. & Heller, B.W. The use of biofeedback for gait retraining: A mapping review. *Clin. Biomech.* **59,** 159-166 (2018).

55. Cherry-Allen K.M., Statton M.A., Celnik P.A., & Bastian A.J. A dual-learning paradigm simultaneously improves multiple features of gait post-stroke. *Neurorehabil. Neur. Repair.* **32**, 810-820 (2018).

56. Colborne G.R., Olney S.J., & Griffin M.P. Feedback of ankle joint angle and soleus electromyography in the rehabilitation of hemiplegic gait. *Arch. Phys. Med. Rehabil.* **74**, 1100-1106 (1993).

57. Aruin A.S., Hanke T.A., & Sharma A. Base of support feedback in gait rehabilitation. *Int. J. Rehabil. Res.* **26**, 309-312 (2003).

58. Montoya R., Dupui P., Pages B. & Bessou P. Step-length biofeedback device for walk rehabilitation. *Med. Biol. Eng. Comput.* **32**, 416-420 (1994).

59. Statton, M.A., Toliver, A. & Bastian, A.J. A dual-learning paradigm can simultaneously train multiple characteristics of walking. *J. Neurophysiol.* **115,** 2692-2700 (2016).

60. Napier, C., MacLean, C.L., Maurer, J., Taunton, J.E. & Hunt, M.A.. Real-time biofeedback of performance to reduce braking forces associated with running-related injury: An exploratory study. *J. Orthop. Sports Phys. Ther.* **49,** 136-144 (2019).

61. Agresta, C. & Brown, A. Gait retraining for injured and healthy runners using augmented feedback: a systematic literature review. *J. Orthop. Sports Phys. Ther.* **45,** 576-584 (2015).

62. An W.W., Ting K.H., Au I.P.H., Zhang J.H., Chan Z.Y.S., Davis I.S., So W.K.Y, Chan R.H.M, & Cheung R.T.H. Neurophysiological correlates of gait retraining with real-time visual and auditory feedback. *IEEE Trans. Neural Syst. Rehabil. Eng.* **27**, 1341-1349 (2019).

63. C.M. Krause. Cognition- and memory-related ERD/ERS responses in the auditory stimulus modality. *Prog. Brain Res.* **159**, 197-207 (2006).

64. Vingerhoets G. & Clauwaert A. Functional connectivity associated with hand shape generation: Imitating novel hand postures and pantomiming tool grips challenge difference nodes of a shared neural network. *Hum. Brain Mapping*. **36**, 3426-3440 (2015).

65. Herzfeld D.J., Vaswani P.A., Marko M.K., & Shadmehr R. A memory of errors in sensorimotor learning. *Science*. **345**, 1349-1353 (2014).

66. Smith M.A., Ghazizadeh A., & Shadmehr R. Interacting adaptive processes with different timescales underlie short-term motor learning. *PLoS Biol.* **4**, (2006).

67. Huang V.S., Haith A., Mazzoni P., & Krakauer J.W. Rethinking motor learning and savings in adaptation paradigms: model-free memory for successful actions combines with internal models. *Neuron*. **70**, 787-801 (2011).

68. Haith A.M., Huberdeau D.M., & Krakauer J.W. The influence of movement preparation time on the expression of visuomotor learning and savings. *J. Neurosci.* **35**, 5109-5117 (2015).

69. Morehead J.R., Qasim S.E., Crossley M.R., & Ivry R. Savings upon re-aiming in visuomotor adaptation. *J. Neurosci.* **35**, 14386-14396 (2015).

70. Zarahn E., Weston G.D., Liang J., Mazzoni P., & Krakauer J.W. Explaining savings for visuomotor adaptation: linear time-invariant state-space models are not sufficient. *J. Neurophysiol.* **100**, 2537-2548 (2008).

71. Ruitenberg M., De Dios Y., Gadd N., Wood S., Reuter-Lorenz P, Kofman I, Bloomberg J, Mulavara A., & Seidler R. Multi-day adaptation and savings in manual and locomotor tasks. *Journal of Motor Behavior*. 1-11 (2017).

72. Seidler R., Gluskin B., & Greeley B. Right prefrontal cortex transcranial direct current stimulation enhances multiday savings in sensorimotor adaptation. *J. Neurophysiol.* **117**, 429-435 (2017).

73. Mawase F., Bar-Haim S, Joubran K., Rubin L., Karniel A., & Shmuelof L. Increased adaptation rates and reduction in trial-by-trial variability in subjects with cerebral palsy following multi-session locomotor adaptation training. *Front. Hum. Neurosci.* **10**, (2016).

74. Leech K.A. & Roemmich R.T. Independent voluntary correction and savings in locomotor learning. *J. Exp. Biol.* **221**, (2018).

75. Huberdeau D., Haith A., & Krakauer J. Formation of long-term memory for visuomotor adaptation following only a few trials of practice. *J. Neurophysiol.* **114**, 969-977 (2015).

76. Orban de Xivry J. & Lefevre P. Formation of model-free motor memories during motor adaptation depends on perturbation schedule. *J. Neurophysiol.* **113**, 2733-2741 (2015).

77. Wang T.Y., Bhatt T., Yang F., & Pai Y.C. Generalization of motor adaptation to repeated-slip perturbation across tasks. *Neuroscience*. **180**, 85-95 (2011).

78. Pai Y.C. & Bhatt T.S. Repeated-slip training: an emerging paradigm for prevention of slip-related falls among older adults. *Phys. Ther.* **87**, 1478-1491 (2007).

79. Yang F., Bhatt T., & Pai Y.C. Generalization of treadmill-slip training to prevent a fall following a sudden (novel) slip in over-ground walking. *J. Biomech.* **46,** 63-69 (2013).

80. Lee A., Bhatt T., & Pai Y.C. Generalization of treadmill perturbation to overground slip during gait: effect of different perturbation distances on slip recovery. *J. Biomech.* **49**, 149-154 (2016).

81. Pai Y.C., Bhatt T., Wang E., Espy D., & Pavol M.J. Inoculation against falls: rapid adaptation by young and older adults to slips during daily activities. *Arch. Phys. Med. Rehabil.* **91**, 452-459 (2010).

82. Bhatt T., Yang F., & Pai Y.C. Learning to resist gait-slip falls: long-term retention in community-dwelling older adults. *Arch. Phys. Med. Rehabil.* **93**, 557-564 (2012).

83. Kwakkel G., van Peppen R., Wagenaar R.C., Wood Dauphinee S., Richards C., Ashburn A., Miller K., Lincoln N., Partridge C., Wellwood I., & Langhorne P. Effects of augmented exercise therapy time after stroke: a meta-analysis. *Stroke*. **35**, 2529-2539 (2004).

84. van Peppen R.P, Kwakkel G., Wood-Dauphinee S., Hendriks H.J., Van der Wees P.J., & Dekker J. The impact of physical therapy on functional outcomes after stroke: what's the evidence? *Clin. Rehabil.* **18**, 833-863 (2004).

85. Lohse K.R., Lang C.E., & Boyd L.A. Is more better? Using metadata to explore dose-response relationships in stroke rehabilitation. *Stroke*. **45,** 2053-2058 (2014).

86. Wagenaar, J.B., Ventura, V. & Weber, D.J. State-space decoding of primary afferent neuron firing rates. *J Neural Eng* **8,** 016002 (2011).

87. Han, S., Chu, J.U., Kim, H., Park, J.W. & Youn, I. Multiunit activity-based real-time limb-state estimation from dorsal root ganglion recordings. *Sci. Rep*. **7,** 44197 (2017).

88. Fathi, Y. & Erfanian, A. A probabilistic recurrent neural network for decoding hind limb kinematics from multi-segment recordings of the dorsal horn neurons. *J. Neural. Eng.* **16,** 036023 (2019).

89. DeLeo, A.T., Dierks, T.A., Ferber, R. & Davis, I.S. Lower extremity joint coupling during running: a current update. *Clin. Biomech.* **19,** 983-991 (2004).

90. Souza, R.B., Arya, S., Pollard, C.D., Salem, G. & Kulig, K. Patellar tendinopathy alters the distribution of lower extremity net joint moments during hopping. *J. Appl. Biomech.* **26,** 249-255 (2010).

91. Dechamps, K. *et al.* A novel approach for the detection and exploration of joint coupling patterns in the lower limb kinetic chain. *Gait Posture* **62,** 272-377 (2018).

92. Christensen, J.C. *et al*. Visual knee-kinetic biofeedback technique normalizes gait abnormalities during high-demand mobility after total knee arthroplasty. *Knee* **25,** 73-82 (2018).

93. Pfeufer, D. *et al*. Training with biofeedback devices improves clinical outcome compared to usual care in patients with unilateral TKA: a systematic review. *Knee. Surg. Sports Traumatol. Arthrosc.* (2018).

94. Luc-Harkey, B.A. *et al*. Real-time biofeedback can increase and decrease vertical ground reaction force, knee flexion excursion, and knee extension moment during walking in individuals with anterior cruciate ligament reconstruction. *J. Biomech.* **76,** 94-102 (2018).

95. Sackley, C.M. & Lincoln, N.B. Single blind randomized controlled trial of visual feedback after stroke: effects of stance symmetry and function. *Disabil. Rehabil.* **19,** 536-546 (1997).

96. Stanton, R., Ada, L., Dean, C.M. & Preston, E. Feedback received while practicing everyday activities during rehabilitation after stroke: An observational study. *Physiother. Res. Int.* **20,** 166-173 (2015).

97. Morawetz, C., Holz, P., Baudewig, J., Treue, S. & Dechent, P. Split of attentional resources in human visual cortex. *Vis. Neurosci.* **24,** 817-826 (2007).

98. Fagioli, S. & Macaluso, E. Attending to multiple visual streams: interactions between location-based and category-based attentional selection. *J. Cogn. Neurosci.* **21,** 1628-1641 (2009).

99. Fagioli, S. & Macaluso, E. Neural correlates of divided attention in natural scenes. *J. Cogn. Neurosci.* **28,** 1392-1405 (2016).

101. Aravind, G. & Lamontagne, A. Dual tasking negatively impacts obstacle avoidance abilities in post-stroke individuals with visuospatial neglect: task complexity matters! *Restor. Neurol. Neurosci.* **35,** 423-436 (2017).

102. Bizama, F., Medley, A., Trudelle-Jackson, E., & Csiza, L. The effect of visual environmental distraction on gait performance in children. *Phys. Occup. Ther. Pediatr.* **38,** 64-73 (2018).

103. Mazaheri, M. *et al*. Effect of aging and dual tasking on step adjustments to perturbations in visually cued walking. *Exp. Brain. Res.* **233,** 3467-3474 (2015).

104. Ranganathan, R. *et al*. Age-dependent differences in learning to control a robot arm using a body-machine interface. *Sci. Rep.* **9,** 1960 (2019).

105. Abdollahi, F. *et al*. Body-machine interface enables people with cervical spinal cord injury to control devices with available body movements: Proof of concept. *Neurorehabil Neural Repair* **31,** 487-493 (2017).

106. Farshchiansadegh, A. *et al*. A body machine interface based on inertial sensors. *Conf. Proc. IEEE Eng. Med. Biol. Soc.* (2014).

107. Pierella, C. *et al*. Body machine interfaces for neuromotor rehabilitation: a case study. *Conf. Proc. IEEE Eng. Med. Biol .Soc.* (2014).

108. Casadio, M., Ranganathan, R., & Mussa-Ivaldi, F.A. The body-machine interface: a new persepective on an old theme. *J. Mot. Behav.* **44,** 419-433 (2012).

109. Dewolf, A.H., Meurisse, G.M., Schepens, B. & Willems, P.A. Effect of walking speed on the intersegmental coordination of lower-limb segments in elderly adults. *Gait Posture* **70,** 156-161 (2019).

110. Martino, G. *et al*. Locomotor coordination in patients with Hereditary Spastic Paraplegia. *J. Electromyogr. Kinesiol.* **45,** 61-69 (2019).

111. Ulman, S., Ranganathan, S., Queen, R. & Srinivasan, D. Using gait variability to predict inter-individual differences in learning rate of a novel obstacle course. *Ann. Biomed. Eng.* **47,** 1191-1202 (2019).

112. Soares, D.P., de Castro, M.P., Mendes, E.A. & Machado, L. Principal component analysis in ground reaction forces and center of pressure gait waveforms of people with transfemoral amputation. *Prosthet. Orthot. Int.* **40,** 729-738 (2016).

113. Franz, J.R., Maletis, M. & Kram, R. Real-time feedback enhances forward propulsion during walking in old adults. *Clin. Biomech.* **29,** 68-74 (2014).

114. Kerrigan, D.C., Gronley, J. & Perry, J. Stiff-legged gait in spastic paresis. A study of quadriceps and hamstrings muscle activity. *Am. J. Phys. Med. Rehabil.* **70,** 294-300 (1991).

115. Piazza, S.J. & Delp, S.L. The influence of muscles on knee flexion during the swing phase of gait. *J. Biomech.* **29,** 723-733 (1996).

116. Luu, T.P. *et al*. Multi-trial gait adaptation of healthy individuals during visual kinematic perturbations. *Front. Hum. Neurosci.* **11,** 320 (2017).

117. Krishnan, C. *et al*. Learning new gait patterns is enhanced by specificity of training rather than progress of task difficulty. *J. Biomech.* **88,** 33-37 (2019).

118. Chisholm, A.E., Qaiser, T., Williams, A.M.M., Eginyan, G., & Lam, T. Acquisition of a precision walking skill and the impact of proprioceptive deficits in people with motor-incomplete spinal cord injury. *J Neurophysiol* **121,** 1078-1084 (2019).

119. Ranganathan, R., Krishnan, C., Dhaher, Y.Y. & Rymer, W.Z. Learning new gait patterns: Exploratory muscles activity during motor learning is not predicted by motor modules. *J. Biomech.* **49,** 718-725 (2016).

120. Fugl-Meyer A.R., Jaasko L., Leyman I., Olsson S., & Steglind S. The post-stroke hemiplegic patients. 1. A methods for evaluation of physical performance. *Scand. J. Rehabil. Med.* **7**, 13-31 (1975).

121. Halligan P.W., Cockburn J., & Wilson B. The behavioral assessment of visual neglect. *Neuropsychological Rehabilitation.* **1**, 5-32 (1991).

122. Nasreddine Z.S., Phillips N.A. Bedirian V., et al. The Montreal Cognitive Assessment, MoCA: a brief screening tool for mild cognitive impairment. *J. Am. Geriatr. Soc.* **53**, 695-699 (2005).

123. Schaffert J., Lee C.M., Neill R., & Bo J. Visuomotor adaptability in older adults with mild cognitive decline. *Acta Psychologica.* **173**, 106-115 (2017).

124. Moussard A., Bigand E., Belleville S., & Peretz I. Music as a mnemonic to learn gesture sequences in normal aging and Alzheimer's disease. *Front. Hum. Neurosci.* **8**, 1-9 (2014).

125. Tippett W.J. & Sergio L.E. Visuomotor integration is impaired in early stage Alzheimer's disease. *Brain Research*. **1102**, 92-102 (2006).

126. van Tilborg I.A.D.A., Kessels R.P.C., & Hulstijn W. L. Learning by observation and guidance in patients with Alzheimer's dementia. *Neurorehabilitation.* **29**, 295-304 (2011).

127. Kal E., van den Brink H., Houdijk H., van der Kamp J., Goossens P.H., van Bennekom C., & Scherder E. How physical therapists instruct patients in stroke:

an observational study on attentional focus during gait rehabilitation after stroke. *Disabil. Rehabil.* **40**, 1154-1165 (2018).

128. Ploughman M., Shears J., Quinton S., Flight C., O'Brien M., MacCallum P., Kirkland M.C., & Byrne J.M. Therapists' cues influence lower limb muscle activation and kinematics during gait training in subacute stroke. *Disabil. Rehabil.* **40**, 3156-3163 (2018).

129. Fasoli S.E., Trombly C.A., Tickle-Degnen L., & Verfaellie M.H. Effects of instructions on functional reach in persons with and without cerebrovascular accident. *Am. J. Occup. Ther.* **56**, 380-390 (2002).

130. Wulf G., Dufek J.S., Lozano L., & Pettigrew C. Increased jump height and reduced EMG activity with an external focus. *Hum. Mov. Sci.* **29**, 440-448 (2010).

131. Lohse K.R., Sherwood D.E., & Healy A.F. How changing the focus of attention affects performance, kinematics, and electromyography in dart throwing. *Hum. Mov. Sci.* **29**, 542-555 (2010).

132. Poolton J.M., Maxwell J.P., Masters R.S.W., & Raab M. Benefits of an external focus on attention: Common coding or conscious processing? *Journal of Sports Science*. **24**, 89-99 (2006).

133. Ward N.S., Brander F., & Kelly F. Intensive upper limb neurorehabiliation in chronic stroke: outcomes from the Queen Square programme. *J. Neurol. Neurosurg. Psychiatry.* **90**, 498-506 (2019).

134. Winstein C., Kim B., Kim S., Martinez C., & Schweighofer N. Dosage matters. *Stroke*. **50**, 1831-1837 (2019).

135. Verstynen T. & Sabes T.N. How each movement changes the next: an experimental and theoretical study of fast adaptive priors in reaching. *J. Neurosci.* **31**, 10050-10059 (2011).

136. Mawase F., Uehara S., Bastian A.J., & Celnik P. Motor learning enhances use-dependent plasticity. *J. Neurosci*. **37**, 2673-2685 (2017).

137. Kim Y.H., You S.H., Ko M.H., Park J.W., Lee K.H., Jang S.H., Yoo W.K., & Hallett M. Repetitive transcranial magnetic stimulation-induced corticomotor excitability and associated motor skill acquisition in chronic stroke. *Stroke*. **37**, 1471-1476 (2006).

138. Quattrocchi G., Greenwood R., Rothwell J.C., Galea J.W., & Bestmann S. Reward and punishment enhance motor adaptation in stroke. *J. Neurol. Neurosurg. Psychiatry*. **88**, 730-736 (2017).

Curriculum Vitae

Kevin Andrew Day was born on May 29, 1992 in Seattle, WA. He grew up outside of Philadelphia, PA and graduated as valedictorian from Garnet Valley High School in 2010. He attended the University of Pittsburgh on a Full Tuition Scholarship and School of Engineering Honors Scholarship. He graduated *summa cum laude* from the Swanson School of Engineering at the University of Pittsburgh with a Bachelor of Science in bioengineering and minors in neuroscience, economics, and chemistry in May 2014. While at the University of Pittsburgh, Kevin conducted research in the Neural Rehab Engineering Lab under the direction of Dr. Doug Weber and the Human Engineering Research Lab under the direction of Dr. Alicia Koontz. He also participated in the Amgen Scholars summer program in which he completed an internship at the Massachusetts Institute of Technology under the direction of Dr. Emilio Bizzi. Kevin began the Biomedical Engineering Ph.D. program at Johns Hopkins University in August 2014. He joined the Center for Movement Studies under the direction of Dr. Amy Bastian where he completed projects related to visuomotor adaptation, human locomotor learning, and stroke rehabilitation. During his time in the Ph.D. program, Kevin participated in the Summer School in Computational Sensory-Motor Neuroscience (CoSMO) in summer 2017 and completed semesters as a teaching assistant for the undergraduate biomedical engineering courses “Introduction to Rehabilitation Engineering”, “Rehabilitation Engineering Design Lab”, and “Biomedical Engineering Modeling and Design”.